January 2015

Hydraulic Hybrid Four Wheel Drive Sport Utility Vehicle - Utilizing the Blended Hybrid Architecture

Tyler Bleazard
Purdue University

Graduate School Form 30
Updated 1/15/2015

PURDUE UNIVERSITY
GRADUATE SCHOOL
Thesis/Dissertation Acceptance

This is to certify that the thesis/dissertation prepared

By Tyler J. Bleazard

Entitled

HYDRAULIC HYBRID FOUR WHEEL DRIVE SPORT UTILITY VEHICLE - UTILIZING THE BLENDED HYBRID ARCHITECTURE

For the degree of Master of Science in Mechanical Engineering

Is approved by the final examining committee:

Monika Ivantysynova
Chair

Andrea Vacca

Gregory Shaver

To the best of my knowledge and as understood by the student in the Thesis/Dissertation Agreement, Publication Delay, and Certification Disclaimer (Graduate School Form 32), this thesis/dissertation adheres to the provisions of Purdue University's "Policy of Integrity in Research" and the use of copyright material.

Approved by Major Professor(s): Monika Ivantysynova

Approved by: Ganesh Subbarayan 7/29/2015

Head of the Departmental Graduate Program Date

HYDRAULIC HYBRID FOUR WHEEL DRIVE SPORT UTILITY VEHICLE - UTILIZING THE BLENDED HYBRID ARCHITECTURE

A Thesis

Submitted to the Faculty

of

Purdue University

by

Tyler J. Bleazard

In Partial Fulfillment of the

Requirements for the Degree

of

Master of Science in Mechanical Engineering

August 2015

Purdue University

West Lafayette, Indiana

To my loving and patient wife, Lacey, and my beautiful children. This work could not have been completed without their support.

ACKNOWLEDGMENTS

This research could not have been possible without the resources and members at the Maha Fluid Power Research Center. I would first like to thank my advisor, Dr. Monika Ivantysynova, who's guidance and encouragement made this work feasible. Special thanks goes to those graduate researchers that were so vital to this project. Micheal Sprengel for his immeasurable assistance in dynamic programming and implementing the blended hydraulic hybrid transmission, which he invented. Ryan Jenkins and Ning Liu for their help in 3D modeling, baseline testing, and instrumentation. Hiral Haria for her great help in 3D modeling, packaging, design and implementation, and Nate Keller for his help in installing the power train.

A special thanks to Anthony Franklin for rebuilding the SUV's engine, fabrication and installation of the blended hydraulic hybrid transmission, without his expertise this project would never have succeeded. Also thanks to Susan Gauger, and Connie McMindes who's administration made procurement. Lastly I would like to thank all those at the Maha Fluid Power Research Center who have made my experience very enjoyable.

TABLE OF CONTENTS

LIST OF TABLES

LIST OF FIGURES

NOMENCLATURE

δ_i	Inner Steering Angle
δ_o	Outer Steering Angle
W	Track
CG	Center of Gravity
R	Turning Radius to Center of Gravity
R_1	Turning Radius to Rear Wheel
R_2	Turning Radius to Front Wheel
O	Turning Radius Origin
l	Wheel Base
a	Length of Rear Wheel to Center of Gravity
F_x	Force in x Direction
F_{xf}	Resultant Force on Front Axle
F_{xr}	Resultant Force on Rear Axle
F_g	Force Due to Gravity
θ	Angle of Incline
F_D	Force Due to Drag
F_{rf}	Force due to Rolling Resistance on Front Axle
F_{rr}	Force due to Rolling Resistance on Rear Axle
C_r	Coefficient of Rolling Resistance
N	Normal Force
W	Vehicle Weight
A_f	Frontal Area
C_d	Coefficient of Drag
ν	Vehicle Velocity
M_{theo}	Theoretical Torque

Q_{theo}	Theoretical Flow
β	Percent Displacement
V	Unit displacement
w	Rotational Speed
M_{eff}	Effective Torque
M_s	Torque Losses
Q_{eff}	Effective Flow
Q_s	Flow Losses
M_{engmax}	Maximum Engine Torque
i	Gear Ratio
p	Pressure
V	Accumulator Volume
n	Adiabatic Coefficient
E	Energy
x	State
u	Control
J	Cost Function

ABBREVIATIONS

BSFC	Brake Specific Fuel Consumption
CVT	Continuously Variable Transmission
DP	Dynamic Programming
EPA	Environmental Protection Agency
FUDS	Federal Urban Driving Schedule
HP	High Pressure
HST	Hydrostatic Transmission
LP	Low Pressure
MAN	Maschinenfabrik Augsburg-Nurnberg
mpg	Miles per Gallon
PGT	Planetary Gear Train
UDDS	Urban Dynamometer Drive Schedule

ABSTRACT

Bleazard,Tyler J. M.S.M.E, Purdue University, August 2015. Hydraulic Hybrid Four Wheel Drive Sport Utility Vehicle - Utilizing the Blended Hybrid Architecture. Major Professor: Monika Ivantysynova, School of Mechanical Engineering.

Improving the fuel economy of on-highway vehicles is of major concern to government agencies, consumers and industry leaders, that has caused an expanding interest in hybrid vehicles. Hydraulic hybrid vehicles show great potential due to their high power density, high efficiency in regenerative braking and low cost of materials. There are many different hydraulic hybrid architectures that allow for better engine management and regenerative braking. The focus for this work is the blended hydraulic hybrid. This transmission achieves high efficiency and response through the use of a hydrostatic power path, additionally a set of check valves enable regenerative braking and blending of engine power and stored power from the accumulator.

A modified blended hybrid circuit was designed to allow for all time four wheel drive operation. Simulation was used to validate the design in four wheel drive turning events.

Optimal control and dynamic simulation were used to understand how the sizing of main components affected the performance and efficiency of this transmission. The main components that were investigated are the hydraulic pump, the two hydraulic motors, the accumulator volume and minimum accumulator pressure, in addition this was compared to a statically sized transmission. This study resulted in the selection of A 100 cc/rev hydraulic pump, two 75 cc/rev hydraulic motors and a 32 liter accumulator was c

A 1999 Range Rover 4.0 Se was selected as the application vehicle, baseline measurements and empirical data were taken to build an appropriate vehicle dynamics model, and engine model to be used for simulation and control. With this information

and results from the parameter study a complete blended hydraulic hybrid transmission was designed, and packaging was completed using 3D modeling. This design was implemented on the application vehicle and different operating modes of the blended hydraulic hybrid were demonstrated.

1. INTRODUCTION

In 1970 the United States reached its peak production of petroleum, for the next 45 years the U.S. dependency on foreign oil continued to increase, with falling output each year. Currently the U.S. is going through an oil boom with the use of hydraulic fracking, but as seen in Figure 1.1 forecasts show that the US is unable to become fully independent of foreign oil. Because of this, great effort is being made in all sectors to reduce our energy consumption. The largest consumer of petroleum in the U.S. is the transportation sector consuming 67% of the total U.S. petroleum use, and 28% of the total U.S. energy use (Davis et al. 2014). Figure 1.2 shows the break down of petroleum use in the transportation sector, of this cars and light trucks consume 63% of the transportation petroleum use, while medium and heavy trucks account for 21% of the petroleum use. Despite the gains that the oil industry is making to increase the supply of crude to the U.S. there is still a great need to reduce the fuel consumed by cars and trucks. Because of these trends in the past 30 years government, academia and industry have researched many ways to save fuel for on and off-highway vehicles.

Of the technologies that have been researched to improve fuel economy, the most successful technology to enter the market is the hybrid transmission. Wouk explained that a hybrid vehicle is one in which propulsion energy is available from two or more sources or converters (1995). There are two main types of hybrid vehicles availiable today, electric and hydraulic. Electric hybrid vehicles use electric motors and generators to convert energy, and batteries or electric capacitors to store energy. On the other hand hydraulic hybrids use hydraulic pumps and motors as energy converters and hydro-pneumatic accumulators to store energy.

The efficiency and fuel economy of a hybrid vehicle can vary greatly depending on many factors such as design, component sizing, and control. Despite these factors though, hybrid vehicles can only save fuel through proper engine management and

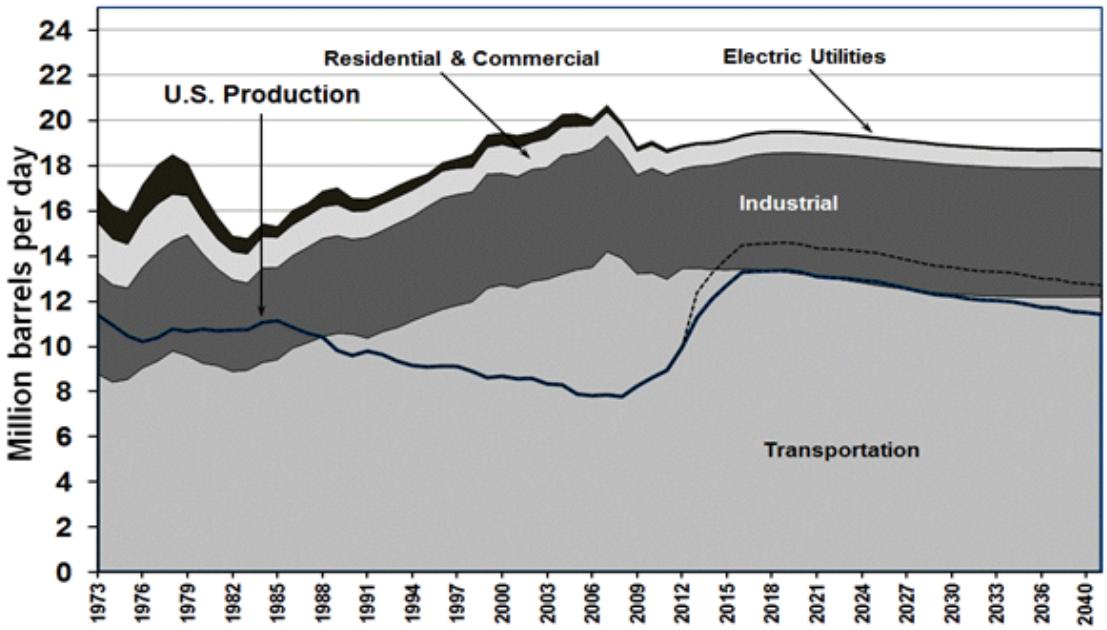

Figure 1.1. United States petroleum production and consumption - all sectors, 1973-2040 (Davis et al. 2014).

regenerative breaking. The combination of these two principles is referred to as power management and will be discussed in the following section.

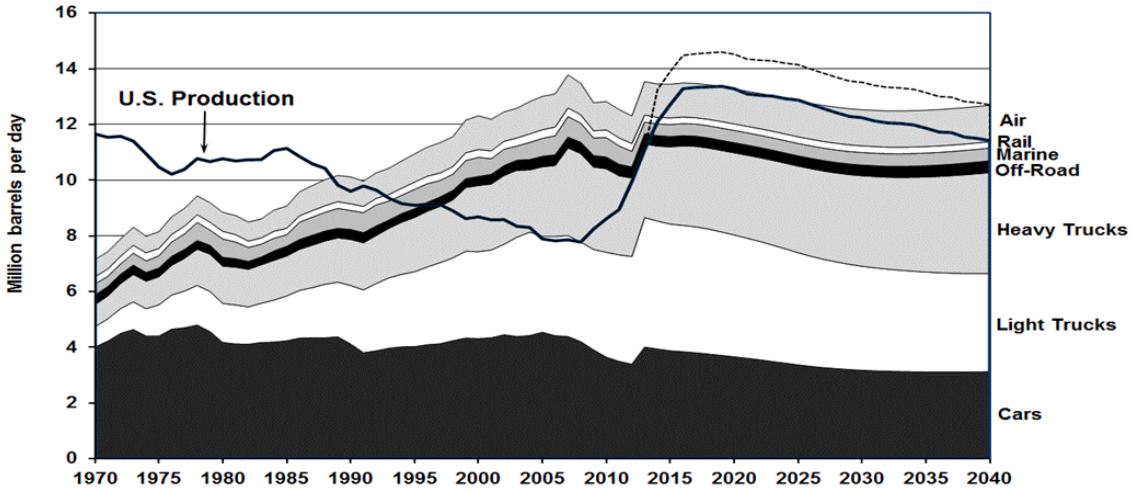

Figure 1.2. United States petroleum production and transportation consumption, 1970-2040 (Davis et al. 2014).

1.1 Engine Management

To fully understand how engine management for hybrid vehicles is beneficial it is important to first understand how a conventional transmission operates. A conventional powertrain consists of an internal combustion engine that is mechanically coupled to the wheels through a mechanical transmission. With a given wheel speed and a given transmission gear ratio the engine speed is fixed. For the user to increase power, the engine torque must increase. Figure 1.3 shows a general brake specific fuel consumption map for a gasoline engine, this map indicates the amount of fuel consumed divided by the power produced. As can be seen in this figure the fuel consumption of a convention transmission is dependent on the current wheel speed, transmission gear ratio, and the torque demand from the driver. Likewise all the energy from the engine must be used when it is produced.

The most simple hybrid power train incorporates the ability to store and release energy. Unlike a conventional transmission the energy consumed by the vehicle does not need to all come from the engine. This allows combustion and kinetic energy

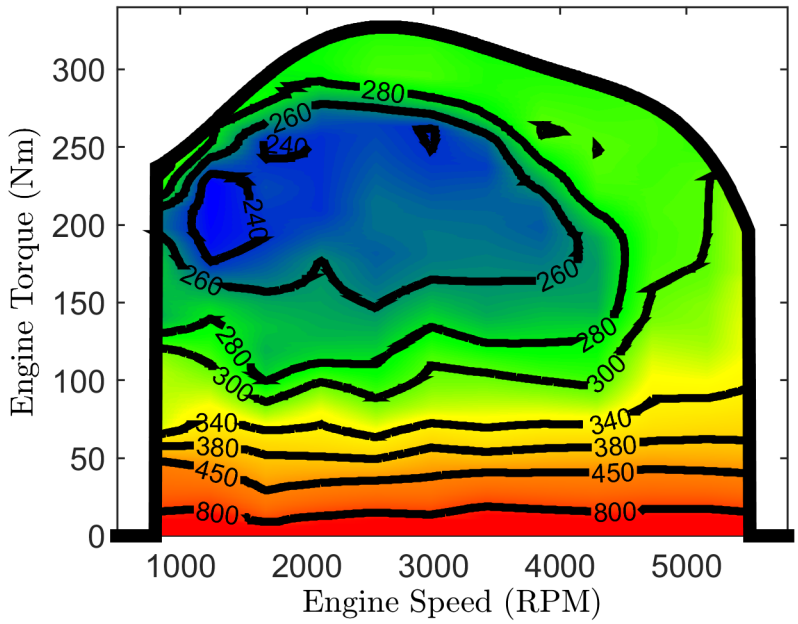

Figure 1.3. BSFC map (kW-h/g).

to be stored as potential energy which can be used at a later time. Though the speed of the engine is still determined by the transmission gear and wheel speed, like a conventional transmission, in a hybrid the engine power can be supplemented by converting the stored potential energy into mechanical energy, thus giving some ability to control the amount of fuel used.

In the past few years Continuously Variable Transmissions (CVT) have made their way into the on-highway market. Where a conventional transmission has discrete gear ratios to choose from, a CVT has an infinite amount of standing gear rations that can be adjusted in order for the engine to operate at almost any speed and still meet the required power at the wheels. For a CVT, fuel consumption can be decreased by choosing the engine speed that has lowest fuel consumption for the required power, a feature not possible in a conventional transmission.

Modern hybrid vehicles combine both energy storage and a CVT. This allows for the required wheel power to be met by either releasing the stored kinetic energy, op-

erating the engine at a speed with low fuel consumption yet meets the power demand, or a combination of both. This gives the greatest freedom in engine management.

1.2 Regenerative Breaking

In addition to engine management, hybrids utilize regenerative braking to save fuel. In a conventional vehicle the kinetic energy is dissipated through friction brakes into heat when the vehicle is braking. Regenerative braking in hybrid vehicles converts the kinetic energy of the vehicle, that would normally be wasted, into a more useful form and then stores that energy for use at another time.

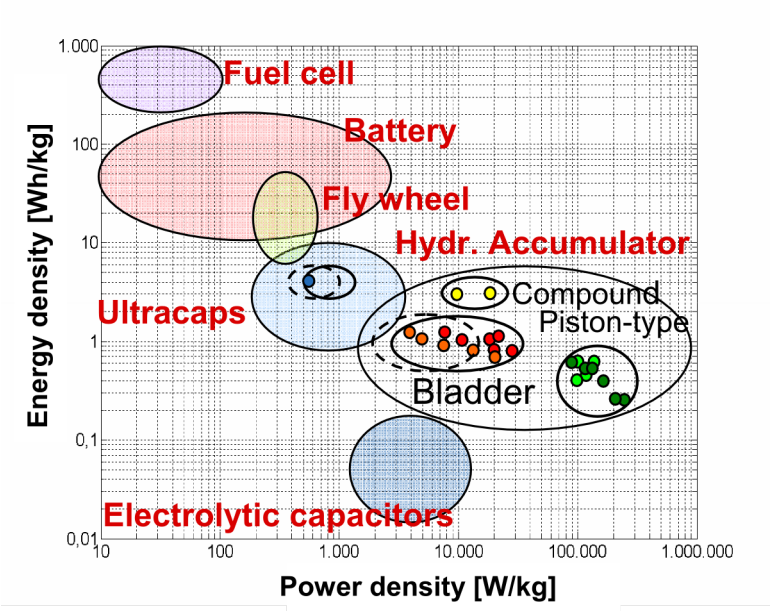

Figure 1.4. Ragone diagram (Baseley et al. 2007).

Regenerative braking is an important feature of all hybrid vehicles, there are many systems that convert and store this kinetic energy. The Ragone diagram shown in Figure 1.4 shows the different power and energy densities of these different systems. The differences in power and energy densities is one of the main contrasts between hydraulic and electric hybrids. For regenerative braking a high power density is of most importance, because a large amount of energy is converted in a relatively short

amount of time, in this area hydraulic hybrids excel. Electric hybrids on the other hand have a low power density compared to hydraulic hybrids. Consequently during most braking events only a portion of the kinetic energy is able to be stored. On the other hand hydraulic hybrids are less energy dense than electric hybrids, resulting less energy storage available. For these reasons hydraulic hybrids have become an attractive alternative to the electric hybrid, especially for large vehicles in urban areas. This thesis will focus only on hydraulic hybrids.

1.3 State of the Art

There have been many different hydraulic hybrid transmissions developed and analyzed, though in the market today three main architectures are most prevalent, these consist of the parallel hybrid, the series hybrid, and a combination of the two called a series-parallel hybrid. The following sections will discuss the operation and development of these systems.

1.3.1 Parallel Hybrid

A parrallel hybrid consists of an energy converter and an energy storage devise coupled mechanically to a conventional transmission, as seen in Figure 1.5. In hydraulic parallel hybrid's the energy converter consists of a hydraulic unit that is typically coupled to the drive shaft, though could also be coupled before the transmission, and a high pressure hydraulic accumulator used for energy storage. Due to the simplicity of this design, it is often used to retrofit existing vehicles.

This hybrid architecture operates by using the hydraulic unit as a pump to store excess energy generated by the engine or convert to kinetic energy during regenerative breaking, the energy is stored in the hydraulic accumulator when fluid is pumped into the accumulator compressing the nitrogen gas. This stored energy can then be released by operating the hydraulic unit as a motor, providing torque to the drive shaft, and propelling the vehicle.

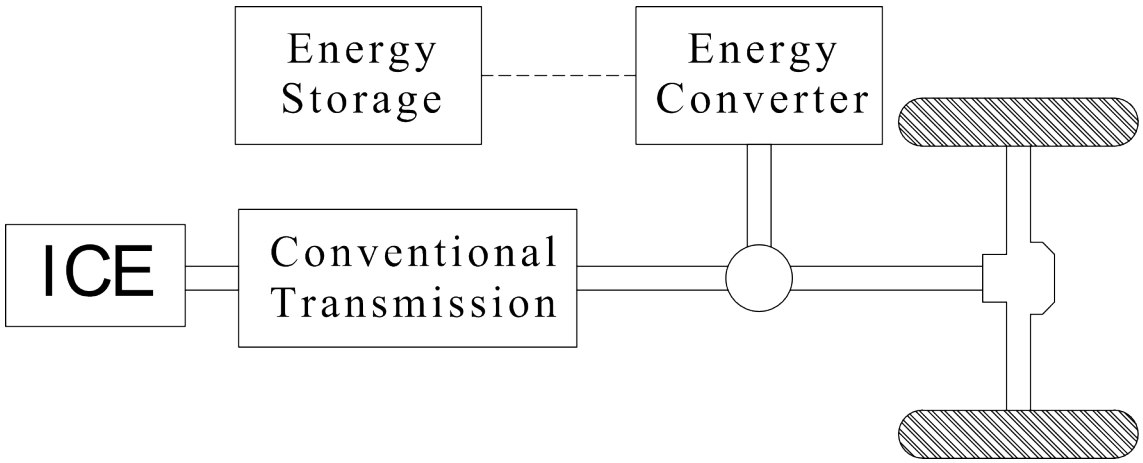

Figure 1.5. Parallel hybrid layout.

Power management has a large impact on the sizing and control of this transmission. A very simple control scheme that is often implemented, is to store energy during braking and then immediate use it during the proceeding acceleration event. More complex power management strategies exist that, in addition to capturing brake energy, excess engine energy is also stored. Also the accumulator could be used more strategically to reduce overall fuel consumption.

Previous research done in this area started in the 1970's using round trip efficiencies. To obtain the round trip efficiency a hydraulic unit is used to store the kinetic energy of a flywheel in a hydraulic accumulator, this energy is then released through the hydraulic unit to the flywheel and its resulting kinetic energy is used to calculate the efficiency. This type of study was first done by Dunn & Wojcienchowski (1972) they found the round trip efficiency of a 19 liter accumulator and a 79 cc/rev hydraulic unit and a 907 kg flywheel to be greater than 50%. Later their studies showed found round trip efficiencies of 66%, from this they determined that 24% of the lost energy was due to losses in the hydraulic unit (1974, 1975). Dewey et al. (1974) additional showed that when accounting for the aerodynamic drag of the flywheel a round trip efficiency of 75% was realized.

Because of the simple control and installation of this transmission in existing vehicles, many prototypes have been developed. In the 1980's a 25% fuel savings was demonstrated by Maschinenfabrik Augsburg-Nurnberg (MAN) in Berlin, Germany on a bus (Martini 1984). Mitsubishi Motors Corp. tested a prototype parallel hybrid bus that received 30% fuel economy gain (Nakzawa et al. 1987). In more recent history Ford Motor Company with the assistance of Eaton and the Environmental Protection Agency (EPA), invented the Hydraulic Power Assist. When doing performance measurements on a 7500 lbs SUV a drop in 0-30 mph acceleration times from 5.4 sec. to 3.5 sec was measured, and a 23.6% improvement in fuel economy on the FTP (Federal Test Procedure) cycle (Kepner 2002). In addition to this numerous other companies and governments have implemented the parallel hybrid on buses, refuse trucks and military vehicles.

1.3.2 Series Hybrid

A series hybrid architecture is shown in Figure 1.6. For this configuration the combustion engine is couple to an energy converter which is then connected in series to an energy storage device and a second energy converter, this is where the name series hybrid comes from. For a hydraulic series hybrid the energy converter (unit 1) coupled to the engine consists of a variable displacement hydraulic pump, a hydraulic accumulator provides energy storage and a second hydraulic unit is coupled to the axles (unit 2).

The use of two hydraulic units that are not coupled with a mechanical shaft form a CVT, allowing the engine speed to be fully decoupled from the wheel speed. This unique feature of the series hybrid creates an opportunity for more advanced power management than the parallel hybrid. The high pressure accumulator in this system has a huge impact on the system operation. Because of the high compliance of the compressed gas in the accumulator, flow from unit 1 has two possible paths, flow may go to the accumulator and the energy can be stored for later use, or flow can go to

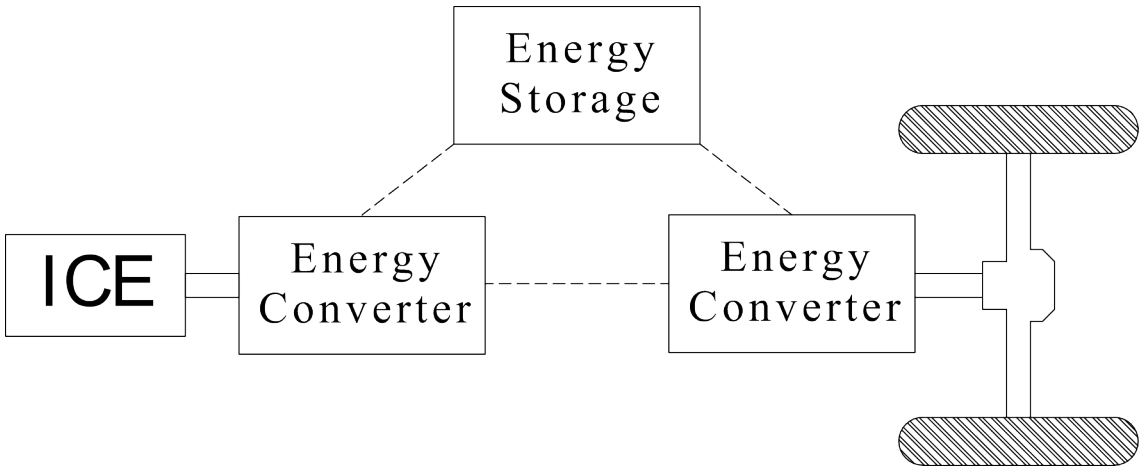

Figure 1.6. Series hybrid layout.

unit 2 and the energy can be used immediately. This allows for greater flexibility in power management because engine energy can be stored independently of the current demanded at the wheels.

The pressure in the system is governed by the compliance of the lines and accumulator and therefore the pressure is a function of the combined flow from unit 1 and unit 2. The most simple control strategy for this transmission consists of using unit 1 to control the pressure, this is done by adjusting the unit displacement and engine speed in order to provide the flow necessary to meet the pressure required by a supervisory controller. Unit 2 on the other hand is controlled to meet a user demanded torque or speed. Because of the high compliance of the accumulator, unit 2 is operated in secondary control, meaning the speed or torque is measured and compared to the demanded speed or torque from the user and the unit displacement is adjusted to meet this demand, while the HP accumulator supplies pressure and flow to the unit.

Braking in a series hybrid is similar to braking in a parallel hybrid. Unit 2 must be an over-center unit, meaning the flow from the unit can be reversed without changing direction of rotation. For an axial piston machine this is typically done by rotating the swash-plate. This allows unit 2 to go from motoring during accelerating, and then

during braking the unit will go over center and begin pumping into the accumulator, converting the kinetic energy into potential energy.

Some draw backs to the series hybrid is that all power to the wheels must come from the unit 2. This often results in a large unit, that under current technology can limit the top speed of the vehicle. Hydraulic units are most efficient when operated at low pressures and high displacements, for a series hybrid, the system pressure is defined by the pressure in the accumulator, and therefore both unit 1 and unit 2 must be exposed to high pressure during operation and can often cause the units to operate inefficiently at high pressures and low displacements.

One of the first studies of the series hybrid, was done by Elder & Otis (1973), simulations were done for 771 kg passenger vehicle on the Federal Urban Driving Schedule (FUDS), this initial study showed that the series hydraulic hybrid could achieve substantial fuel savings and was feasible for passenger vehicles. Soon after this fuel savings of 17% and 22% were investigated for a series hybrid vehicle that incorporated a de-cluching mechanisim called a "mechanical bypass" Heggie & Sandri (1979). In 1985 Wu et al. simulated a series hybrid passenger vehicle capable of 60 mpg on the FUDS and incorporating engine shut off.

Prototype vehicles of the series hybrid began two decades after the parallel hybrid in the 1990's. A series hybrid was applied to a bus using secondary control, called the Cumulo Hydrostatic Drive, saw a 48% fuel savings on a trapezoidal start-stop drive cycle (Hugosson 1993). Government and industry partnered in 2006 to develop series hybrid Class 5 UPS delivery truck, this also included an advanced engine over the typical delivery truck. When field tested in Detroit, MI this vehicle saw 60% to 70% fuel savings (Wendel et al. 2007). Also in 2012 the U.S. Federal Transit Authority teamed with multiple corporations to design, build and test a series hydraulic hybrid on a transit bus, title the Altair Bus. This project, unlike others which normally retrofired an existing vehicle, designed an entire bus from the ground up, including a more advanced engine, lighter frame and materials, advanced HVAC system and many other features in an effort to create the most efficient and cost effective transit

bus. With these advancements they were able to show a 29% increase in fuel economy over the most efficient electric hybrid, and a 47% increase in fuel economy over an identical non hybrid bus. When compared to a conventional transit bus, the Altair Bus increases the fuel economy 109% (Heskitt et al. 2012).

1.3.3 Series-Parallel Hybrid

The series-parallel hybrids, are considered to be the most efficient of hybrid architectures. These architectures combine aspects of both the series hybrid and the parallel hybrid, and are often referred to as a power split hybrid transmission. There are many different power split architectures ranging from output coupled, input coupled, or more complex architectures that incorporate multiple planetary gear trains (PGT) and clutches such as the dual stage and compound power split transmissions, though different in operation the main principle is the same for each. Figure 1.7 shows a simple output coupled power split architecture, which consists of an internal combustion engine, a planetary gear train, two energy converters, and an energy storage device.

The PGT forms the heart of all power split transmission. This mechanism allows a single power input to be split onto two shafts. Thus power from the engine is input into the planetary gear and then split between an efficient mechanical path, and a continuously variable hydraulic path, in this case a series hybrid architecture. The power is then added together before the wheels through unit 2, similar to a parallel hybrid. In a series hybrid all power must transmit though the hydraulics, which are much less efficient than a mechanical shaft, thus making the power split transmission more efficient.

During initial acceleration, when the wheels are not rotating, all engine power is transmitted through the hydraulic path and torque is added to the drive shaft through unit 2. As the wheels speed up the PGT causes unit 1 to slow down, thus decreasing the power through the hydraulic path and power through the mechanical

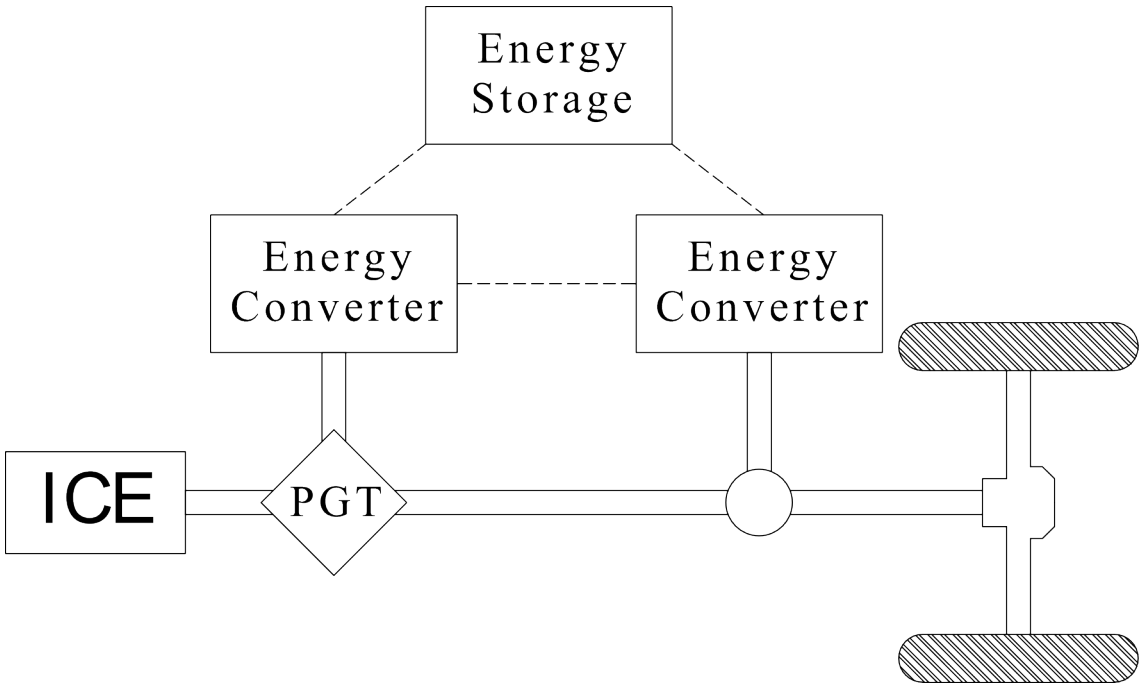

Figure 1.7. Series-parallel hybrid layout.

shaft starts to increase. At a velocity specified by the transmission designer, unit 1 will stop rotating and all power will be transmitted through the mechanical shaft, thus becoming highly efficient at higher speeds. The energy storage device for this transmission operates similar to the other hybrid transmission discussed, where unit 2 is able will go over center and pump hydraulic fluid into the accumulator thus converting kinetic energy to potential energy to be used at another time. Similar to the series hybrid, unit 1 is able to store excess engine energy in the accumulator as well.

Initial work on the power-split transmission began in the late 1970's and early 1980's when Shiber (1980) first patented the power split hydraulic hybrid transmission. He also prototyped this transmission for a 1360 kg VW Jetta, their data showed a doubling of fuel economy compared to the non hybrid vehicle (1979). In Germany, MAN did a second iteration of their hydraulic hybrid bus, called Hydrous II, this transmission consisted of a hydraulic hybrid power split transmission, in testing they

measured 18 to 33% increase in fuel economy over a conventional bus (Martini 1984). In 2012 the United Postal Service installed 20 power split transmissions developed by Parker Hannifin in to gasoline powered delivery trucks in the Baltimore MD area, these transmission incorporated engine shut off during idle. To get a better representation of their potential data, GPS data was taken from these 20 vehicles and a representative drive cycle was developed and then the vehicle was tested on a chassis dynamometer for the designed drive cycle. The power split parcel delivery van demonstrated a 19-52% better fuel economy than a conventional diesel depending on the cycle, and a 30-56% better fuel economy than the conventional gasoline (Lammert et al. 2014). Most recently PSA-Peugeot-Citroen has begun developing a hydraulic hybrid power split transmission for a passenger vehicle, called the Air Hybrid. They have reported a 45% fuel savings in city driving and an average of 35% fuel savings in overall driving (PSA-Peugeot-Citroen 2014). There do exist other power split transmission developed by other companies, though the list is limited due to the high development costs.

1.4 Thesis Statement

The aim of this thesis is to implement an optimally sized blended hydraulic hybrid transmission in an all time four wheel drive on-highway SUV. More specifically these include:

- Modify the blended hybrid circuit to allow for four wheel drive operation, and develop a simulation model to validate this circuit design during turning events.
- Instrument and take baseline fuel measurements of the application vehicle, including developing multiple drive cycles to capture most operating conditions of the vehicle.
- Obtain baseline performance measurements to compare transmission design in simulation.

- Use empirical data to develop a model of the vehicle, including engine torque curve, fuel map, and vehicle dynamics parameters.
- Use the traditional static sizing approach to size the blended hydraulic hybrid transmission. This includes sizing of the hydraulic units, accumulator volume, and minimum working pressure.
- Develop a new methodology for optimally sizing of hybrid transmissions in order maximize efficiency and vehicle performance.
- Perform a parameter variation study to investigate the affects of unit 1, unit 2, unit 3, accumulator volume and minimum accumulator pressure on performance and efficiency.
- Size all other components that are not critical to performance, including charge pump, LP accumulator, oil cooler
- Develop and implement a throttle actuation system to control engine speed.
- Develop a modified brake pedal to incorporate regenerative braking without loosing the ability for operator to manually actuate hydraulic friction brakes.
- Design the blended hybrid transmission using 3d modeling to be implemented in the application vehicle.
- Implement the design, including manufacturing of custom parts and assembly of the transmission
- Implement basic control strategy and demonstrate operation in all modes of operation.

2. THE BLENDED HYDRAULIC HYBRID

The focus of this thesis is on a new hydraulic hybrid transmission that was developed in the Maha Fluid Power Research Center called the Blended Hydraulic Hybrid. This transmission was developed to overcome some of the weaknesses that more conventional hydraulic hybrid transmissions experience.

This chapter will discuss the weaknesses in conventional hydraulic hybrid transmissions, and how the blended hybrid transmission overcomes these. In addition, previous research done on the blended hydraulic hybrid will be discussed. Following this a modified blended hybrid architecture will be introduced that allows all time four wheel drive operation. A derivation and simulation of a four wheel drive turning event for this architecture will be presented.

2.1 The Blended Hydraulic Hybrid Transmission

The most common and widely used fully hydraulic hybrid is the series hybrid, which was discussed in Section 1.3.2. While this transmission has proven to increase fuel economy, there exists a few drawbacks. First, the system pressure is governed by the pressure in the high pressure accumulator, thus the hydraulic units are always exposed to the high pressure accumulator's pressure. Thus the units often operate inefficiently at high pressure and low displacement. Second, the series hybrid often has a slow response to demanded torque, resulting in a poor driver feel. Torque at the wheels is a function of system pressure and unit displacement. Because of this, when the current accumulator pressure is relatively low, and the torque demand is high, the user must wait until unit 1 pumps enough fluid into the high pressure accumulator to raise the pressure to meet the desired torque demand.

The last weakness of the series hybrid, is that they require over-center hydraulic units. Over center units. When braking in the series hybrid, unit 2 must go over center, providing a resistive torque to stop the vehicle. Currently only a limited number of hydraulic units sold on the market are capable of going over-center, more importantly an even smaller amount of the high efficiency bent-axis units go over-center.

To address these concerns the blended hydraulic hybrid was developed at the Maha Fluid Power Research Center, this was first introduced by Sprengel & Ivantysynova (2012). The reason it is termed the blended hybrid is because it combines both a hydrostatic transmission and a parallel hybrid. To truly understand the blended hybrid it is important to first understand the hydrostatic transmission (HST)

A hydrostatic transmission is the most common hydraulic transmission in industry, and has been widely used in many applications for years. Figure 2.1 shows the hydraulic circuit for a hydrostatic transmission. This transmission converts power from the engine through a variable displacement pump mechanically connected to the engine. A second hydraulic unit is mechanically connected to the wheels. This system is often described as flow controlled, meaning that the flow from unit 1 must go through unit 2. During operation, a given engine speed and displacement of unit 1 results in a flow that must pass through unit 2 connected to the axle and wheels, thus the displacement of unit 2 will determine the speed of the axle. The hydraulic lines in this system are not very compliant when compared to a hydraulic accumulator and as such the system pressure, normally Line A, will increase almost instantly to the pressure needed to meet the required unit 2 torque. Unit 2 can be either a fixed displacement unit or a variable displacement unit. Since unit 1 is variable displacement the system becomes a continuously variable transmission. Typically the hydrostatic transmission is controlled sequentially, meaning that unit 2 will stay at 100% displacement while unit 1 increases displacement and flow. Once unit 1 reaches full displacement then unit 2 will decrease displacement to continue increasing speed. When slowing down the opposite process is taken, as such unit 2

will produce more flow than unit 1 and Line B will become the high pressure line and a resistive torque will be applied to the wheels as unit 2 pumps high pressure fluid into Line B, decelerating the vehicle.

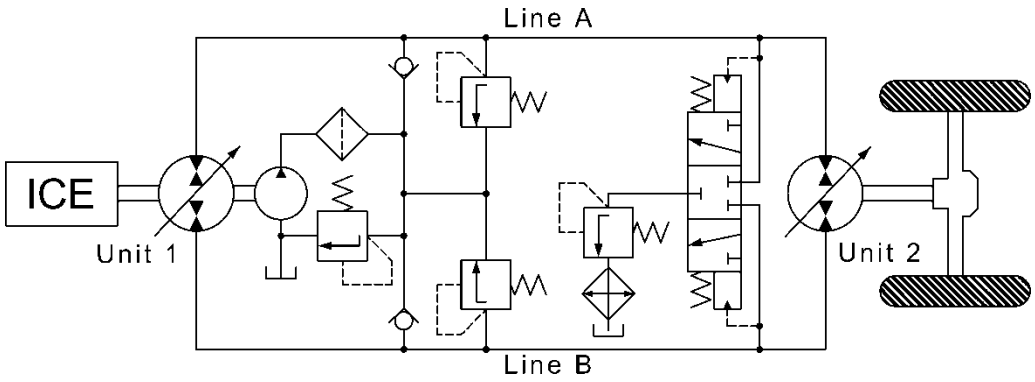

Figure 2.1. Hydrostatic transmission.

In contrast to the series hybrid, a hydrostatic transmission operates the hydraulic units very efficiently. Because the system pressure increases to meet the required torque of unit 2, the units never operate at higher pressures than necessary. One draw back of a HST is that it does not have energy storage capabilities, and therefore the series hybrid consistently has lower fuel consumption over a HST.

The blended hybrid is designed to combine the efficiency of a hydrostatic transmission and the energy storage of a parallel hybrid. The circuit for this transmission is seen in Figure 2.2.

The blended hydraulic hybrid transmission is simply a hydrostatic transmission when the enabling valve (18) is closed, preventing flow from the accumulator into Line C. When compared to Figure 2.1 an additional hydraulic unit was added to the axle, this is common for hydrostatic transmissions, allowing the use of smaller units with lower losses and high speeds while still meeting the displacement needed for high torque demands. The additional check valves (15, 17) allow unit 3 to be connected either to unit 1 as a hydrostatic transmission or to the HP accumulator in secondary control. A third check valve (20) was added which allows flow from Line B into to HP accumulator, this feature allows both unit 2 and unit 3 to provide braking torque

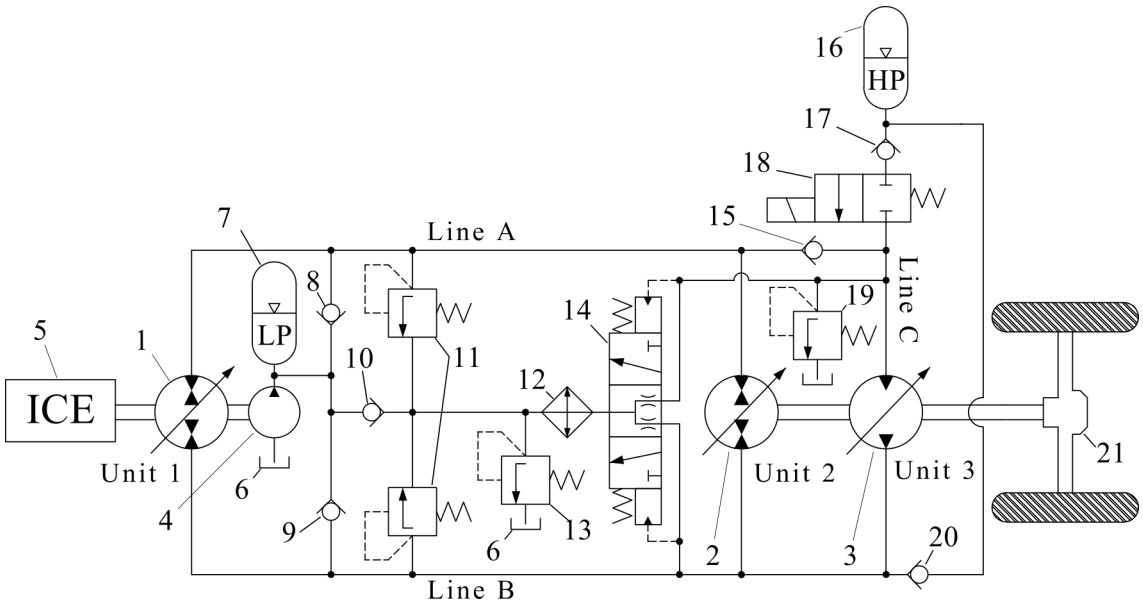

1. Unit 1	2. Unit 2	3. Unit 3
4. Charge Pump	5. Combustion Engine	6. Tank
7. LP Accumulator	8. Check Valve	9. Check Valve
10. Check Valve	11. HP Relief Valve	12. Oil Cooler
13. LP Relief Valve	14. Flushing Valve	15. Check Valve
16. HP Accumulator	17. Check Valve	18. Enabling Valve
19. HP Relief Valve	20. Check Valve	21. Axle and Wheels

Figure 2.2. Blended hydraulic hybrid circuit (Sprengel & Ivantysynova 2014*c*).

without going over-center, in this operation Line B becomes the high pressure line, and line A and Line C become low pressure lines.

In addition to changes in the high pressure operation, the low pressure system of the blended hybrid accomplishes a few extra functions over the traditional low pressure system of the HST. Typical to a hydrostatic transmission the LP charge pump (4) provides the pressure needed for control, and flushes the fluid in order to cool and filter the oil in the system. In addition to this, the LP charge pump (6) and the LP accumulator (7) provide flow to unit 2 and through check valve (15) to

unit 3 when braking. Another slight difference is with the flushing valve. During events when the enabling valve (18) is open and the HP accumulator is being used, pilot pressure shifts the flushing valve (14) so that oil entering Line B will go through the oil cooler (12) and either over the LP relief valve (13) to tank or charge the LP accumulator (7).

The following sections detail the different modes of operation for the blended hydraulic hybrid.

Hydrostatic Driving without HP Accumulator

As stated before when the enabling valve (18) is closed the blended hybrid works as a hydrostatic transmission. When starting Unit 2 and Unit 3 are both at 100% displacement, to begin moving, the engine spins Unit 1 and the displacement begins increasing and supplying flow to Line A. The check valve (15) opens in order for Line A and Line C to be connected. The flow form Unit 1 must be absorbed by Unit 2 and 3, this flow determines the speed of these Units, and the pressure builds up to meet the needed torque.

Driving With HP Accumulator

To use energy from the accumulator enabling valve (18) is moved to the open position, thus exposing Line C and therefore Unit 3 to the high pressure from the accumulator. If the pressure in Line C is greater than the pressure in Line A check valve (15) closes, preventing flow form Line C to Line A. Unit 3 is then able to release the stored energy of the accumulator to the wheels. This Unit is controlled in secondary control, meaning the displacement of Unit 3 is adjusted to either meet the torque or speed commanded by the user. Unit 2 can also provide power to the wheels by working as a hydrostatic transmission with Unit 1 as described in the section before, yet in this case, the pressure in Line A increase to meet the required wheel torque minus the torque provided by Unit 3. Thus power is blended between

a hydrostatic transmission and a parallel hybrid as long as the pressure in Line C is greater than that of Line A. If the pressure in Line C drops below the pressure in Line A than flow from Line A will enter Line C through check valve (15) and check valve (17) will close preventing flow from the accumulator, and the transmission again operates as a hydrostatic transmission.

Regenerative Braking

Just like a traditional hydrostatic transmission high pressure will switch from Line A and Line C to Line B during a braking event. The flow from Unit 2 and Unit 3 during braking has 2 different flow paths. First is that flow could go through Unit 1 which would then operate in motoring mode and help power parasitic losses. Flow could also be captured and reused at a later time in the HP accumulator. This occurs when the pressure in Line B increases above the pressure in the HP accumulator, at which point check valve (20) opens and allows high pressure flow from Unit 2 and Unit 3 into the accumulator. These units would then be controlled in secondary control and their displacement would be adjusted to meet the resistive torque demand at the wheels. In this case flow to Unit 2 and Unit 3 must come from the charge pump (4) and the LP accumulator (7) through check valve (8). Any excess flow from Unit 2 and Unit 3 that does not go into the HP accumulator or through Unit 1 would then go over relief valve (10) or Unit 2 and Unit 3 could go to a lower displacement and friction brakes will be needed to supplement the required breaking torque.

Reverse Operation

To drive in reverse, Unit 1 will go over center providing flow to Line B, because of check valves (15) and (17) Unit 3 will need to go to zero displacement and unit 2 will go to 100% displacement. HP relief valve (19) is needed for safety in case Unit 3 is not at zero displacement. The pressure in this line will increase in order to meet the required torque at the wheels, if this pressure is greater than the pressure in the

HP accumulator than check valve (20) will open and the Unit 1 must then charge the accumulator until the required pressure is met. When braking during reverse, the high pressure switches to Line A providing a resistive torque at the wheels. The flow from Units 2 can then be absorbed through Unit 1 to overcome parasitic losses or through HP relief valve (11) to either charge the LP accumulator or go through the LP relief valve (13). This reverse operation is required if Unit 2 and Unit 3 do not go over-center. If Unit 2 and Unit 3 are over-center units than to go in revers, the displacement of Unit 2 and 3 will go to -100% and the transmission would then be operated exactly as it is in forward operation. This is very useful, because regenerative braking would be realized in reverse operation, along with full power and speed during revers. Having this type of operation is very beneficial for off-highway and construction equipment.

2.2 Previous Research in the Blended Hydraulic Hybrid

As stated before the blended hydraulic hybrid was first invented and researched at the Maha Fluid Power Research Center by Sprengel & Ivantysynova (2012). In their first work they discussed different architectures that accomplished the same thing as the blended hybrid, this is done by using slightly different logical elements, they also surveyed existing transmissions that are similar to the blended hybrid. The researchers then compared the fuel consumption of the blended hydraulic hybrid to an automatic transmission, and a series hybrid for a class II pickup truck (Sprengel & Ivantysynova 2013*b*). An optimization tool called dynamic programming was used to optimally control each transmission over the UDDS cycle minimizing the fuel consumption. The results showed the blended hybrid achieving a fuel economy of 21.1 mpg, a 37% increase over the automatic transmission, while the series hybrid achieved 22.3 mpg, which was a 44.8% increase in fuel economy over the automatic transmission. Additionally a general control strategy was developed for the different operating modes of the blended hydraulic hybrid (Sprengel & Ivantysynova 2013*a*).

The blended hybrid is a continuously variable transmission, and therefore can act as the variating unit to more complex transmissions. Because of this researchers at Maha Fluid Power Research Center performed an energetic analysis of the power split transmission using the blended hybrid as the hydraulic path (Sprengel & Ivantysynova 2014*b*). This study again used the dynamic programming and the UDDS cycle to compare the blended hybrid power split transmission to a manual transmission, and a series hybrid power split transmission for a compact SUV with a diesel engine. This study showed that the manual transmission achieved 7.89 l/100 km, while the series hybrid power split transmission acheived 7.34 l/100 km, a 7.0% improvement in fuel economy over the manual transmission. The blended hybrid power split transmission simulated 7.28 l/100 km, which is 7.7% better fuel economy than the manual transmission and 0.8% better than the series hybrid power split transmission. One important note by these researchers is that sizing of the transmission plays a critical role in fuel consumption of each transmission. A similar study was also presented by these researchers in which they compared an automatic transmission, a manual transmission, a series hybrid transmission, a blended hybrid transmission, a series hybrid power split transmission, and a blended hybrid power split transmission (Sprengel & Ivantysynova 2014*c*). This again was done on a compact SUV using dynamic programming for the UDDS cycle. The results of this study are listed in the Table 2.1.

In an effort to verify simulation results and to test the top level control strategy that was developed, the same researchers then designed a hardware in the loop test rig for the blended hydraulic hybrid (Sprengel & Ivantysynova 2014*a*). This hardware in the loop test rig was designed to simulate a passenger vehicle. The transmission consisted of Sauer S90 42cc/rev for Unit 1, 2 and 3 with a 20 L accumulator. Electric motors were used to simulate the engine and the load on the axles. From this the researchers were able to validate the control strategy and prove physically the potential of the blended hybrid.

Table 2.1. Fuel economy and energy consumption of various transmissions Sprengel & Ivantysynova (2014*c*).

Transmission	**Fuel Economy [l/100 km]**	**Fuel Economy [mpg]**	**Engine Energy Generation [MJ]**
Automatic	9.01	26.11	11.14
Automatic (no lockup clutch)	11.37	20.68	13.37
Manual	8.12	28.96	9.38
Series Hybrid	8.09	29.07	11.28
Blended Hybrid	8.02	29.34	10.58
Series Hybrid PST	7.77	30.28	10.55
Blended Hybrid PST	7.68	30.64	9.28

2.3 The Four Wheel Drive Blended Hydraulic Hybrid

One of the goals of this work is to apply the blended hydraulic hybrid to a four wheel drive SUV replacing the conventional automatic transmission. In straight line driving there is no major difference between a four wheel drive transmission and a two wheel drive transmission, but during turning events there is a potential issue. Figure 2.3 shows that during a turning event all wheels follow a different radius of curvature, and therefore when turning each wheel spins at a different rate.

A conventional all time four wheel drive transmission is also depicted in Figure 2.3. To allow differences in speed between the left and right wheels every vehicle employs a front and rear differential, this allows the right and left wheels to spin at different speeds. Another other issues arises when both the front and rear axles are to be driven, during straight line driving the drive shafts rotate at the same speed, but during turning the rear wheels will turn at a different radius than the front wheels. To correct this, an all time four wheel drive vehicle will have a transfer case that couples the transmission output to both the front and rear axles and allows the two axles to

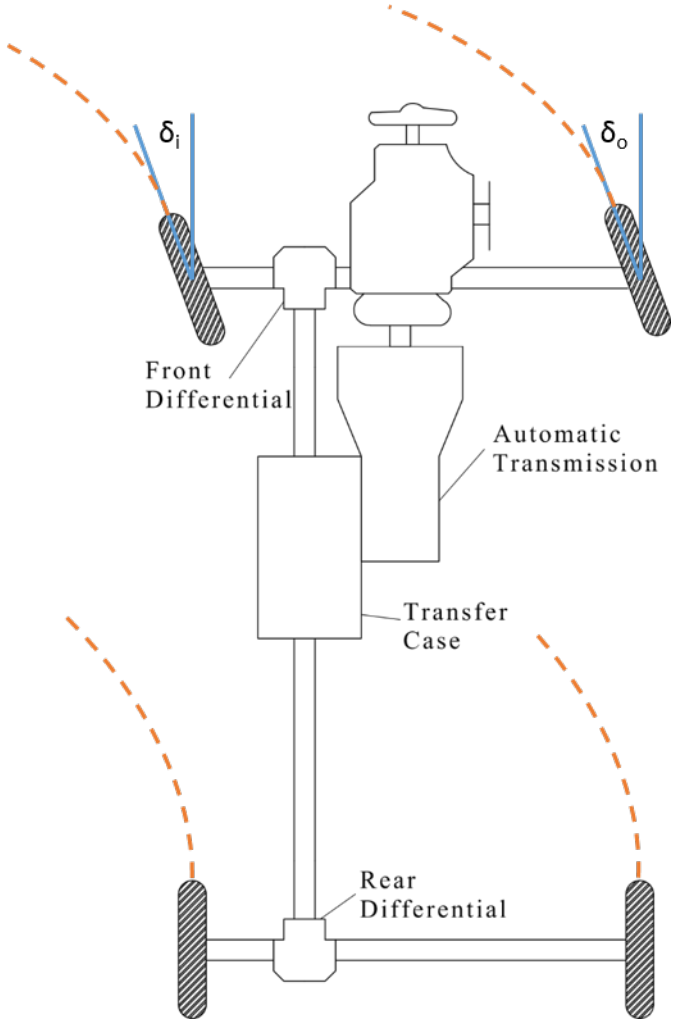

Figure 2.3. Individual wheel turning radius.

spin at different rates. For vehicles that are not all time four wheel drive the two axles are usually rigidly connected when four wheel drive is needed, but this should only be done on low friction surfaces. If done on concrete or asphalt the difference in wheel speeds between the front and rear will cause the vehicle to hop, increase tire wear, and potentially damage the transmission.

2.3.1 Four Wheel Drive Architecture

Often for hydraulic transmissions a transfer case or differential is used to couple the hydraulic motor to both the front and rear axles. For this thesis limited space is available in retrofitting an existing vehicle, especially if the existing transfer case was to be used. Likewise it is beneficial if the proposed blended hybrid transmission is capable of requiring less parts, making it both cheaper and lighter, and still provide the same four wheel drive benefits of the original automatic transmission. For these reasons one goal of this project is to modify the blended hybrid system architecture to have all time four wheel drive without the use of a transfer case.

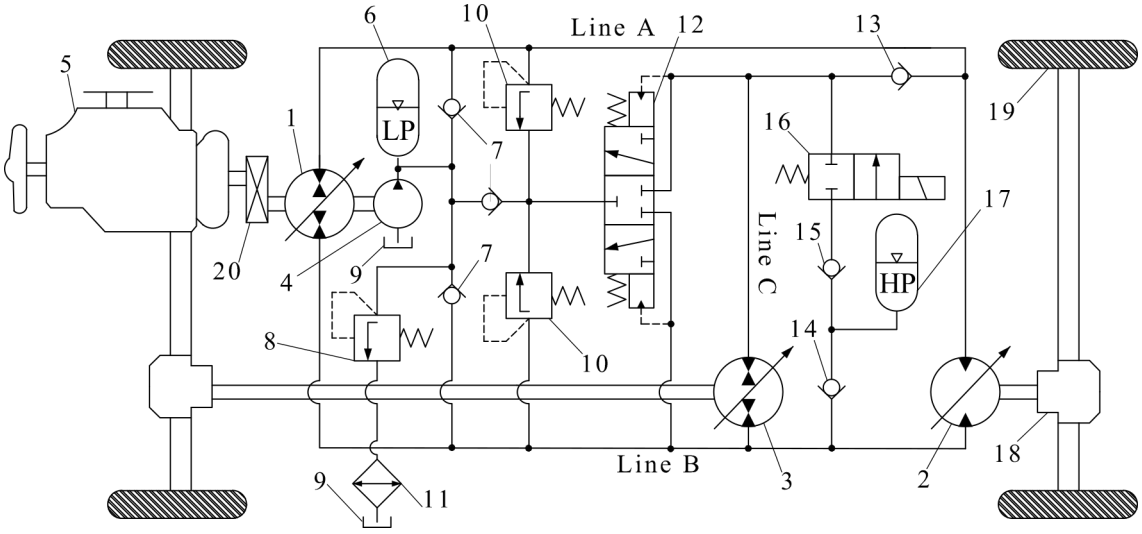

1. Unit 1
2. Unit 2
3. Unit 3
4. Charge Pump
5. Combustion Engine
6. LP Accumulator
7. LP Check Valve
8. LP Relief Valve
9. Tank
10. HP Relief Valve
11. Oil Cooler
12. Flushing Valve
13. Check Valve
14. Check Valve
15. Check Valve
16. Enabling Valve
17. HP Accumulator
18. Axle
19. Wheels
20. Gear Box

Figure 2.4. Four wheel drive blended hydraulic hybrid circuit.

Figure 2.4 shows the four wheel drive blended hybrid circuit. This circuit has slight modifications to the circuit seen in Figure 2.2. Notice that in this design Unit 2 and Unit 3 are not coupled together on the same shaft. In this design Unit 2 is coupled to the rear axle while unit 3 is couple to the front axle. These two units are hydraulic linked in parallel, meaning the flow through each unit is independent of the other. Thus in this configuration the rear axle will always be driven as a HST, and front axle will be driven as a HST when the enabling valve (16) is closed. When the enabling valve is open and the pressure in the HP accumulator is greater than the pressure in Line A than the front axle will be driven is secondary control with flow coming from the accumulator.

2.3.2 Derivation and Simulation of Four Wheel Drive Turning

To ensure that this design is feasible a simulation was needed to help prove the concept. In order to do this a kinematic model was created to find the different axle speeds during a turning event. This kinematic model is shown in Figure 2.5. This model assumes that our vehicle has Ackermann steering geometry for all steering inputs. As seen in the figure this arrangement ensures that when turning all tires rotate around the same point, this ensures a no slip situation. Though our vehicle does not have Ackermann steering at all points, most vehicles have a steering arrangement that is close to Ackermann and therefore this assumption is valid in order make a model for the four wheel drive blended hybrid during a turning event.

In Figure 2.5 δ_i and δ_o indicate the steering input of the inner and outer front wheels respectively. O is the origin that all the wheels are rotating about, l is the distance between the front and rear axle, while a is the distance of the center of gravity from the rear axle. Lastly R_1 is the distance from the origin to the center of the vehicle, and W is the width of the vehicle.

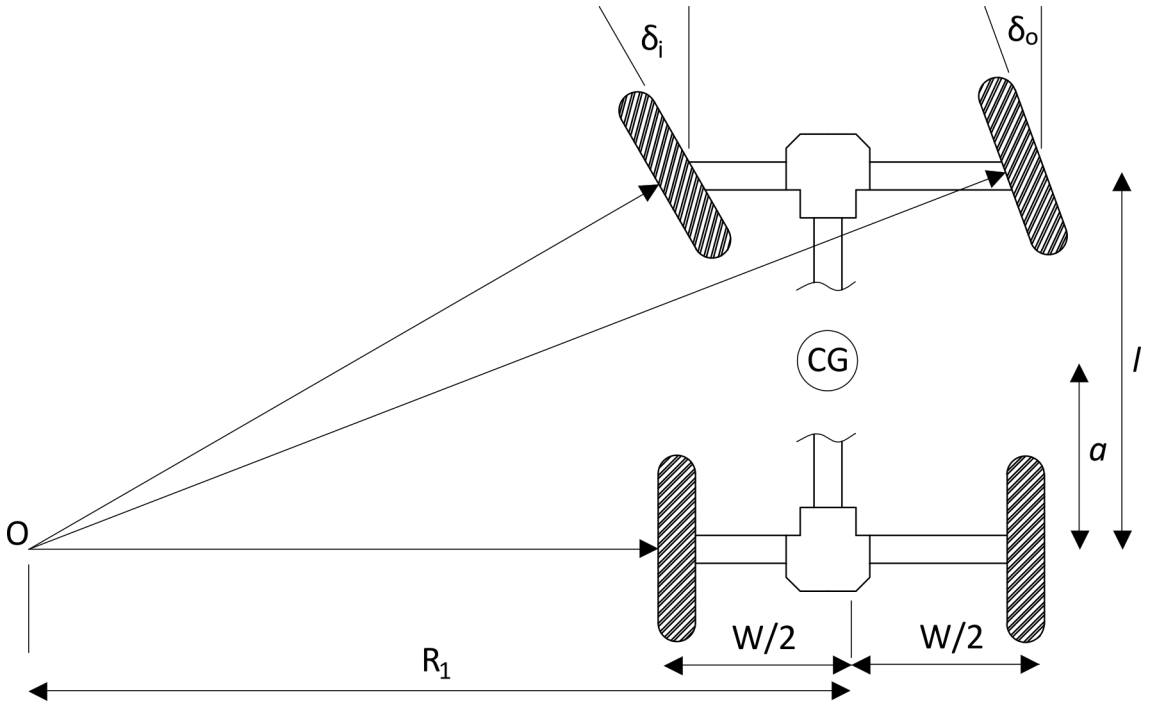

Figure 2.5. Ackermann steering geometry.

From this figure we know the following:

$$tan(\delta_i) = \frac{l}{R_1 - \frac{w}{2}}$$
$$tan(\delta_o) = \frac{l}{R_1 + \frac{w}{2}}$$

Combining these equations we can solve for R_1:

$$R_1 = \frac{l}{tan(\delta_i)} + \frac{w}{2} = \frac{l}{tan(\delta_i)} - \frac{w}{2}$$

$$\frac{w}{l} = cot(\delta_o) - cot(\delta_i) \tag{2.1}$$

Equation (2.1) shows the simple relationship needed to meet Ackermann steering. To simplify our model development, the four wheel Ackermann model can be condensed to what is termed the bicycle model as seen in Figure 2.6. The bicycle model simply averages the steering input of δ_i and δ_o into δ, and places the wheels at the center of the vehicle as seen in Figure 2.6.

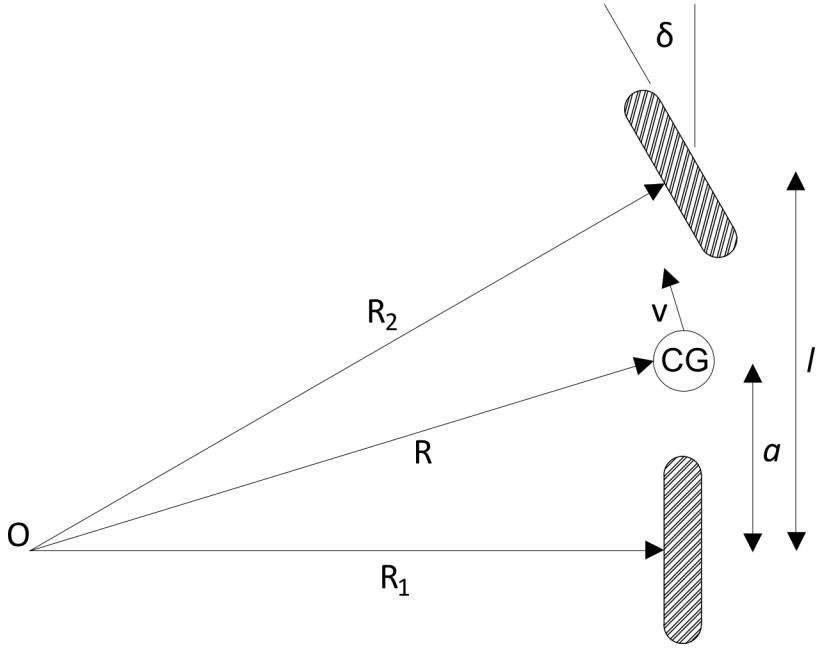

Figure 2.6. Ackermann steering: bicycle model.

We will define the vehicles turning radius as R, which is perpendicular to the velocity vector located at the center of gravity. Using this model the following characteristics are obtained:

$$R^2 = a^2 + R_1^2$$

$$cot(\delta) = \frac{R_1}{l} = \frac{cot(\delta_i) + cot(\delta_o)}{2}$$

$$R = \sqrt{a^2 + l^2 cot^2(\delta)} \tag{2.2}$$

From this we can find the turning radius of the front axle (R_2)and the turning radius of the rear axle (R_1) in terms of the steering input and basic vehicle dimensions.

$$R_1 = \sqrt{R^2 - a^2}$$

Substitute in Equation (2.2):

$$R_1 = \sqrt{a^2 + l^2 cot^2(\delta) - a^2}$$

$$R_1 = l cot(\delta) \tag{2.3}$$

$$R_2 = \sqrt{R_1^2 + l^2}$$

$$R_2 = \sqrt{l^2 cot^2(\delta) + l^2}$$

$$R_2 = l\sqrt{l + cot^2(\delta)} \tag{2.4}$$

If we neglect slip at the wheels and assume rigid body mechanics it is possible to determine the relative velocity of the front and rear axles using the velocity at the center of gravity of the vehicle:

$$\dot{\theta} = \frac{v_{veh}}{R} = \frac{v_{front}}{R_2} = \frac{v_{rear}}{R_1}$$

Therefore:

$$v_{front} = \frac{v_{veh} l\sqrt{l + cot^2(\delta)}}{\sqrt{a^2 + l^2 cot^2(\delta)}} \tag{2.5}$$

$$v_{rear} = \frac{v_{veh} l cot(\delta)}{\sqrt{a^2 + l^2 cot^2(\delta)}} \tag{2.6}$$

This model is very useful because of its simplicity. The velocity of both the front and rear axle is simply the function of the current velocity at the center of gravity and the steering input

To further verify that the blended hybrid in a four wheel drive circuit will operate successfully during turning events the relationships in Equations (2.5) and (2.6) were incorporated into a dynamic model of the blended hydraulic hybrid. To model the vehicle dynamics, the torque from the front and rear axle result in a force acting at the center of gravity, this force acts of the vehicle to either accelerate or decelerate. The resulting speed of the vehicle is what determines the speed of the hydraulic units, this speed combined with the unit displacement determines the flow. In a conventional blended hybrid circuit, when both Unit 2 and Unit 3 are coupled to the same shaft, the vehicle speed determines the speed of both units. When simulating the four wheel drive blended hybrid in a turning event, the current vehicle speed and steering input are used to determine the speed of Unit 2 and Unit 3. Figure 2.7 shows the results of this simulation.

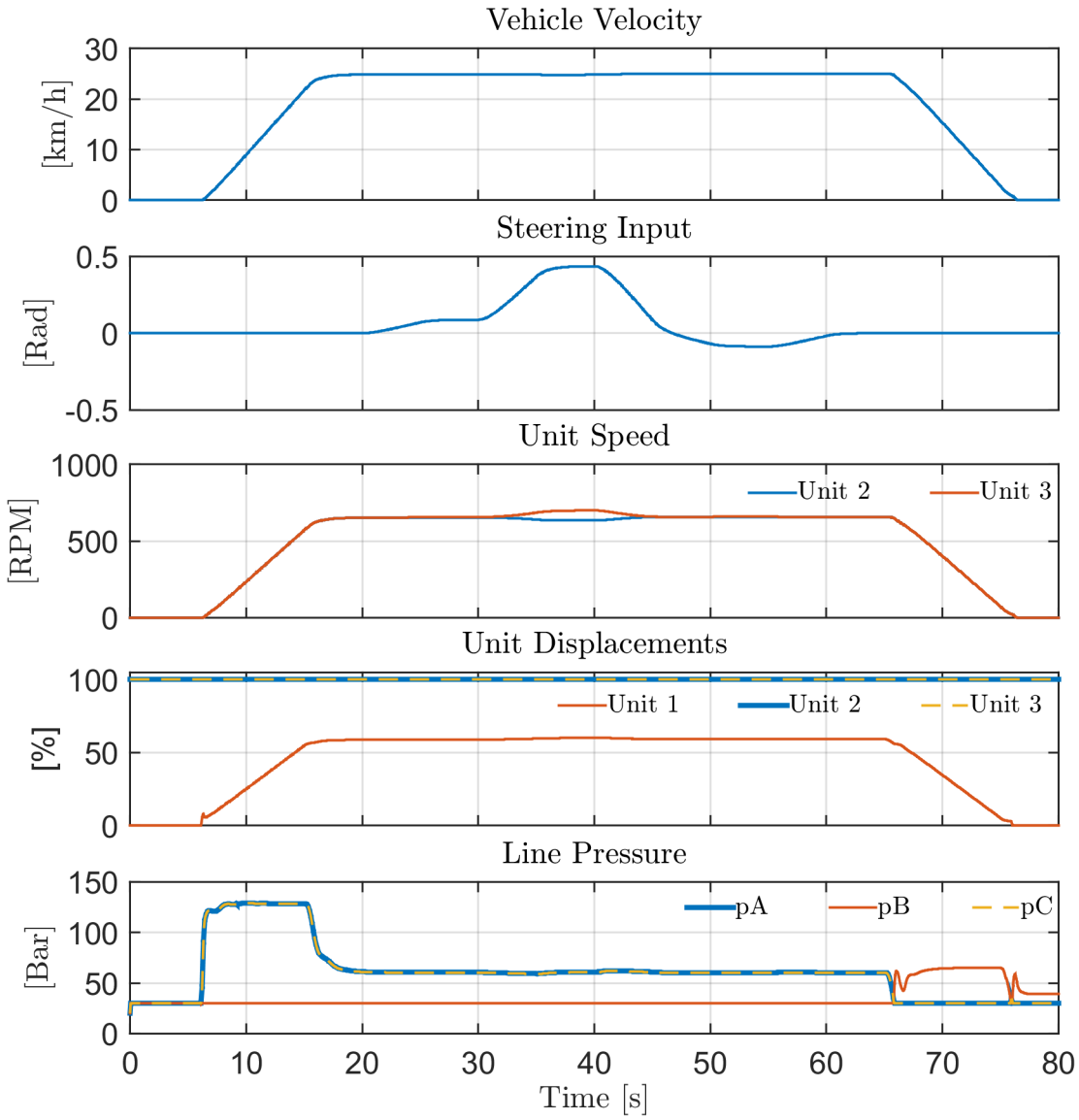

Figure 2.7. Simulation of the four wheel drive blended hybrid during a turning event.

For this simulation the application was an SUV with a wheel base (l) of 3 m and the distance of the rear axle to the center of gravity to the vehicle (a) of 1.5 m. As can be seen in the figure the transmission was operated in hydrostatic mode and accelerated to 25 km/h, while maintaining this speed, both Units 2 and 3 were held

at a constant displacement. During this time a series of steering inputs were applied to the vehicle, in both the left and right direction. As can be seen in the results when turning sharply there is a significant difference in the speed of Unit 2 and Unit 3. This simulation does verify that the speed was able to be maintained during the turning event. There is a slight disturbance to the pressure during the turning event due to the nonlinear efficiencies of the hydraulic units. The promising results of this simulation though is that none of the controls needed to be changed from normal straight line driving. Thus, this simulation verifies that the four wheel drive blended hybrid circuit is capable of driving in all time four wheel drive during turning events, and that the parallel arrangement of units 2 and 3 allow this transmission to be controlled uniformly during both straight line driving, when units 2 and 3 have the same speed, and during turning events when units 2 and 3 are spinning at different speeds. An important note though, is if the speed of each unit was being controlled than special care would need to be taken during a turning event.

3. APPLICATION VEHICLE

3.1 Vehicle Parameters

For this work the reference vehicle is a 1999 Range Rover 4.0 SE, built by Land Rover. This vehicle, seen in Figure 3.1, was donated to the Maha Fluid Power Research Center by a third party. The donated vehicle has a 4.0 liter, V-8 engine with an automatic transmission and all time four wheel drive. Table 3.1 and Table 3.2 shows the known vehicle parameters and gear ratios of the conventional four speed transmission for this vehicle. The automatic transmission has a lockup clutch on the torque converter and the reported fuel consumption is 12 mpg city and 15 mgp on highway U.S. Department of Energy (2015).

Figure 3.1. Application vehicle: 1999 Range Rover 4.0 SE.

This work consists of two main parts. First, developing and applying on the blended hybrid a new methodology for sizing hybrid transmissions, which utilizes optimal control for efficiency and dynamic simulation for performance. The second focus of this work, consists of removing the current automatic transmission form the Range Rover and installing and testing a blended hydraulic hybrid transmission on the vehicle.

Table 3.1. Range Rover 4.0 SE parameters.

Parameter	**Unit**	**Symbol**	**Value**
Curb Mass	kg	m_{curb}	2170
Gross Mass	kg	m_{gross}	2780
Max Power	kW	P_{engmax}	142 @ 4750 RPM
Max Torque	Nm	M_{engmax}	320 @ 2600 RPM
Rolling Radius	m	r_r	0.358
Frontal Area	m	A_f	2.78

Tables 3.1 and 3.2 shows the vehicle parameters supplied by the manufacturer. These parameters are needed for all aspects of this work including sizing, modeling and control. Other parameters such as aerodynamic drag, rolling resistance and the engine torque curve were not provided and for this reason were derived empirically.

Table 3.2. Range Rover 4.0 SE gear ratios.

Gear	Gear Ratio: High	Overall Ratio
1st	2.480:1	10.67:1
2nd	1.480:1	6.37:1
3rd	1:1	4.30:1
4th	0.728:1	3.13:1
Reverse	0.086:1	3.13:1
Transfer High	1.22:1	-
Transfer Low	3.27:1	-
Axle	3.54:1	-

3.2 Engine Torque Curve

This vehicle has a 4.0 liter V8 gasoline engine. No information or models of this engine have been published. In order to move forward with sizing the transmission a model of the torque and power of the engine was needed. To do this properly the engine would be removed and mounted to a dynamometer and torque would be measured over the entire engine speed range at maximum throttle. This empirical method is costly and time consuming. This section overviews how a approximation of the torque curve was developed that met both the time and budget constraints for this project.

Instead of using an engine dynamometer to extract torque data on the engine an inertia chassis dynamometer capable of measuring power of a four wheel drive vehicle was used, this can be seen in Figure 3.2. This type of dynamometer uses the known inertia of the drums under the front and rear axles to determine the power output to the wheels. It is usually used for racing to determine how changes to the power train and engine effect the power output throughout acceleration. Two different runs were recored, each run started at a low speed and then a full throttle input was given to

Figure 3.2. Four wheel drive inertial dynamometer testing of the 1999 Range Rover 4.0 SE.

the engine. The engine speed and vehicle speed were recored. The acceleration and inertia of the drums were used to calculate the output power. Figure 3.3 details the results of these two runs.

Figure 3.3(a) shows the engine speed as the vehicle accelerates on the dynamometer, notice that the transmission went from 2nd to 4th gear during each run. Figure 3.3(b) shows the power output to the wheels, Figure 3.3(c) shows the overall gear ratio, meaning the engine speed divided by the wheel speed throughout the run. Notice in this figure the second order nature of the overall gear ratio at the beginning of each gear. This second order response is due to the torque converter. The torque converter allows slip between the engine and the transmission during acceleration, but when the lock up clutch engages the ratio becomes fixed. The lockup clutch engaging also causes the large spikes in power and calculated torque seen in Figure 3.3(d). Because of the non-consistent gear ratio and low efficiencies when the torque converter is not

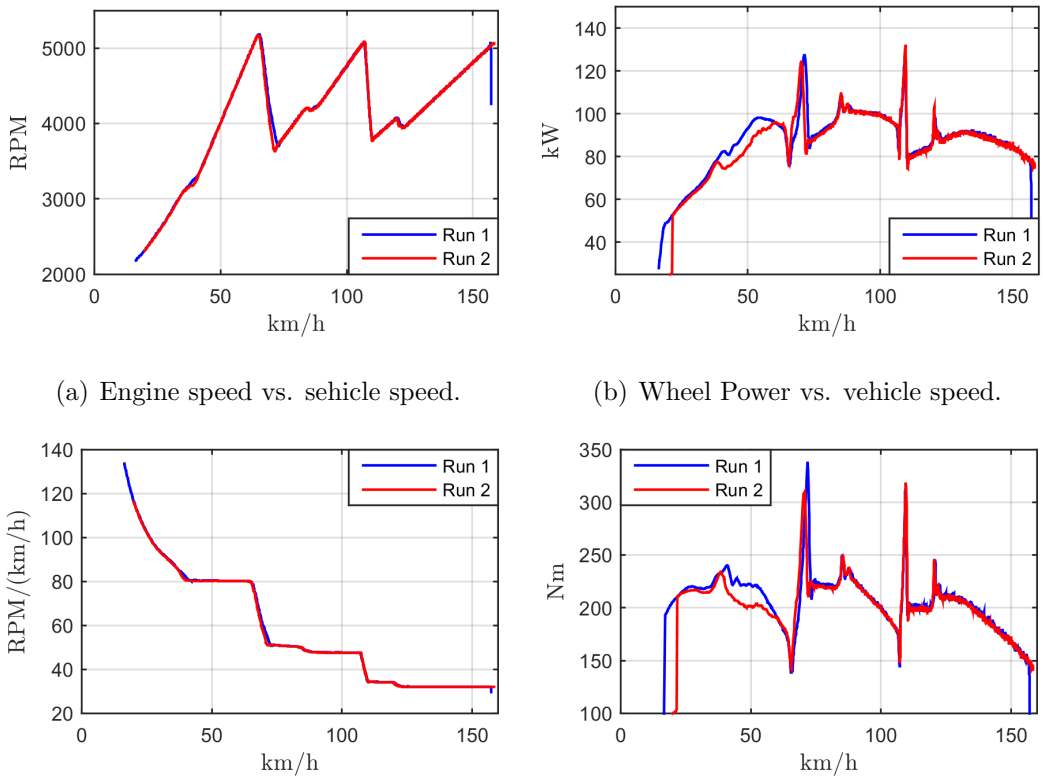

(a) Engine speed vs. sehicle speed.

(b) Wheel Power vs. vehicle speed.

(c) Overall gear ratio vs. vehicle speed.

(d) Torque vs. vehicle speed.

Figure 3.3. Inertial dynamometer testing results.

locked up, the only data that is useful for developing the power and torque curve is during the times when the lock up clutch is activated, forcing the gear ratio to be constant.

With the information from the dynamometer test the power was able to be scaled due to the efficiency of the transmission. A power curve was then able to be extrapolated from this data and the power points provided by the manufacture. With this power curve a representative torque curve was also created. The torque and power curve are shown in Figure 3.4.

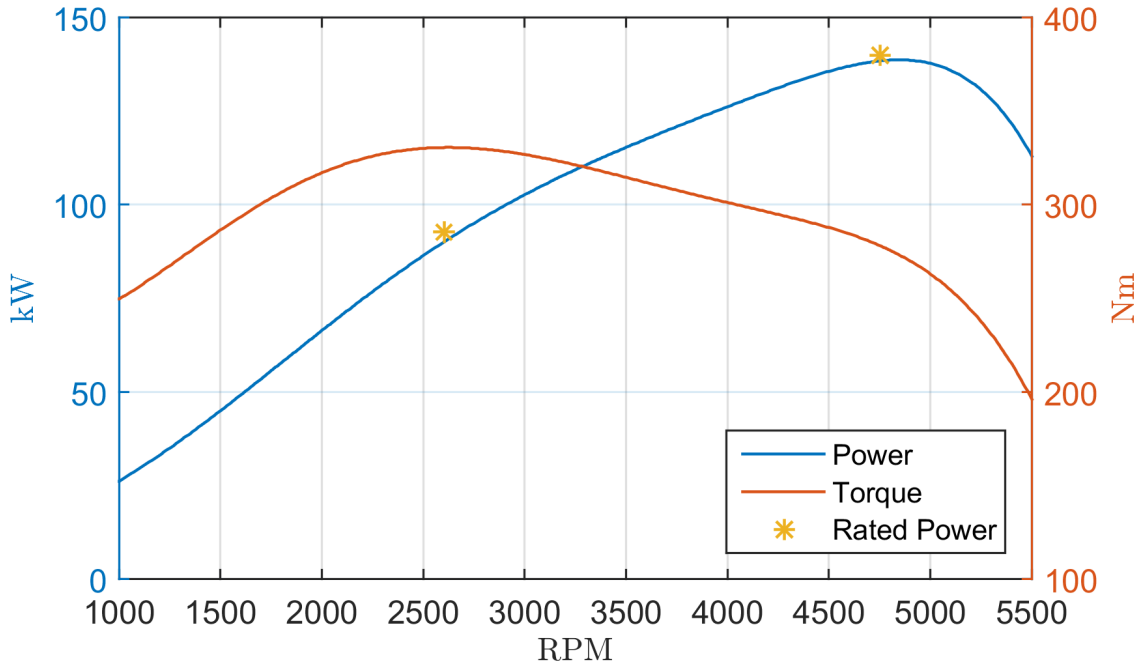

Figure 3.4. Range rover 4.0 SE torque and power curve.

3.2.1 Engine Fuel Map

In addition to the torque curve, a fuel map of the engine is used to better determine fuel consumption in the simulation environment. In this work a representative fuel map is necessary for optimizing controls that minimize fuel consumption. Figure 3.5 shows the BSFC map that was used for the Range Rover, the BSFC map indicates the amount power generated by the engine for a given amount of fuel.

Similar to the torque curve, the fuel map and BSFC map where not provided for this work. In order to obtain an approximate fuel map an assumption was made that all gasoline engines have similar trends in their BSFC maps, with this assumption a BSFC map was scaled from a different engine to match the power of the Range Rover. The reason this approach is appropriate for this work is because only the trends in the fuel map are needed for optimizing control strategies, the goal of this work is not to accurately predict fuel consumption.

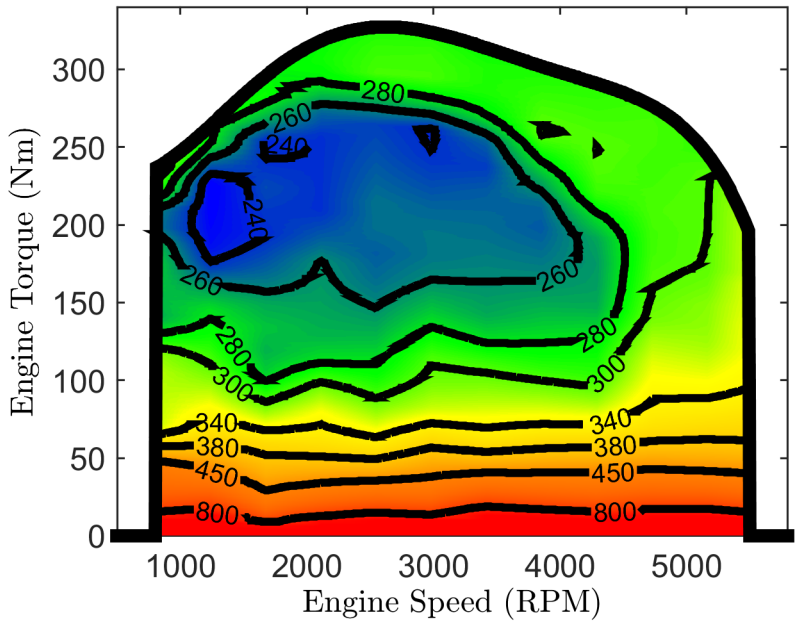

Figure 3.5. Range rover BSFC map (kW-h/g).

3.3 Drag and Rolling Resistance

Other important values that are needed for sizing and simulation are the resistive forces that act on the vehicle. Figure 3.6 shows a free body diagram of the range rover. The resulting propulsion force in the x direction is as follows:

$$F_x = F_{xr} + F_{xf} - F_g - F_D - F_{rr} - F_{rf} \tag{3.1}$$

Where F_{xr} and F_{xf} are the resulting forces from the torque supplied from the engine through the transmission. Because the transfer case provides a 50/50 torque split between front and rear axles, F_{xr} and F_{xf} are equal. The weight of the vehicle results in a force, F_g due to the grade, θ, thus:

$$F_g = W sin(\theta) \tag{3.2}$$

The rolling resistance on the front axle is combined with the rolling resistance on the rear axle, thus the total rolling resistance is:

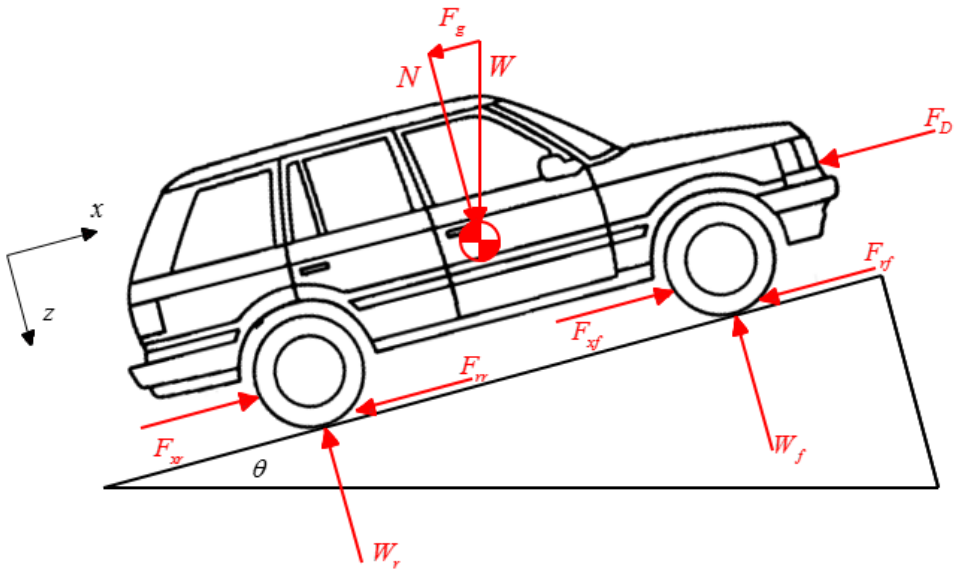

Figure 3.6. Free body diagram of the Range Rover.

$$F_r = F_{rr} + F_{rf} = W cos(\theta) C_r \tag{3.3}$$

Where C_r is the coefficient of rolling resistance. The aerodynamic drag, F_D, is:

$$F_D = \frac{1}{2} \rho A_f C_d \nu^2 \tag{3.4}$$

Where A_f is the frontal area, ν is the vehicle velocity and C_d is the coefficient of aerodynamic drag.

The equations above are used to develop a model and size the transmission, all of the parameters are known except C_d, the coefficient of aerodynamic drag, and C_r the coefficient of rolling resistance. These values where obtained empirically.

Figure 3.7 shows three different coast down test that were performed with the vehicle. To do this the vehicle was brought to approximately 110 km/h on a straight flat road. At this point the transmission was put into neutral to decreases losses due to the gear train, and eliminate churning losses in the torque converter. The vehicle was then allowed to coast down. As can be seen in the figure the results were very repeatable.

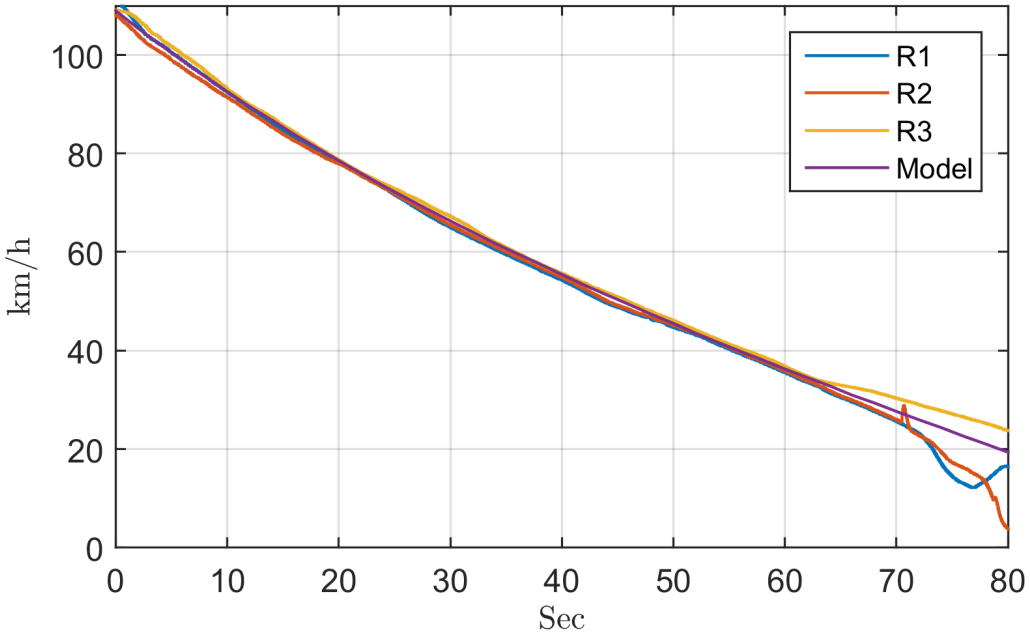

Figure 3.7. Rolling resistance and aerodynamic drag model validation.

A hill in the road occurred around 60 seconds, therefore coasting ended around 35 km/h. A vehicle model was developed using the equations discussed before and the values of C_d and C_r where tuned so the vehicle model matched the coast down of the measured results. Figure 3.7 shows the excellent correlation with a vehicle model that has drag and rolling resistance parameters equal to those found in Table 3.3.

Table 3.3. Rolling resistance and aerodynamic drag parameters.

Parameter	**Symbol**	**Value**
Rolling Resistance	C_R	0.022
Aerodynamic Drag	C_D	0.4

3.4 Baseline Measurements

In addition to determining coefficients needed for sizing and simulation additional measurements where taken in order to determine baseline fuel consumption for a given cycle and maximum performance.

3.4.1 Fuel Consumption

The application vehicle was retrofitted with a removable fuel tank that is discussed in Chapter 6. The weight of the fuel tank was measured at the beginning and the end of each cycle to measure the total fuel consumed.

Though this approach is far from being completely robust, seven different drive cycles were created with varying degrees of city type driving with lots of stop and go, and highway driving with a steady high speed. Table 3.4 shows the results of these drive cycles that were each performed at least three times.

Table 3.4. Fuel consumption measurement results.

Cycle	**Length (km)**	**Average MPG**	**Std. Dev.**
Route 1	7.48	13.86	0.95
Route 2	11.50	16.13	1.64
Route 3	8.54	11.29	1.65
Route 4	14.25	10.51	3.11
Route 5	23.58	9.52	1.06
Route 6	1.72	5.79	0.17
Route 7	3.65	7.35	0.96

As can be seen depending on the drive cycle there is large variation in fuel consumption. Appendix A shows maps, velocity profiles and results for each of the test runs.

3.4.2 Performance

In addition to fuel consumption one goal of this project is to develop a blended hybrid transmission that is able to perform similarly to the baseline vehicle.

To do this acceleration runs were performed on a flat straight road. The vehicle started at zero velocity and then was given a wide open throttle input and allowed to accelerate to approximately 130 km/h. These results were compared to a simulated performance run produced by a third party (Automobile Catalog 2015). Figure 3.8 shows the results of these performance runs.

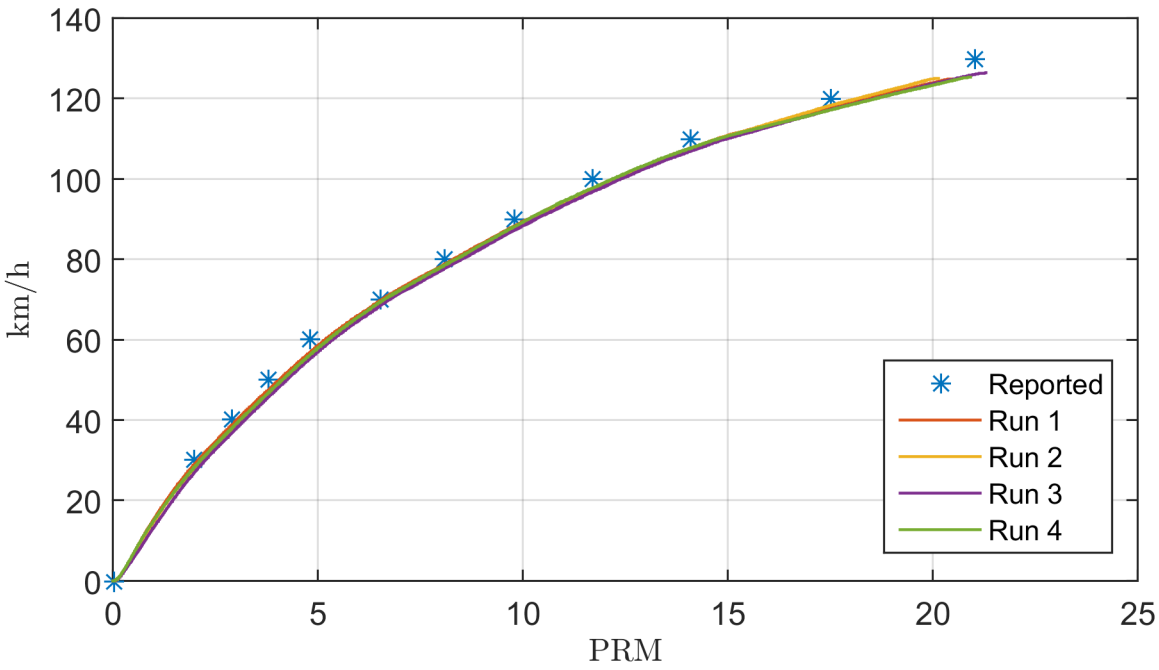

Figure 3.8. Measured and reported acceleration.

As can be seen the performance runs match nicely with the simulated performance. likewise the four acceleration runs had good repeatability.

4. SYSTEM MODELING AND STATIC SIZING FOR THE BLENDED HYDRAULIC HYBRID

4.1 Component Description and Static Sizing

Chapter 2 provides an overview of how the blended hybrid operates. This chapter focuses on the physics of the individual components that make up the blended hydraulic hybrid and from this understanding each component can be sized accordingly and the physical equations can be used to simulate the system.

In general the main components of the blended hybrid power train are the engine, hydrualic units, 2 and 3, the gearing between unit 1 and the engine, the gearing between unit 2 and 3 and the wheels, and the high pressure accumulator. The goal of this project is to size the transmission for a Range Rover, and therefore throughout this work the size and properties of the engine will be assumed to be the same as the Range Rover engine discussed in Chapter 3.

Figure 4.1 shows the overall static sizing approach for the blended hybrid. From this, vehicle parameters and performance requirements are used to first size unit 2 and 3 and then size unit 1, the same parameters and performance metrics are used in sizing the accumulator.

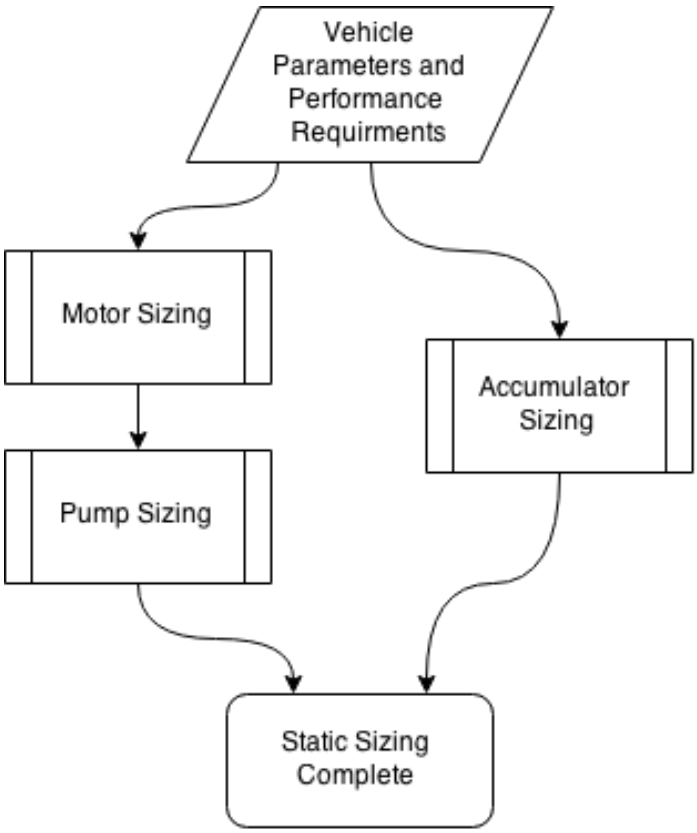

Figure 4.1. Static sizing flow chart.

4.1.1 Hydraulic Pump and Motor

The hydrualic unit is the basis of a hydraulic transmission. These units are the main energy converters. The pump converts the mechanical power (torque and speed) of the engine into fluid power (flow under pressure). Motors act in the opposite manner, converting fluid into mechanical power, thus taking pressurized fluid and transforming it into torque and speed on a shaft. Hydraulic pumps and motors consist of identical hardware, and therefore a hydraulic unit pumps when work is being done on the fluid and motors when the fluid is doing the work. In hydraulic systems the role of pumping and motoring can be switch back and forth often. Though there are many types of pumps and motors that can move hydraulic fluid, for this work only axial piston machines will be considered. These types of hydraulic units are

chosen for this work because of their ability to operate at high pressures and speeds with relatively high efficiencies. The following equations define the theoretical torque, M_{theo} and theoretical flow, Q_{theo}:

$$M_{theo} = \beta \frac{\Delta p V_i}{2\pi} \tag{4.1}$$

$$Q_{theo} = \beta \frac{w V_i}{2\pi} \tag{4.2}$$

The theoretical torque is governed by the difference in pressure between the high and low pressure port, Δp, and the derived displacement, V_i, of the hydraulic unit and the percent of total displacement, β. The flow on the other hand is depended on the speed of the unit, w, the derived displacement, V_i, and the percent of total displacement, β.

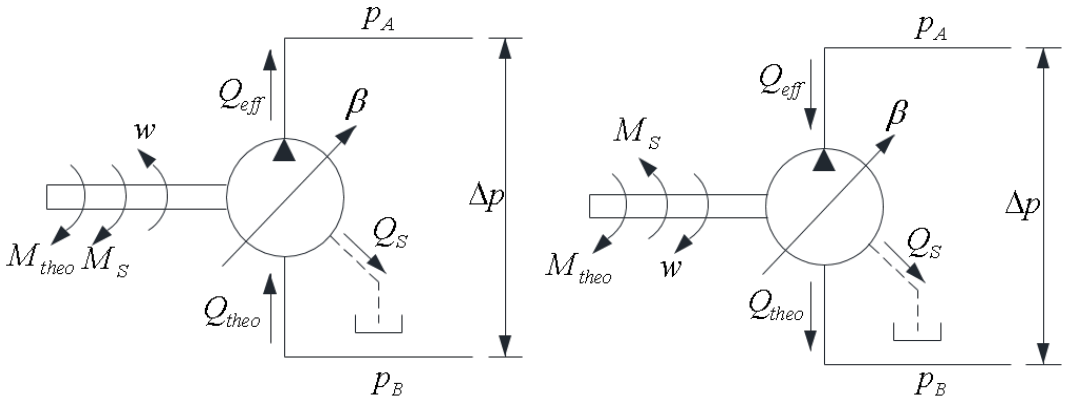

(a) Pump schematic.

(b) Motor schematic.

Figure 4.2. Hydraulic pump and motor schematics.

To improve the use of the theoretical equations for the pump and motors, empirically obtained torque and volumetric losses are used to find the effective torque and flow of a hydraulic unit. The torque and volumetric losses are obtained by mounting the hydraulic unit of interest to a test rig that is has been instrumented to capture

speed, torque, flows, temperatures and pressures. The hydraulic unit is then ran at many different speed, pressure and displacement points and the steady state torque and volumetric losses are recorded. With this data a polynomial model is then used to describe the losses at all points of operation. Thus the effective torque and flow are given by the following equations:

Pumping:

$$M_{eff} = M_{theo} + M_s = \beta \frac{\Delta p V_i}{2\pi} + f_M(\omega, \Delta p, \beta) \tag{4.3}$$

$$Q_{eff} = Q_{theo} - Q_s = \beta \frac{w V_i}{2\pi} - f_q(\omega, \Delta p, \beta) \tag{4.4}$$

Motoring:

$$M_{eff} = M_{theo} - M_s = \beta \frac{\Delta p V_i}{2\pi} - f_M(\omega, \Delta p, \beta) \tag{4.5}$$

$$Q_{eff} = Q_{theo} + Q_s = \beta \frac{w V_i}{2\pi} + f_q(\omega, \Delta p, \beta) \tag{4.6}$$

Though these equations are needed for creating high fidelity simulation models that will be used for this work, for static sizing a simpler approach is taken. The efficiencies for both flow and torque will be approximated when statically sizing each unit.

Unit 2 and Unit 3 Sizing

When sizing the blended hybrid it is important to first start with sizing unit 2 and unit 3. Unit 2 and 3 are the only power source to the wheels. Because of this unit 2 and 3 must be sized in order to meet all the power requirements, torque requirements, and the top speed of the vehicle.

For the blended hydraulic hybrid, units 2 and 3 use pressurized fluid coming from either unit 1 or the HP accumulator and convert that pressurized fluid to power at the wheels. Because the original vehicle has a 50/50 torque split, meaning that the front and rear axles provide the same amount of torque, therefore for this work unit

2 and 3 will be constrained to being the same size. In operation this allows the most conveinient way to accomplish a 50/50 torque split.

Figure 4.3 shows a general flow chart for sizing units 2 and 3 which can be done at the same time. It begins by considering the power requirements at the wheel. From the power requirements a unit size can be chosen, this is don't by looking at catalog data to find hydraulic units that have the torque and speed to meet the required power requirements at the wheel. With a chosen unit 2 and 3 from the catalog, an axle ratio is determined. This axle ration includes any gear box after unit 2 and 3, the differential and the axles. The axle ratio is sized so that the hydraulic unit is capable of meeting the maximum vehicle speed requirement. With this axle ratio and maximum torque of the chose hydrualic unit the maximum tractive force is calculated, if the combination does not meet the required torque than the hydraulic unit is too small, if the hydraulic unit exceeds the maximum torque requirement than the hydraulic unit is too large. This is an iterative process until the appropriately sized unit is chosen. Throughout this process appropriate unit efficiencies and gear efficiencies are used so the unit is not undersized unintentional.

For this project a slightly different approach was taken. The goal for this work is to design a blended hybrid transmission that can be retrofitted onto an existing Range Rover. As such designing a gear box and differential to suit our needs would be beyond the scope of this work, therefore in sizing for the Range Rover it was assumed the units 2 and 3 would be mechanically connected to the wheels through the existing drive shafts and therefore the existing axle ratio would be the axle ratio of 3.54:1. Likewise to design a vehicle with similar performance units 2 and 3 must provide a maximum torque equal to the maximum torque of conventional transmission in normal operation. This is seen in first gear, at the maximum torque of the engine.

Using this sizing approach resulted in approximately 81 cc/rev for both unit 2 and unit 3, using catalog data the closest size is a 75 cc/rev or a 100 cc/rev unit. To meet the torque demand at all points it would be required to go to the next sized unit and use a 100 cc/rev unit. Because this is work is for a prototype vehicle the

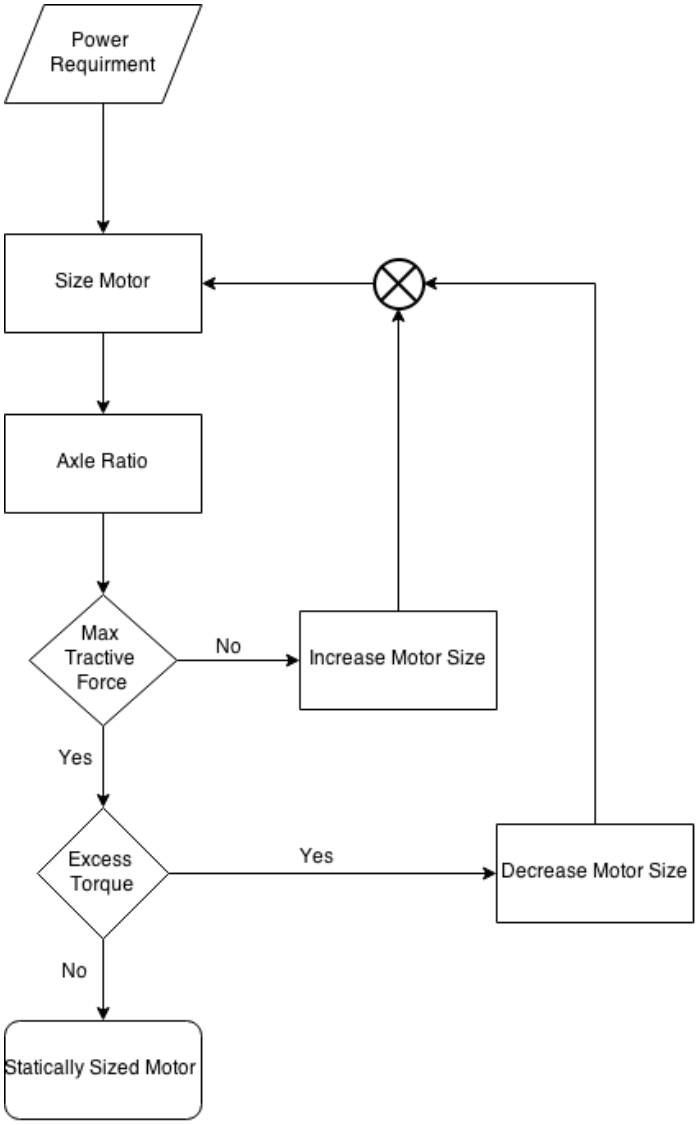

Figure 4.3. Static sizing flow chart.

top speed is of less concern than if this was for production. Using a 100 cc/rev unit would limit the top speed to 137 km/h (85 mph), while a 75 cc/rev unit would allow nearly 153 km/h (95 mph).

Unit 1 Sizing

There are a few different approaches to sizing unit 1 and the associated gear between the engine and the primary unit. It is important to remember that unit 1 is the first energy converter in the transmission. Thus it plays a vital role in the performance and fuel consumption of the vehicle. Larger units tend to have higher torque and volumetric losses, therefore it is common practice to size unit 1 to be the smallest unit that fills the requirements of the designer.

One approach is to size the hydraulic unit and gear to provide the required flow to unit 2 and unit 3 at maximum speed. The problem with this approach though is that the required flow is often difficult to approximate, usually this is done by calculating the required displacement to maintain max vehicle speed at maximum pressure. Unit 1 and gear i_1, would then be sized to meet this flow. This approach results in the smallest possible unit 1. Sizing this way often leads to a unit 1 not being able to meet the maximum torque of the engine, thus limiting the operation of the engine. Using this approach for the Range Rover resulted in a 52 cc/rev hydraulic unit.

A more robust approach is to size the hydraulic unit and gear to fully load the engine at maximum pressure. This results in the following equation:

$$V_1 = \frac{2\pi i_1 M_{engmax}}{\Delta p} \tag{4.7}$$

The following must be true to obtain all available engine power:

$$i_1 \omega_{1,maxspeed} > \omega_{eng,maxpower} \tag{4.8}$$

In this approach a gear, i_1, is first chosen and then a required unit 1 displacement is determined. Following this Equation (4.8) is checked to ensure that maximum engine power is obtainable. This approach allows all the power from the engine to be extracted by unit 1 and converted into fluid power. For the blended hydraulic hybrid a gear box with a ratio of 1.48:1 was used. Though there exist hydraulic units that could load the engine without a gear box, the use of the gear box allows the units to

operate at a slower speed which minimizes noise that is prevalent in these machines. For the range rover this results in a 73 cc/rev unit, therefore a commercially available 75 cc/rev unit will be selected for the statically sized unit 1 for the blended hydraulic hybrid.

4.1.2 Hydro-Pneumatic Accumulator

The hydro-pneumatic accumulator is the device that turns a hydrostatic transmission into a hydraulic hybrid. Its sole purpose for the blended hybrid is to store and release brake energy. This energy storage is critical, it aids the engine during high power propulsion events (load leveling), and stores kinetic energy that has been converted to pressurized fluid by units 2 and 3 (regenerative braking). In a series hybrid the accumulator increases the capacitance of the high pressure line, thus allowing more options in powertrain optimization, for the blended hybrid the accumulator is used similar to a parallel hybrid and therefore does not increase the capacitance of line A. As a result all engine power must be used immediately by the transmission, and cannot be stored for use at a later time.

A hydro-pneumatic accumulator utilizes the compressibility of gas to store energy in the form of compressed fluid. Hydraulic accumulators come in many designs, the most common for hydraulic hybrids are bladder type and piston type accumulators. The difference in these two accumulators is how the hydraulic fluid and nitrogen gas are separated. In bladder type accumulator an elastic membrane separates the hydraulic fluid from the nitrogen gas, while a piston accumulator used a piston capable of sliding to separate the two fluids. For all accumulators the hydraulic oil, nitrogen gas, and separation devise are enclosed in a pressure vessel typically made of steel, or more recently low weight carbon fiber.

Static Sizing of the Accumulator Pre-charge Pressure

The core of the hydro-pneumatic accumulator is the nitrogen gas. Energy storage occurs by pumping hydrualic oil into the oil side of the accumulator, this process compresses the nitrogen gas, thus storing energy. Nitrogen is an ideal gas, and therefore the ideal gas law can be used to effectively model the polytropic process of the accumulator by the following equation:

$$pV^n = c \tag{4.9}$$

Therefore:

$$p_o V_o^n = pV^n \tag{4.10}$$

Where p_o is the initial pre-charge pressure of the nitrogen gas, and V_o is the accumulator volume. From these equations the change in accumulator volume is given by the following equation:

$$\Delta V = V_o \left[\left(\frac{p_o}{p_1} \right)^{\frac{1}{n}} - \left(\frac{p_o}{p_2} \right)^{\frac{1}{n}} \right] \tag{4.11}$$

To increase the life of the accumulator typically a minimum pressure is chosen so the accumulator does not completely discharge during operation. Common practice and the standard used in this work is to have the pre-charge pressure be 90% of the minimum system pressure. As discussed before the maximum pressure in the system is set by limits of the hydraulic units, thus there are two variables needed for sizing the high pressure accumulator, the pre-charge pressure, p_o, and the accumulator volume, V_o.

The approach used to determine the pre-charge pressure was developed by Cross (2011). Because the accumulator is an energy storage device the goal in designing the accumulator is to store as much energy as possible, while minimizing the size of the

accumulator and therefore the weight of the accumulator. Using this idea, Equation (4.10) can be used to find the energy used to compress the nitrogen gas:

$$E_{1\to 2} = \int_{V_1}^{V_2} p dV \tag{4.12}$$

$$= \int_{V_1}^{V_2} \frac{p_o V_o^n}{V^n} dV \tag{4.13}$$

$$= \frac{p_o V_o^n}{1-n}(V_2^{1-n} - V_1^{1-n}) \tag{4.14}$$

V_1 and V_2 volume of gas at pressure p_1 (minimum pressure) and pressure p_2 (maximum pressure) respectively. n is the adiabatic coefficient describing how close to being an adiabatic or an isothermal process this is, where 1.4 is fully adiabatic and 1 is fully isothermal.

By substituting Equation (4.10) into Equation (4.14) the following equation for accumulator volume due to energy and minimum accumulator pressure is developed:

$$V_1 = \frac{E_{1\to 2}(1-n)}{p_1(\frac{p_1}{p_2})^{\frac{1-n}{n}} - p_1} \tag{4.15}$$

This equation shows that for a given amount of energy to be captured and a maximum pressure p_2 there exists a minimum pressure that minimizes the accumulator volume.

Figure 4.4 shows the results of for three different energy storage amounts. As seen in the figure, there is one minimum accumulator pressure that results in the smallest accumulator volume, 144 bar, for all energy storage amounts. Thus no matter what size accumulator is selected the pre-charge pressure should be $0.9 * p_1$ thus the pre-charge pressure for the blended hydraulic hybrid Range Rover should be 130 Bar.

Static Sizing of the High Pressure Accumulator Volume

The next step is determining the volume of the HP accumulator. Form the information discussed before, this simply means determining the amount of energy storage desired. There is not a perfect way to determine the optimal energy storage, a larger accumulator will store more energy, but the weight of the vehicle and the possibility

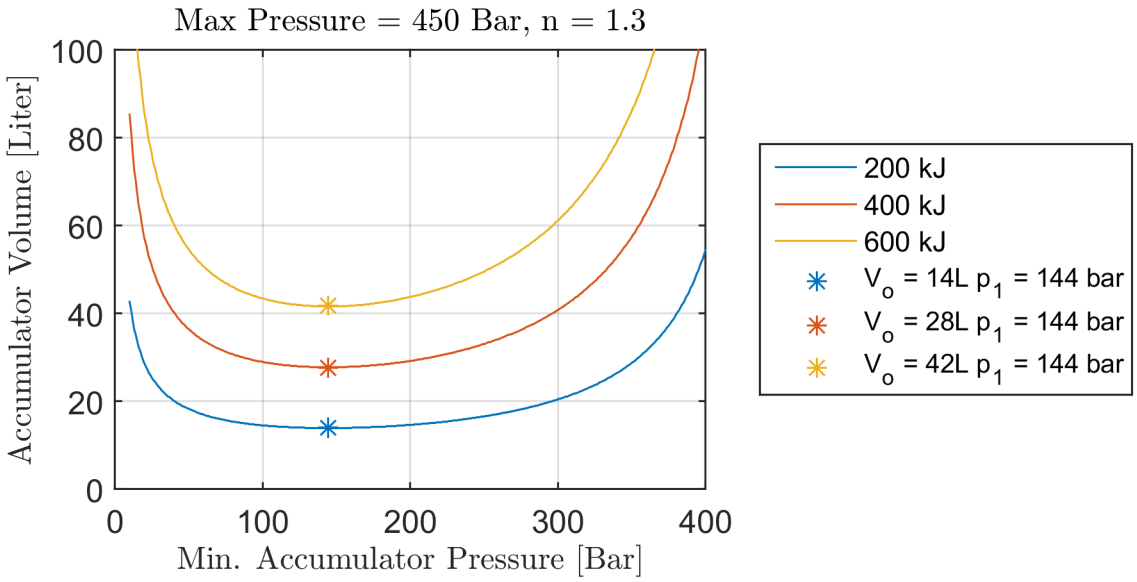

Figure 4.4. Accumulator volume vs. minimum accumulator pressure.

of packaging the accumulator must also be taken into consideration. Previous investigations have been done to size the accumulator for a drive cycle. Kumar (2010) organized a drive cycle into different velocities, this information was used to select a velocity, and therefore a kinetic energy and accumulator size that would capture a certain percentage of braking energy from the cycle.

A second approach implemented by Kumar (2010) and Cross (2011) and used in this thesis is to determine the amount of power during each braking event in the drive cycle and then calculating the amount of braking energy available in each event. Figure 4.5 shows the braking events for the UDDS cycle. This approach is much more comprehensive because the vehicle has energy losses due to rolling resistance and aerodynamic drag that limit the amount of kinetic energy that can be stored. Notice in the figure that some deceleration events are not considered braking events, because drag and rolling resistance provide all the necessary resistance to decelerate.

Using the vehicle parameters and the information from the UDDS cycle the amount of power at each time step can be determined, integrating this power over the

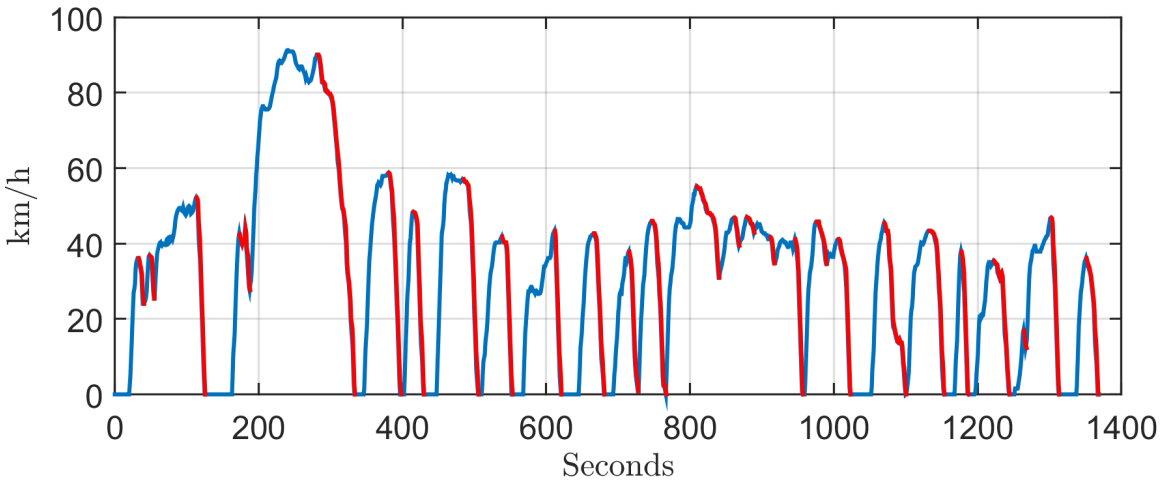

Figure 4.5. Braking events of the UDDS cycle.

entire braking event yields the amount of possible brake energy that can be stored in the HP accumulator. Figure 4.6 shows the available brake energy to be stored during each braking event. Combining this brake energy and Equation (4.15) the corresponding minimum accumulator volume needed for each braking event can be determined, this is also shown in the figure.

Considering traditional available bladder type accumulators shows that a 20 liter accumulator would not be large enough to capture all the energy from the largest braking event. The next size of accumulator would be a 32 liter accumulator which is much larger and heavier. For this reason a 20 liter accumulator will be chosen for static sizing, though a small amount of energy will not be captured during the largest braking event.

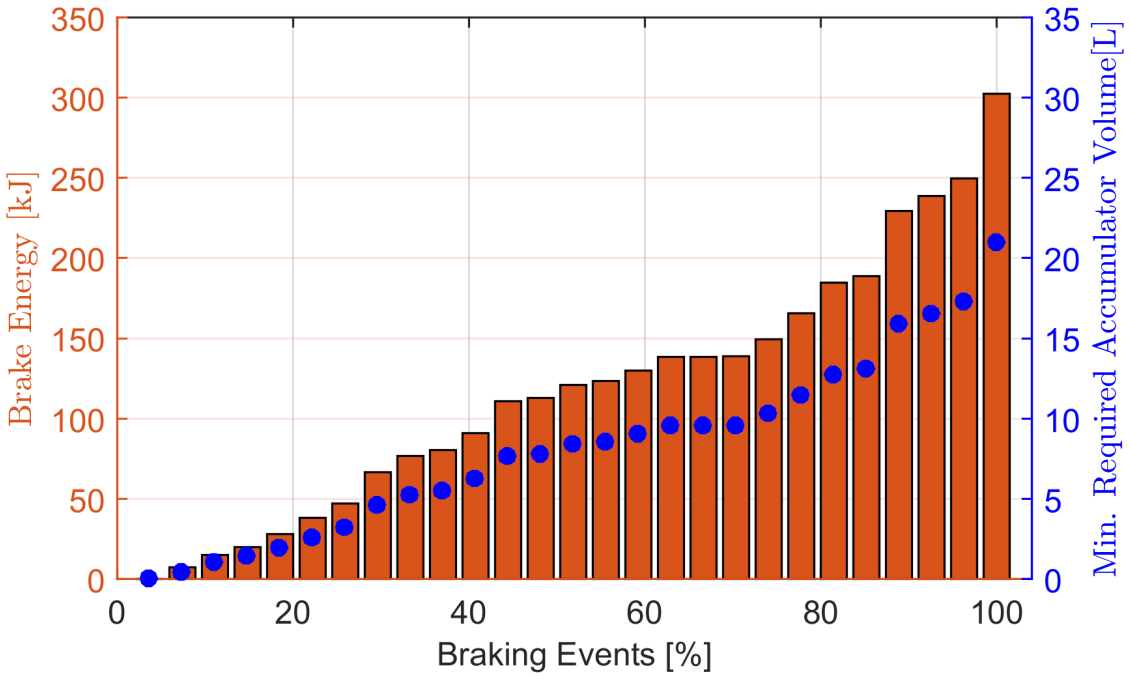

Figure 4.6. UDDS braking energy and accumulator volumes.

4.2 Range Rover Static Sizing Selection

The previous section outlined the static sizing for Unit 1, Units 2 and 3, the minimum accumulator pressure and volume. Each item was chosen from currently existing units and assumptions of current technology were considered. Table 4.1 shows the results of static sizing for the blended hydraulic hybrid.

Table 4.1. Fuel consumption measurement results.

Component	Symbol	Size	Units
Unit 1	V_1	75	cc/rev
Unit 2	V_2	100	cc/rev
Unit 3	V_3	100	cc/rev
Accumulator	V_o	20	L
Min. Accumulator Pressure	p_1	144	bar

4.3 Dynamic Simulation and Testing

Dynamic models are often used in hydraulic transmission design to test and develop control strategies, and determine the performance or functionality of a design. A dynamic model of the blended hybrid was created using the component sizes seen in Table 4.1. Figure 4.7 shows the results of an acceleration run of the blended hydraulic hybrid compared to the measured acceleration of the automatic transmission.

A non-optimal control strategy was implemented in an effort to obtain close to the maximum acceleration. To do this the engine was operated 4750 rpm, the engine speed at which max power is obtained. Unit 1 was held at maximum displacement, with an anti-stall controller to limit unit displacement if it would over load the engine. Units 2 and 3 where controlled sequentially, meaning each stayed at 100% displacement until unit 1 reached 100% displacement. This allowed for the maximum amount of energy from the engine to be extracted and converted to fluid power. In addition to extracting the maximum amount of engine power, the accumulator was assumed to begin at maximum pressure and the enabling valve was open during the entire run.

This strategy could be improved upon, by taking into account unit efficiencies, and studying when the best time to release the accumulator energy would be. Nevertheless, an improved controller would only see minimal increases in performance.

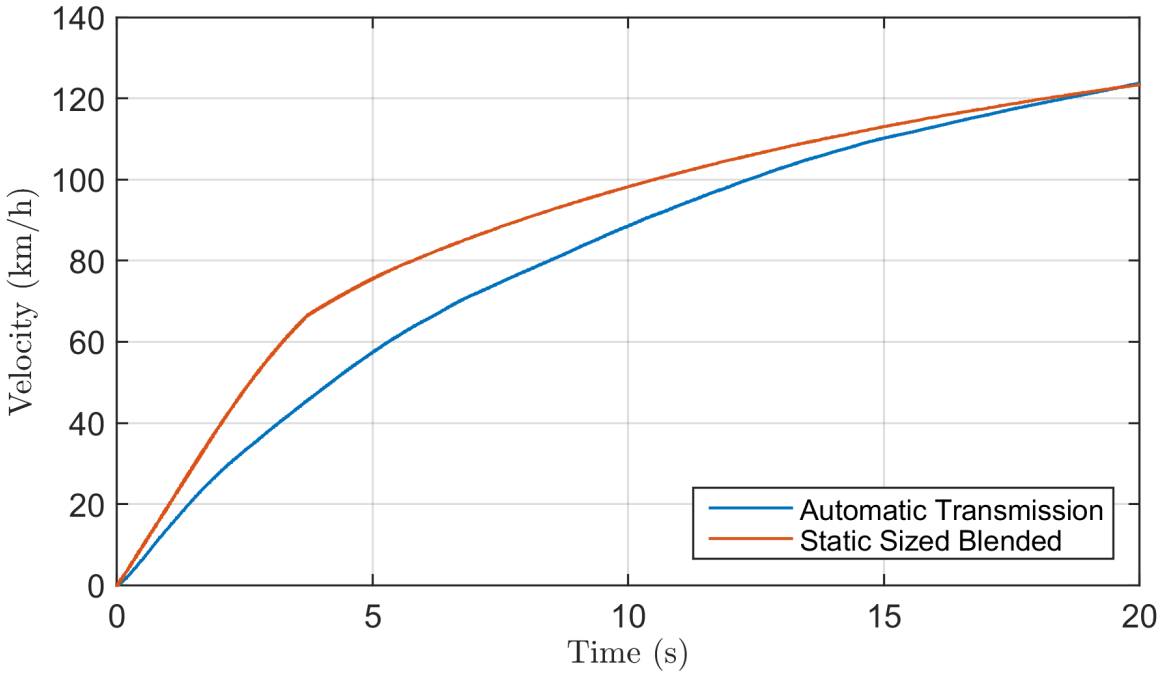

Figure 4.7. statically sized blended hydraulic hybrid transmission max acceleration.

4.4 Limitations in Static Sizing and Dynamic Simulation

The static sizing outlined in this chapter shows that with relative ease approximate component sizes for a hydraulic hybrid vehicle can be determined. It is important to note that some assumptions and approximations were made during this sizing approach that has the potential to limit the effectiveness when designing a hydraulic hybrid vehicle. With proper computational tools, time and satisfactory simulation environments the sizing could be more accurate.

Assumptions and Approximations

- Using smaller hydraulic units will be more efficient and therefore result in better fuel economy.

- That maximizing the energy density of the accumulator will result in better fuel economy.
- The accumulator can be modeled by the ideal gas law, including assumptions about heat transfer and the polytropic coefficient.
- That the assumed volumetric and torque efficiencies of the hydraulic units are valid.
- The amount of energy that the accumulator should be able to store.

Using these assumptions and approximations can result in poor design, or at least designs that are far from optimal. Static sizing is an iterative process with choices that the designer must make at each step in the process, this approach is very subjective and often leads to bias.

As discussed throughout this chapter the goal in sizing each component is to maximize performance and minimize fuel consumption. The dynamic testing used in design does a decent job in understanding performance and testing control, but it is very difficult to use dynamic testing in order to measure a designs fuel consumption. This is due to control, an efficient transmission that is controlled poorly can consume more fuel that a transmission that is designed poorly but controlled well. For this reason only an optimal control approach is appropriate when comparing efficiency of different designs.

5. SIZING USING OPTIMAL CONTROL AND DYNAMIC SIMULATION

One of the main goals of this work is to develop a new methodology for sizing hydraulic hybrid powertrains. This chapter outlines the work that was done in sizing a blended hybrid transmission to be applied to an on-highway SUV. This new methodology blends optimal sizing for efficiency and sizing for maximum vehicle performance in a goal to design a transmission that can perform similar to an existing vehicle with an automatic transmission with as minimal fuel consumption as possible. This new methodology incorporates optimal control for a globally optimum cycle efficiency and dynamic simulation of performance, this approach will be outlined in this chapter.

5.1 Optimal Control

In modeling and designing a powertrain, especially hydraulic powertrains, a control strategy must be used to determine the inputs to the system. For hydraulic hybrid transmissions these inputs include the engine throttle, pump and motor displacements, and in the case of the blended hydraulic hybrid, valve control. The control strategy for these inputs has a great affect on vehicle performance, fuel economy, and emissions to name a few. For very simple systems, such as a single input single output (SISO) system, a simple trial and error approach can be used to tune the controls and find the best strategy. However for many modern systems, especially nonlinear systems that have multiple inputs and multiple outputs a trial and error approach is simply infeasible. To overcome these obstacles, optimal control theory provides a direct approach.

As stated simply by Kirk (2004) "The objective of optimal control theory is to determine the control signals that will cause a process to satisfy the physical constraints and at the same time minimize (or maximize) some performance criterion". This tool

provides several opportunities when designing a power train. First optimal control eliminates the effects of a suboptimal controller on performance, and will therefore yield the global optimal control to maximize a performance criteria. This allows a fair comparison between powertrains or shows the true effect of changing different system parameters or components. Second is that optimal control gives a baseline for suboptimal controllers to be compared too, and lastly this tool is often used in designing suboptimal control laws. This work will focus mainly on using optimal control in understanding the blended hydraulic hybrid especially in how component and system parameters affect the powertrain performance and efficiency.

5.2 Dynamic programming

To obtain optimal control, a tool referred to as Dynamic Programming (DP) was used for this work. Like all optimal control routines require, DP involves the use of a dynamic model of the proposed powertrain with constraints on both inputs and states and a performance criteria that is to be minimized or maximized. This technique is based on the principle of optimality stated by Bellman (1957) "An optimal policy has the property that, whatever the initial state and optimal first decision may be, the remaining decisions constitute an optimal policy with regard to the state resulting from the first decision". Thus the past control effort does not affect the optimization of the future. This algorithm will be described below.

The dynamics of a powertrain can be described as a discrete-time system:

$$x_{k+1} = f(x_k, u_k, d_k), \tag{5.1}$$

Where x_k is the state vector, u_k is the control vector and d_k is the disturbance vector. The optimization will yield u_k, the sequence of control inputs that results in the minimizing or maximizing a chosen cost function. For Dynamic programming, the problem is divided into N stages and the cost function takes the following form:

$$C^*_{k,N}(x(k), u(k)) = J_{k,k+1}(x(k), u(k)) + J^*_{k+1,N}(x(k+1)) \tag{5.2}$$

Where $C^*_{k,N}$ is the total cost of operating the transmission from stage k to stage N. $J_{k,k+1}$ is the transitional cost from stage k to $k+1$ for a given state, $x(k)$, and a given control input, $u(k)$. $J^*_{k+1,N}$ is the minimum cost to finish the operation from $k+1$ to N. The global minimum cost to operate the system from k to N is therefore:

$$J^*_{k,N}(x(k)) = \min_{u(k)}[C^*_{k,N}(x(k), u(k))] \tag{5.3}$$

Equations (5.2) and (5.3) are the *functional equations of dynamic programming* (Kirk 2004). A vital concept in applying DP to a computation algorithm is the formation of a recurrence relation, an equation that defines the sequence of operations to obtain the optimal control. The recurrence relation for DP takes advantage of the principle of optimality, in that whatever the initial state may be the remaining controls must be optimal:

$$\begin{aligned} J^*_{N-k,N}(x(N-k)) = \min_{u(k)}[g_D(x(N-K), u(N-K)) + \\ J^*_{N-(K-1)}(a_D(x(N-K), u(N-K)))] \end{aligned} \tag{5.4}$$

In Equation (5.4), N is the final stage in the process, K is a counter making $N-K$ the current stage in the process. Thus the DP algorithm begins at the end of the process and works backwards until it reaches the beginning. This is vital to obtaining a globally optimum control strategy. DP is able to take advantage of knowing the future states and therefore, as the algorithm works backwards in time it is able to update the cost function $J^*_{N-k,N}$ finding the global minimum cost to operate the system from time step $N-k$, to the end of the cycle. It is important to note how this is different from other controls termed optimal control, if the future states where not known that an optimal control could be applied to the current states and projected forward, though this type of optimization that only depends on past and current states would only yield a local minimum and would not guarantee a global minimum operation for the entire cycle. Often the control trajectory resulting from dynamic programming results in controlling the system in an inefficient manner for a short time in order to meet the global optimum control trajectory for the entire cycle.

Another important aspect of DP is dealing with a nonlinear system with discrete states and discrete controls. The output of a nonlinear system with discrete states and discrete inputs will practically never result in a discrete state, thus linear interpolation is required. This is especially useful for obtaining the cost function which must be interpolated based on the cost at discrete states.

5.2.1 Dynamic Programming for the Blended Hydraulic Hybrid

To properly formulate an optimal control problem, three aspects of the problem must be defined (Kirk 2004):

1. The Mathematical Model
2. The Physical Constraints
3. The Performance Measure

5.2.2 The Mathmatical Model

The most common approach to modeling time varying nonlinear systems is by state space representation. A state space model consists of state variables, which consist of variables in the system that are of interest and are denoted by $x_i(t)$. These state variables are acted upon by the control inputs denoted as $u_i(t)$. With multiple states and controls for a system a state vector and a control vector can be formulated:

$$x(t) = \begin{pmatrix} x_1(t) \\ x_2(t) \\ \vdots \\ x_n(t) \end{pmatrix} \qquad u(t) = \begin{pmatrix} u_1(t) \\ u_2(t) \\ \vdots \\ u_m(t) \end{pmatrix} \tag{5.5}$$

From these the following first order differential can be developed:

$$\dot{x}(t) = a(x(t), u(t), t) \tag{5.6}$$

Thus this model represents how the states will change over time as the control inputs act on the current states through out time. For the blended hybrid the following states fully describe the system:

$$x(t) = \begin{pmatrix} \omega_{eng} \\ \omega_{wheel} \\ p_A \\ p_B \\ p_C \\ p_{acm} \\ p_{LP} \end{pmatrix} \tag{5.7}$$

Where p_A, p_B, p_C, p_{acm} and p_{LP} are the pressures in Line A, B, C, the HP accumulator, and the low pressure system respectively. ω_{eng} and ω_{wheel} is the speed of the engine and wheels. To completely define the system a control vector is needed:

$$u(t) = \begin{pmatrix} u_{eng} \\ \beta_1 \\ \beta_2 \\ \beta_3 \\ u_{enab} \end{pmatrix} \tag{5.8}$$

The controls consist of the engine throttle, u_{eng}, the unit displacements β_1, β_2, β_3 and, the control of the enabling valve, u_{enab}. This results in a state space system with seven states and five controls. To reduce computational expense it is important to simplify the model as much as possible while still representing the system.

The first simplification is found when the transmission is in HST mode, as discussed before the system is a flow controlled system and normally operates in sequential control. Meaning Unit 2 and 3 must be at 100% displacement until Unit 1 reaches 100% displacement, because the system is flow controlled the displacements of all three units are a function of the engine speed and the current wheels speed. With these values determined by the states, ω_{eng} and ω_{wheel}, the controls, β_1, β_2, and

β_3, are no longer necessary in the control vector, because they can be calculated from existing states.

Additional as discussed in Section 2.1, when in HST mode the system is very stiff and the pressures increase to meet the required torque much faster than the system operates. Because of this the dynamics of the pressure building up in the lines can be neglected. A simpler approach is to determine the pressure needed in the lines from the drive cycle that the transmission is being optimized for. With the derived displacements of Unit 2 and 3, the drive cycle will determine the amount of acceleration, drag and rolling resistance these units must overcome, and thus the pressure in the lines can be calculated to meet the required torque. The low pressure system can be neglected, and simply be considered a constant pressure source.

Dynamic programming will use a predefined drive cycle, and therefore the speed of the wheels ω_{wheel} is predefined.

The last simplification is with the enabling valve during hybrid operation. When this valve is open the Unit 3 is controlled in secondary control using pressure and flow from the accumulator. Whenever the enabling valve is open, Unit 3 will be controlled separate from unit 2 and therefore the control of the enabling valve and Unit 3 can be combined into one control input. These simplifications result in the following state space model:

$$x(t) = \begin{pmatrix} \omega_{eng} \\ p_{acm} \end{pmatrix} \qquad u(t) = \begin{pmatrix} u_{eng} \\ \beta_3 \end{pmatrix} \tag{5.9}$$

There are a few added benefits of simplifying our state space system. First is that the states that were removed are now deterministic, as discussed before these states are calculated based on the information from other states. The benefit of this is these states are now continuous because they are no longer a discretized state. This results in a more accurate simulation. The second and more obvious benefit is that the total amount of states and controls is reduced, this results in a significant reduction in computational time because it reduces the amount of possible decisions per stage. Figure 5.1 shows how dynamic programming handles the reduced states

and controls. At each state every control combination is applied which projects to the next time step a new state, thus minimizing the amount of states and controls greatly minimizes the computational expense.

5.2.3 The Physical Constraints and Control Constraints

Whenever describing a physical system there are always limits that can not be surpassed. For this reason there are constraints on the states, and on the controls. This is an important concept in optimal control theory, if constraints are understood correctly the computational burden can be reduced. Consequently if constraints are not properly understood than often the optimal control sequence and trajectory found through optimal control will be physically impossible. Due to this control inputs are limited to those feasible by the system and the resulting states that exceed the physical constraints are deemed inadmissible. Figure 5.1 shows a representation of an inadmissible state. An important note that is not obvious in the figure is that a state becomes inadmissible if either a state in the state space model is outside the constraints or the deterministic states, such as pressure in the lines, are outside of the physical constraints.

There are three factors taken in considering the constraints on engine speed for the blended hybrid. First is the limitation of the engine as reported by the manufacture. As stated before the red-line of the 4.0 liter engine is 5,500 RPM, this can not be exceeded. The second factor is that the engine is mechanically connected to Unit 1 through a gear box that has a gear ratio of 1.48 and thus the engine speed must not result in a Unit 1 speed greater than 3,300 RPM. The third factor is engine power, the maximum power for this engine is obtained at a speed of 4,750 RPM. To maximize performance it is desirable to reach the max power point of the engine, going above this speed the power begins dropping. For these reasons the max engine speed is constrained to 4,750 RPM, thus maximum power is obtainable and both the engine and Unit 1 are operated within their physical limits. The minimum engine speed was

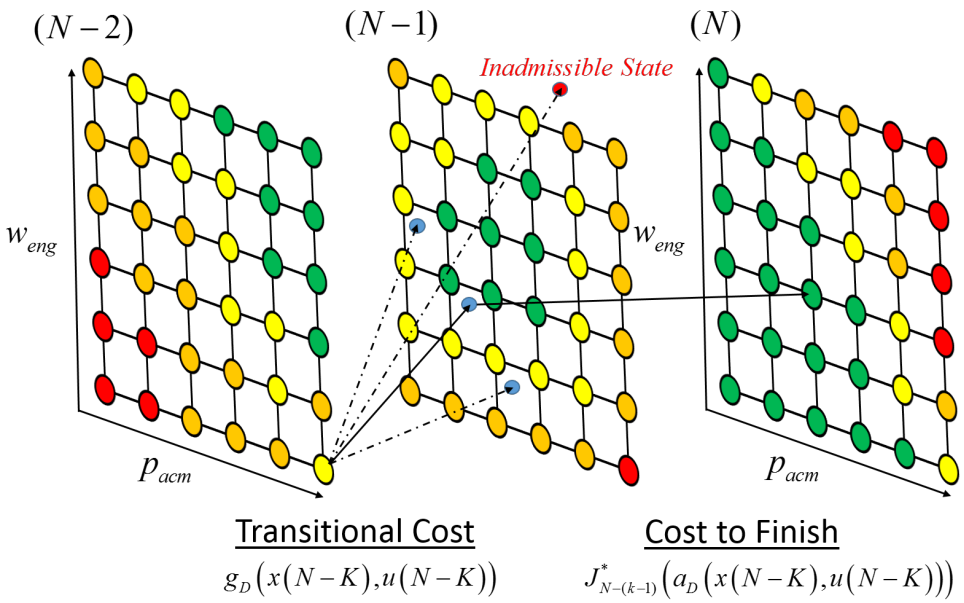

Figure 5.1. Dynamic programming state projection.

set to 1000 rpm due to fuel map data, even though the engine idle of the application vehicle is at 660 rpm.

Maximum accumulator pressure is limited by the hydraulic units. Currently hoses, accumulators and valves are capable of reaching higher pressures than typical swash plate type hydraulic units. For this work Danfoss S90 swash plate type hydraulic units will be used for both simulation and application, these units have a maximum operating pressure of 450 bar, while the hydraulic hose, accumulator and valves have a maximum pressure of at least 500 bar, because the hose and valves are always connected to the pumps the maximum pressure for the system is set to 450 bar.

The minimum pressure is dealt with different for hydraulic lines and the HP accumulator because the check valves in blended hybrid allow for the hydraulic lines, and the HP accumulator to have different pressures. For the hydraulic lines, the pressure is able to go to zero, but with the presence of a low pressure system, the charge pump will continue pumping low pressure fluid into the lines. In dynamic programming the hydraulic lines are limited to a low pressure of 20 bar. The gas in accumulators is always charged to a user defined pressure before they are installed,

this is referred to as the pre-charge pressure. Typically this pressure is set to 90% of the minimum pressure of the HP accumulator required by the transmission designer. For both the physical transmission and in DP this is how the minimum pressure in the accumulator is dealt with, though in simulation it is important to ensure that flow stops when the minimum pressure is reached.

The hydraulic Units 2 and 3 that are connected to the wheels also must not be operated in an over-speeding scenario. For these though, there is not a constraint that is built into dynamic programming. Dynamic programming follows a reference drive cycle and therefore the speed of Unit 2 and 3 are governed by this cycle. Therefore this constraint is met by ensuring that the top speed of the drive cycle does not exceed the speed of the hydraulic units.

Table 5.1 shows the physical constraints that were used in dynamic programming of the Blended Hybrid.

Table 5.1. Physical system constraints.

State	**Symbol**	**Minimum**	**Maximum**
Engine Speed	ω_{eng}	1,000 [RPM]	4,750 [RPM]
Line Pressure	p_A, p_B, p_C	20 [Bar]	450 [bar]
Accumulator Pressure	p_{acm}	User Defined	450 [Bar]

In addition to physical constraints there are also constraints on the control inputs. The different actuators that are used to control the system can only provide an input consistent with what is available to the physical system. For instance the throttle input can go from fully closed to fully open. This results in a percentage of the max available torque at a given engine speed. It is impossible to give a throttle input greater than 100% in the physical system, therefore it is important to build this constraint into dynamic programming otherwise the algorithm could easily find an optimal control input that is physically impossible to obtain. In addition to the throttle input the displacement of each of the units is also constrained to the maximum

displacement of the hydraulic units. For normal forward operation Units 1, 2 and 3 will never go overcenter and therefore the minimum displacement is set to 0%.

Table 5.2 details the control input constraints that were used in dynamic programming for the blended hybrid:

Table 5.2. Control constraints.

Control Input	**Symbol**	**Minimum**	**Maximum**
Engine Throttle	u_{eng}	0 %	100 %
Unit 1 Displacement	β_1	0 %	100 %
Unit 2 Displacement	β_2	0 %	100 %
Unit 3 Displacement	β_3	0 %	100 %
Enabling Valve	u_{enab}	On	Off

5.2.4 The Performance Measure

The performance measure is a vital aspect of dynamic programming. This metric is used to compare results of applying every control input to each state combination. The combination of state and control that minimizes or maximizes the desired performance metric is what determines the optimal control policy.

For this work the fuel consumption of the engine was used as the performance metric that was to be minimized. The fuel map outputs a fuel rate (g/s) for a given engine speed and engine torque. Thus dynamic programming guarantees that the optimal control policy will be found that minimizes the amount of fuel consumed by the vehicle. The cost function is therefore:

$$J = \dot{Fuel}(\omega_{eng}, M_{eng}) \tag{5.10}$$

For this work a representative fuel map was created and used for dynamic programming, because this map is not an empirically formulated fuel map of the engine

the results will be presented as the amount of energy output from the engine in mega-joules (MJ).

5.2.5 Discretization

In addition to a proper model of the system, constraints on states and controls and a performance metric, the extent to which a system is discretized play a large role in the accuracy and computational expense for dynamic programming. There are three areas that will be discretized, the states, the controls, and time, or the amount of stages. Having a fine discretization increases the accuracy of the model because a larger discretization results in a closer approximation to a continuous system. On the other hand though, the more states, controls and time steps the larger the computational costs will be. Computational cost can become very important with large studies such as this one.

There are two states to be discretized for the blended hybrid, engine speed, ω_{eng}, and accumulator pressure, p_{acm}. The discretization of states used for DP in this work is shown in Table 5.3.

Table 5.3. State discretization.

State	**Range**	**Discretization**
ω_{eng}	1,000-4,750 RPM	[1000:50:2000] [2100:100:3000] [3250:250:4750]
p_{acm}	User Defined - 450 bar	[User Defined:5:450]

The engine speed, ω_{eng}, does not have a constant discretization. The reason for this is to increase modeling accuracy, at lower engine speeds the fuel consumption rate tends to be lower and therefore DP will often operate the engine at speeds of 1,000 to 3,000 RPM therefore it is important to have a finer mesh in these areas. Rarely will the engine need to operate at very high speeds and therefore a courser

discretization higher engine speeds reduces computational cost. A total of 38 engine speed possibilities or states were used for this work.

The accumulator pressure is an important state that should see wide ranges of operation and therefore has a fine discretization throughout its operation. For this work many different minimum accumulator pressures will be tested and as such each simulation will have a different amount of pressure possibilities. For the worst case scenario of 50 Bar, p_{acm} will have 81 possibilities. Combining these two states results in a total of 3,078 state combinations.

In addition to state combinations the controls must also be discretized. Table 5.3 shows the discretization for the two control inputs. Notice that a change has been made, before the first control input was u_{eng}, representing the engine throttle. For some dynamic systems a small change in input has a minimal effect on the output, the opposite is true for an engine, a small change in throttle position results in a small difference in the shaft and load torque, a small difference in torque has a fast impact on the engine speed. For this reason a very fine discretization would be needed for the throttle in order to control the engine speed. To solve this a new control input is created, the desired engine speed, ω_{des}. Dynamic programming handles this new control input by taking the new desired engine speed and then controlling the engine throttle continuously in the model for the entire time step trying to reach the new desired speed, if the new engine speed state is the same as the desired engine speed state it is admissible, if the engine is not able to meet the desired engine speed the control is inadmissible (Sprengel & Ivantysynova 2014*c*). This allows for a courser control discretization, decreasing the computational expense.

Table 5.4. Control discretization.

State	**Range**	**Discretization**
ω_{des}	1,000-4,750 RPM	[1000:50:2000] [2100:100:3000] [3250:250:4750]
β_3	0 - 100 %	[0:10:100] %

With a resolution of 10% for β_3 and keeping the same resolution for ω_{des} as that of ω_{eng} there are a total of 418 control inputs. Combining the 3,078 states and the 418 control inputs results in 1,286,604 operations at each stage.

The last factor that affects both the accuracy and the computational costs is the number of stages used in the algorithm. Because a driving cycle is being used the number of stages can be thought of as time steps. Thus the number of stages if found by the following equation:

$$N = \frac{TotalDriveCycleTime(s)}{TimeStep(s)} \tag{5.11}$$

Similar to states and controls there are both benefits and draw backs when selecting the time step, or number of stages, for dynamic programing. A small time step results in many stages and therefore better accuracy when modeling, but also increases the computational expense, likewise a small time step limits how much a state is able to change between stages. An important note is that in DP the controls are held constant through the entire time step but the model it self does not need to be solved using this same time step. Thus when applying the controls to the model any ODE solver may be used as long as the controls are held constant for the duration of the entire stage. Figure 5.2 shows an example of how DP steps backwards through the cycle, this gives a visual of how a fine discretization will give better accuracy when following the drive cycle.

The last important factor in determining the time step or number of stages for the DP algorithm is the dynamics of the control system. In the model for DP of the blended hybrid the control dynamics are neglected. This is only possible if the time step is large enough to neglect the dynamics, if the time step becomes too small the dynamics of the control systems must be considered, namely the throttle bandwidth, and the bandwidth of Unit 1, 2 and 3. To properly account for the control system dynamics would make dynamic programming significantly more complicated and computationally expensive. Due to the overall system dynamics being relatively slow a time step of one second is acceptable.

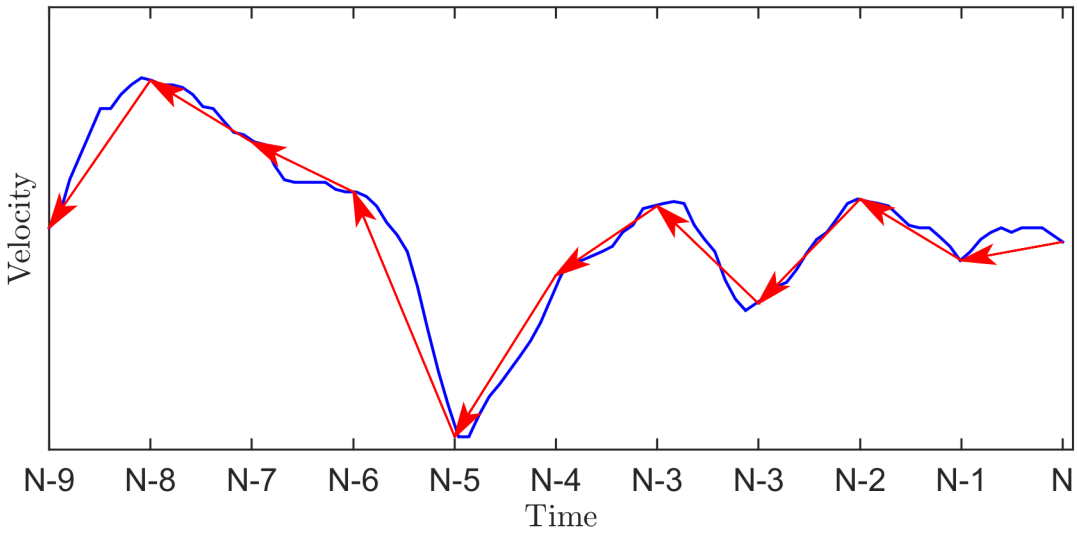

Figure 5.2. Dynamic programming time discretization.

For this work the blended hybrid will be optimized over the Urban Dynamometer Driving Schedule (UDDS) as seen in Figure 5.3. This is an EPA cycle that is 1369 seconds long and is the standard for evaluating hybrid powertrains due to the many acceleration and deceleration periods.

With a total of 1,370 stages, the total number of operations are shown in Table 5.5. Where the maximum is at 50 bar minimum accumulator pressure and the minimum amount of operations is at 240 bar for this thesis.

Table 5.5. Computational expense for blended hybrid study.

Min p_{acm}	**State Combinations**	**Control Combinations**	**Stages**	**Calculations**
50 [Bar]	3,078	418	1370	1,762,647,480
240 [Bar]	1,634	418	1370	935,726,440

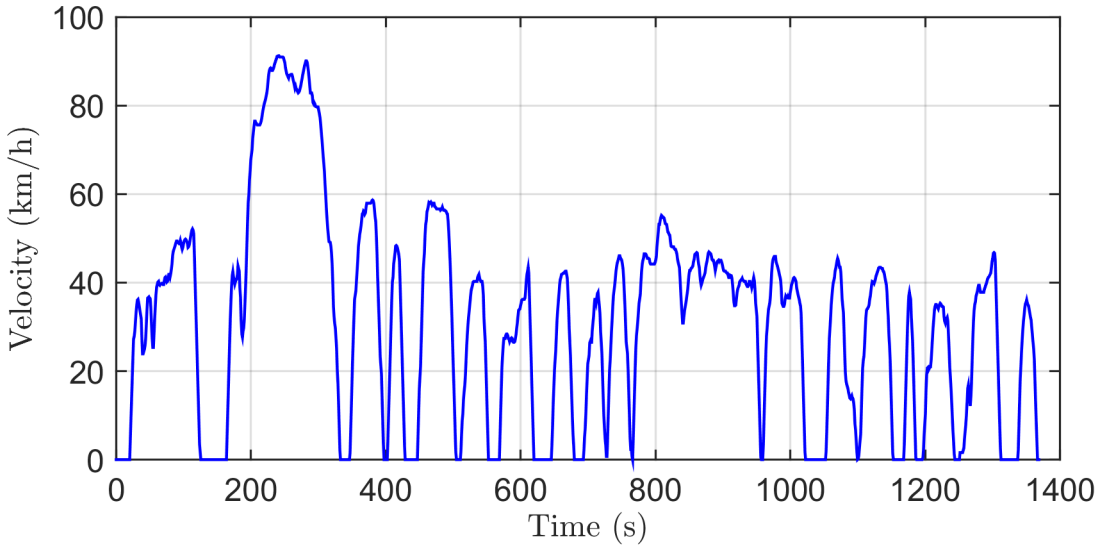

Figure 5.3. Urban dynamometer driving schedule (UDDS).

5.3 Parameter Study

One of the main goals of this work is to discover the resulting trends in sizing of the blended hybrid, this work results in a new methodology for sizing hybrid powertrains. Which incorporates both effects of efficiency and performance.

The first step of the parameter study looks at various sizes for Unit 1, Unit 2, Unit 3, HP accumulator volume, and minimum accumulator pressure. Dynamic programming is used to optimally control each design over the UDDS cycle and affects of efficiency are recorded. By using dynamic programming for optimal control to minimize the fuel consumption, or as reported in this work, the engine energy, a fair comparison of designs is accomplished because control is no longer a factor in efficiency. Dynamic programming optimizes the control strategy thus maximizing the efficiency of each component.

In the past similar approaches have been taken for sizing hydraulic hybrid architectures. Cross (2011) used dynamic programming to optimally size a series hybrid transmission for the United States Postal Service (USPS) Long Life Vehicle (LLV).

This sizing study used a large parameter approach, comparing 2000 designs, over both the UDDS cycle and a portion of the Goodyear Driving Schedule. Similarly Zhao (2012) used dynamic programming to optimally size a hydraulic hybrid output coupled power split transmission for a Toyota Prius. In this work the variating path of the power split transmission was a series hybrid, a total of 600 designs were optimally controlled over the UDDS cycle.

An important addition to this work not done in previous work is also looking at performance. When optimally sizing for a drive cycle there is no guarantee that the transmission will meet the users performance requirements. Most EPA drive cycles are very mild in acceleration and power demand, modern vehicles today have much more power than required for following the UDDS cycle. For on-highway applications users desire both fuel efficiency and performance, therefore one goal of this work is to developed a sizing methodology that can maximize fuel economy and meet the current performance of an on highway SUV. In order to do this a sub-optimal controller was applied to each design that maximized performance. A 20 second cycle of the maximum acceleration was recorded and then combined with dynamic programming result in order to obtain trends in performance and efficiency.

5.3.1 Parameter Study Setup

As mentioned before, this work consists of studying a full factorial of unit 1 size, unit 2 and 3 size, accumulator volume and minimum pressure. The different sizes of each component are shown in Table 5.6. There are a total of five different sizes for unit 1. For unit 2 and 3 seven different sizes were investigated. Five of the options held the size of unit 2 and 3 equal. In order to see the affect of having a different sized unit 2 and 3 two designs consisted a combination of unit 2 and unit 3 at 55 and 100 cc/rev. Thus in one combination unit 2 was 55 cc/rev and unit 3 was 100 cc/rev, in the other combination unit 2 was 100 cc/rev and unit 3 was 55 cc/rev. A total of 3 different accumulator volumes were investigated along with 7 different

minimum accumulator pressures. The precharge pressure for each simulation followed the convetion of $p_{pre} = 0.9 * p_{min}$.

Table 5.6. Component combinations.

Component	Combinations
Unit 1	42, 55, 75, 100, 130 cc/rev
Unit 2 x Unit 3	42x42, 55x55, 75x75, 55x100, 100x55, 100x100, 130x130 cc/rev
Accumulator Vol.	20, 32, 54 L
Min. Accumulator Pressure	50, 90, 120, 145, 170, 200, 240 Bar

Sizes for the hydraulic units and the accumulator were based off commercially available units. Minimum pressure was chosen in order to get a wide range of pressures. This study results in a total of 735 dynamic programing simulations. Each simulation was ran on the entire UDDS cycle. As stated before combinations with a lower minimum accumulator pressure results in a larger state grid and therefore take longer to run. Using parallel processing the longest runs took approximately 8 hours while combinations with higher minimum pressures took approximately 4.5 hours to run.

5.4 Efficiency Study Results

This section outlines the effects of component sizing on transmission efficiency for the UDDS cycle. The dynamic programming algorithm used for this work was developed by Sprengel & Ivantysynova (2013*a*,*b*, 2014*c*). For this study the transmission model was modified to incorporate the torque and volumetric losses of the hydrualic units that will be used on this vehicle. Likewise the vehicle model includes the drag and rolling resistance and other vehicle parameters for the Range Rover. The engine

model was also changed to incorporate the Range Rover torque curve and the representative fuel map. The state and control discretization were modified to represent the discretization discussed before.

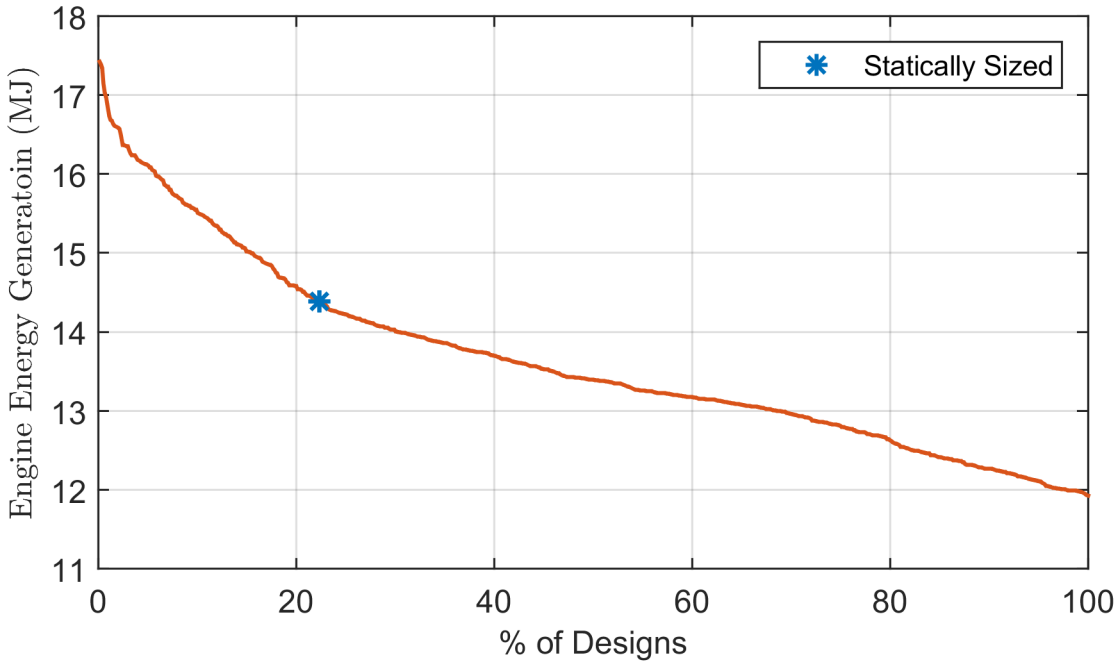

Figure 5.4. Engine energy generation over all designs.

All 735 designs were ran using dynamic programming. Figure 5.4 shows the results of all DP simulations over the UDDS driving cycle. Because an accurate fuel map was not available the amount of required engine energy needed for the cycle was used for reporting instead of the fuel consumption. From these results it is seen that the best design resulted in 11.9 MJ of energy provided by the engine, while the worst design provides 17.4 MJ of energy from the engine. The statically sized design is also indicated. This design was in the 22nd percentile for efficiency and the engine provided 14.4 MJ of energy. An important note is that each of these results shows the best possible efficiency over a cycle due to the use of optimal control. Using a different cycle or sub-optimal control could produce different results, or could even be beyond of the performance ability of the design.

5.4.1 Trends in Efficiency due to Unit 1 Size

The bar graph seen in Figure 5.5 shows the average engine energy that is consumed over the different unit 1 sizes. The error bars on the figure indicate the maximum and minimum engine energy for a given transmission combination using the indicated unit 1 size. From this we can see that a 100 cc/rev unit 1 results in the average lowest engine energy consumption, while the lowest engine energy consumption was seen with smaller units.

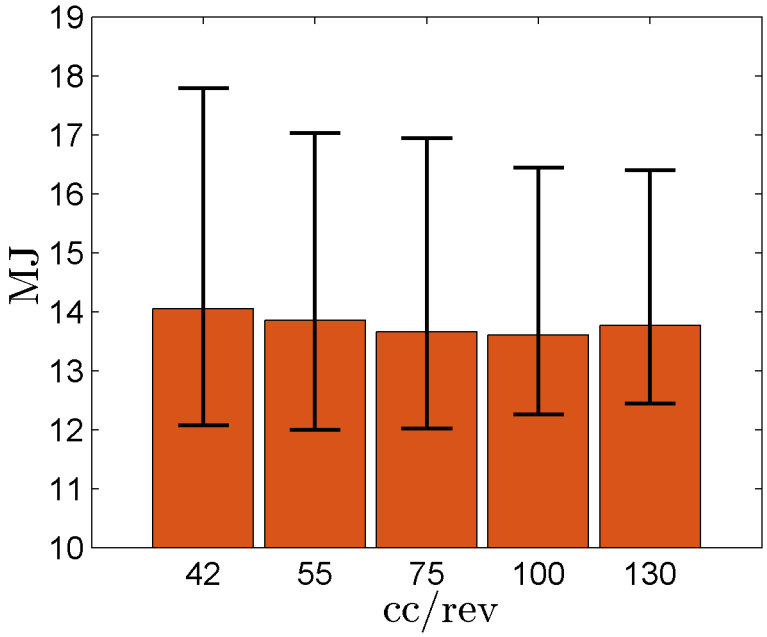

Figure 5.5. Engine energy generation for varying unit 1 size.

Hydraulic units tend to be most efficient when run at low pressures and high displacements, and in general smaller units tend to have lower torque and volumetric losses than larger units. Likewise the DP algorithm was minimizing fuel consumption and therefore tends to operate the engine at lower speeds and higher torques.

There are a several reasons we see these trends in unit 1 size. A larger pump allows the engine to operate at lower speeds and still be able to maintain the necessary flow. This allows the engine to operate at a more efficient point of the engine map

where as a smaller unit would require a higher engine speed and a less efficient point on the engine map. On the other hand the larger pump has higher torque and volumetric losses which will influence the efficiency of the system. The fact that some transmission combinations that contain smaller pumps have lower engine energy consumption indicates that there is an interaction between unit 1 size and the other components when minimizing engine energy. This will be discussed later in this thesis.

5.4.2 Trends in Efficiency due to Unit 2 and Unit 3 Size

Figure 5.6 shows the results when considering unit 2 and 3. As can be seen there is a constant trend that engine energy for the UDDS cycle increases as the size of unit 2 and 3 increase. This is to be expected, a smaller unit 2 and 3 will allow for larger displacements at lower system pressures and therefore will convert the fluid power to mechanical power more efficiently. Though it is important to note that if unit 2 and 3 are too small they will not be able to provide the torque required to meet the drive cycle. Also for this study the influence of having a different unit 2 and unit 3 sizes was explored. Having a 100 cc/rev unit 2 and a 55 cc/rev unit 3 tends to be more efficient than having a 55 cc/rev unit 2 and a 100 cc/rev unit 3. During hydrostatic driving these transmissions will have the same efficiency and losses, but when using the accumulator for propulsion they will not. The 55 cc/rev unit 3 will more efficiently use the power from the accumulator because it will operate at higher displacements than the 100 cc/rev unit.

5.4.3 Trends in Efficiency due to Accumulator Volume

The trends for accumulator volume are minimal as seen in Figure 5.7. Unlike the series hybrid the accumulator of the blended hybrid cannot store energy from the engine and can only store energy during braking. Because of this, as long as the accumulator can store all of the energy the efficiency should be comparable. The larger accumulator will allow the energy to be stored at a lower pressure and therefore

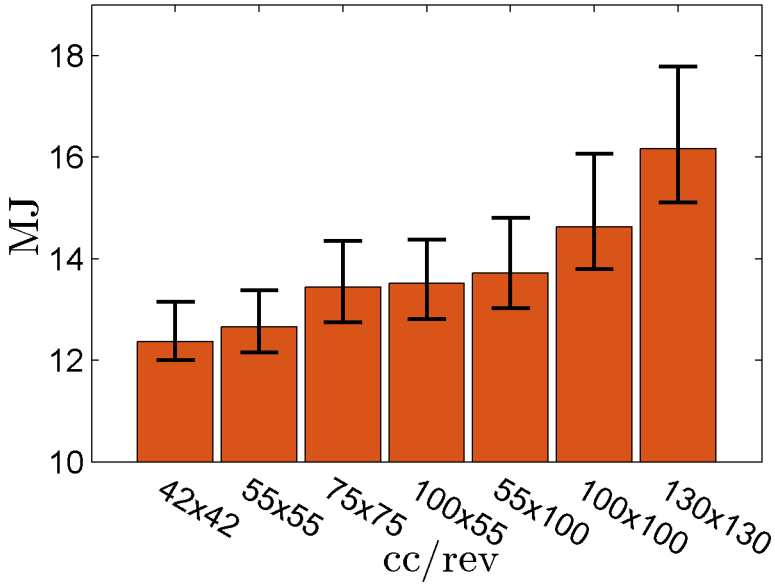

Figure 5.6. Engine energy generation for varying unit 2 and unit 3 size.

unit 3 will be able to reuse the energy more efficiently. This explains the small increase in efficiency due to accumulator size.

5.4.4 Trends in Efficiency due to Minimum Accumulator Pressure

The last metric that was analyzed for this paper was the influence of the minimum accumulator pressure seen in Figure 5.8. The minimum average engine energy occurs at a minimum accumulator pressure of 90 bar, while the absolute minimum engine energy occurs at 120 bar. As discussed in static sizing, the maximum energy density of the accumulator is a function of the maximum pressure and the minimum pressure, thus for a maximum pressure of 450 bar, the minimum pressure that results in the highest energy density is approximately 145 bar (Cross 2011) despite the size of the accumulator. This means that for every accumulator, 145 bar minimum pressure will allow the accumulator to capture the most amount of energy if the max pressure is 450 bar. The reason on average the 90 bar minimum accumulator pressure is better

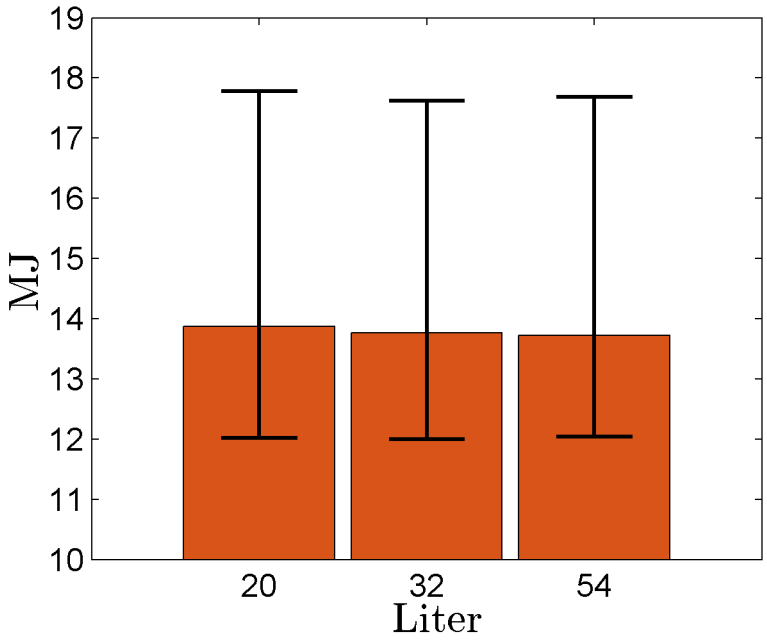

Figure 5.7. Engine energy generation for varying accumulator size.

is because the UDDS cycle is not very aggressive and therefore with optimal control the accumulator is not filled completely. Thus a lower minimum pressure allows the braking energy to be stored at a lower pressure which therefore allows the units to operate at higher displacements. The reason pressures lower than 90 bar result in more engine energy consumption is because the minimum accumulator pressure sets the initial maximum braking toque of the accumulator, therefore lower minimum pressures will result in need for fiction brakes during more aggressive braking events. Using friction brakes dissipates the kinetic energy into heat.

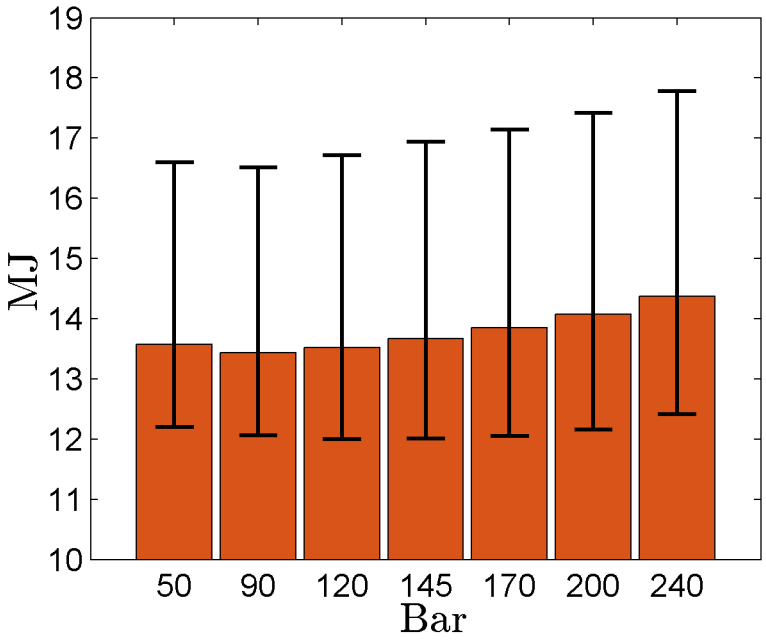

Figure 5.8. Engine energy generation for varying minimum accumulator pressure.

5.5 Performance Simulations

In addition to developing a transmission that is highly efficient it is important to design the transmission to meet performance requirements. For this study each transmission was run for a 20 second cycle that maximized the acceleration of the vehicle. To obtain maximum acceleration the engine was run at its maximum power point of 4750 rpm, and unit 1 was controlled to maximize the power extracted from the engine. The accumulator had maximum energy so the initial pressure was at 450 bar, and the enabling valve was open during the entire run. Units 2 and 3 were controlled using sequential control, meaning they stayed at maximum displacement until unit 1 reached maximum displacement. Then units 2 and 3 decreased displacement at a rate that kept the pressure high enough to fully load the engine. This control strategy ensured that the maximum amount of engine power was being extracted from the engine and then converted back to mechanical power to accelerate the vehicle. Each

of these acceleration runs were also compared to the measured acceleration of our application vehicle. A simplified vehicle model was used that neglected tire dynamics.

5.5.1 Trends in Performance due to Unit 1 Size

Figure 5.9 shows all 735 simulated acceleration runs with different unit 1 indicated by color. The measured acceleration run of the application vehicle is also plotted in this figure. What is interesting in this figure is that unit 1 has a direct relationship to performance. As unit 1 size increases the acceleration performance also increases but with diminishing returns. The reason we see these trends is because unit 1 is used to convert engine power to hydraulic power. Smaller units, are not able to extract all of the engine power and therefore the performance suffers. Likewise there comes a point when increasing the unit size will not allow more power to be extracted. This is seen with the 130 cc/rev unit which has does not increase in acceleration performance over the 100 cc/rev unit.

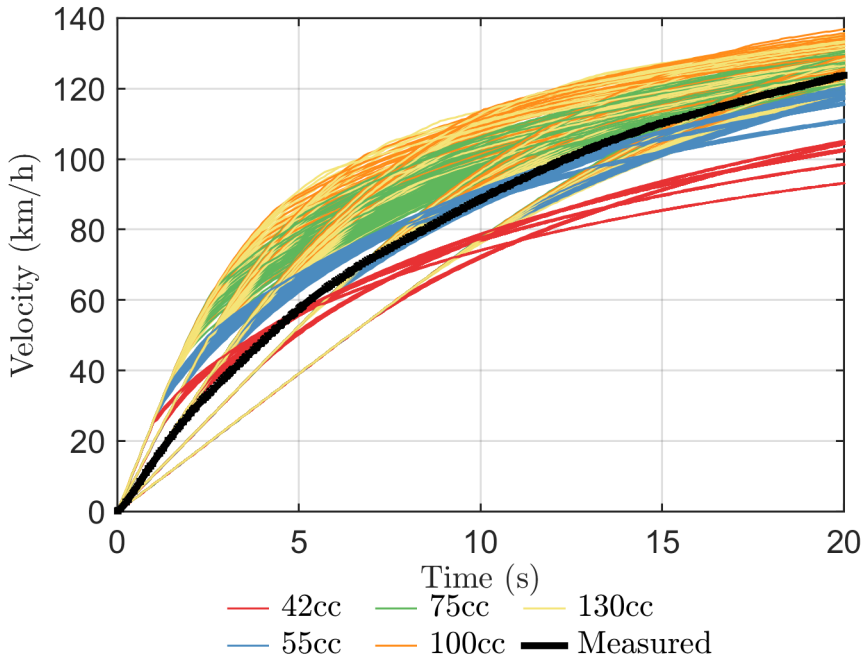

Figure 5.9. Simulated acceleration showing unit 1 trends.

5.5.2 Trends in Performance due to Unit 2 and Unit 3 Size

Figure 5.10 shows the same data as Figure 5.9 except each unit 2 and 3 combination is indicated by color. This figure shows that at higher speeds the size of unit 2 and unit 3 do not have a major trend in performance. At low speeds the transmission is not able to convert all the hydraulic power to the wheels, and as a result the system pressure stays at a maximum until the transmission is able convert all of the engine power to the wheels. This results in lines of constant torque when the vehicle is at lower speeds. Thus unit 2 and 3 mainly affect initial acceleration.

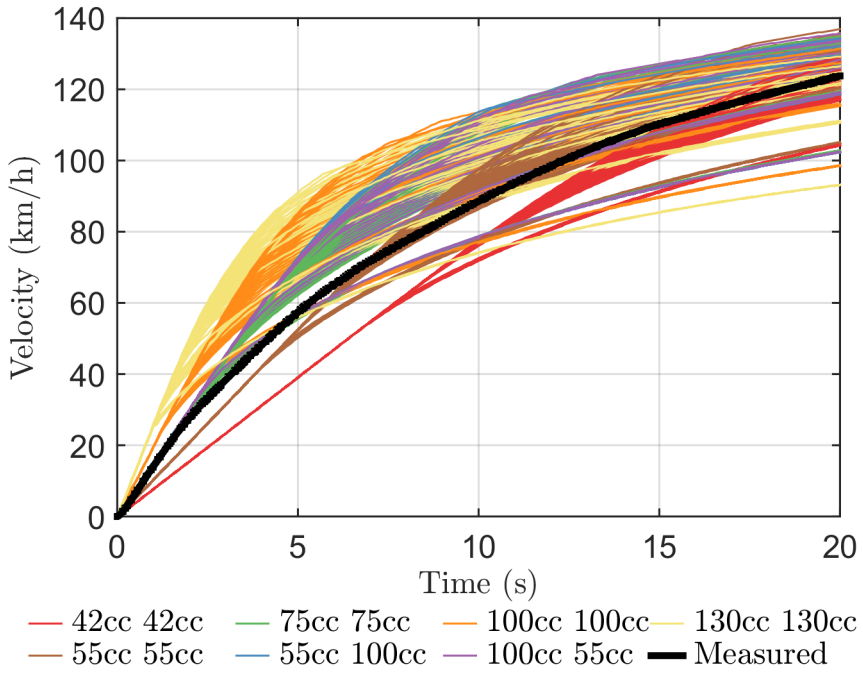

Figure 5.10. Simulated acceleration showing unit 2 and 3 trends.

5.5.3 Accumulator Influence in Performance

To show the influence that the HP accumulator has on performance, all the transmission combinations were simulated with the enabling valve closed, thus removing the accumulator from the system, as shown in Figure 5.11. This shows that the ac-

cumulator has a great influence on vehicle performance. A mechanical transmission should convert engine power to wheel power at a higher efficiency than a hydraulic transmission. Yet during the first 13 seconds of the simulation some combinations have higher performance than the measured transmission. This occurs because the blended hybrid is a continuously variable transmission and therefore the engine can continuously operate at a higher power point than the traditional mechanical power-train, and therefore output more power to the wheels despite the lower efficiency.

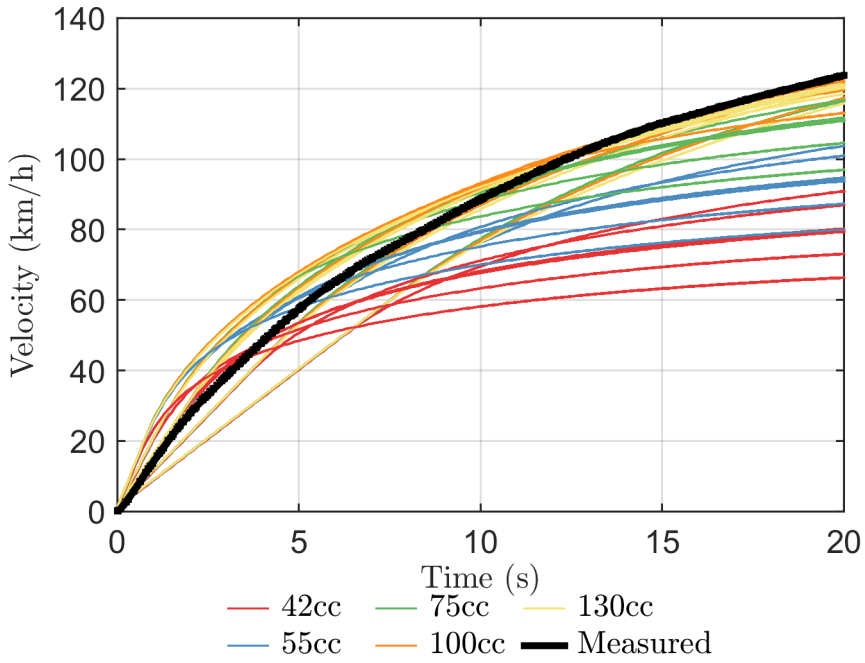

Figure 5.11. Simulated acceleration showing unit 1 trends without an accumulator.

5.6 Combined Efficiency and Performance Results

To go further into how sizing affects performance and efficiency the results have been normalized and combined into a pareto front that maximizes both efficiency and performance. The efficiency was normalized so that the least efficient transmission was set to zero and the most efficient transmission was set to 1. To normalize acceleration performance the results of each run were integrated to give the total distance traveled

in 20 seconds and the measured distance was subtracted from each run, this was then normalized so that a value of 1 indicates the best performing transmission, a value of 0 indicates performance equal to the measured cycle and a negative value indicates a transmission that performed less than the measured.

5.6.1 Unit 1 Combined Trends

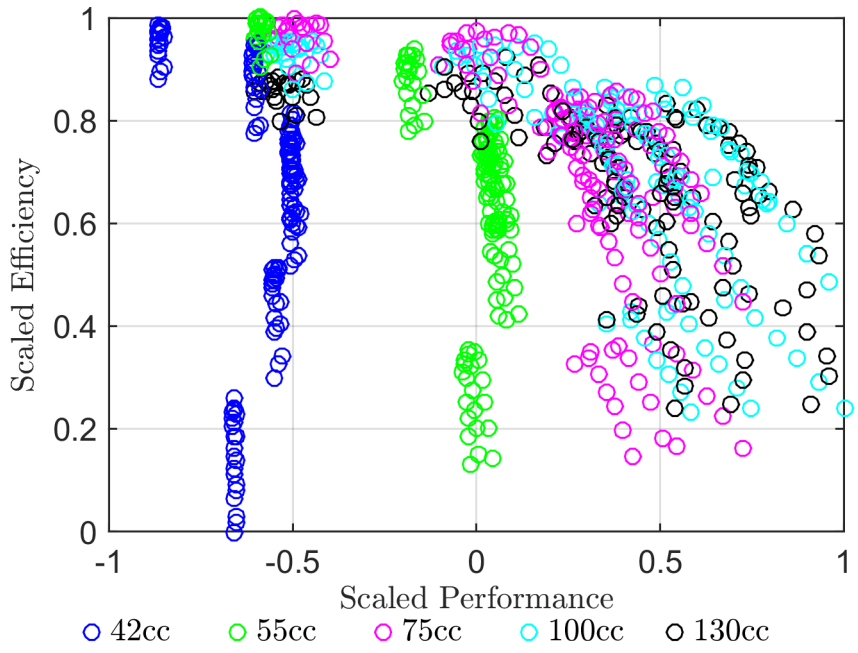

Figure 5.12. Combined efficiency and performance showing unit 1 trends.

The results with unit 1 indicated by color are shown in Figure 5.12. As discussed before, this shows that unit 1 has a large impact on vehicle performance. Where smaller units provide a slower acceleration, and larger units provide faster acceleration. This figure shows that there is not a major trend in efficiency for unit 1, depending on the other component sizes the transmission efficiency varies greatly. As performance increases though, the efficiency decreases.

5.6.2 Unit 2 and Unit 3 Combined Trends

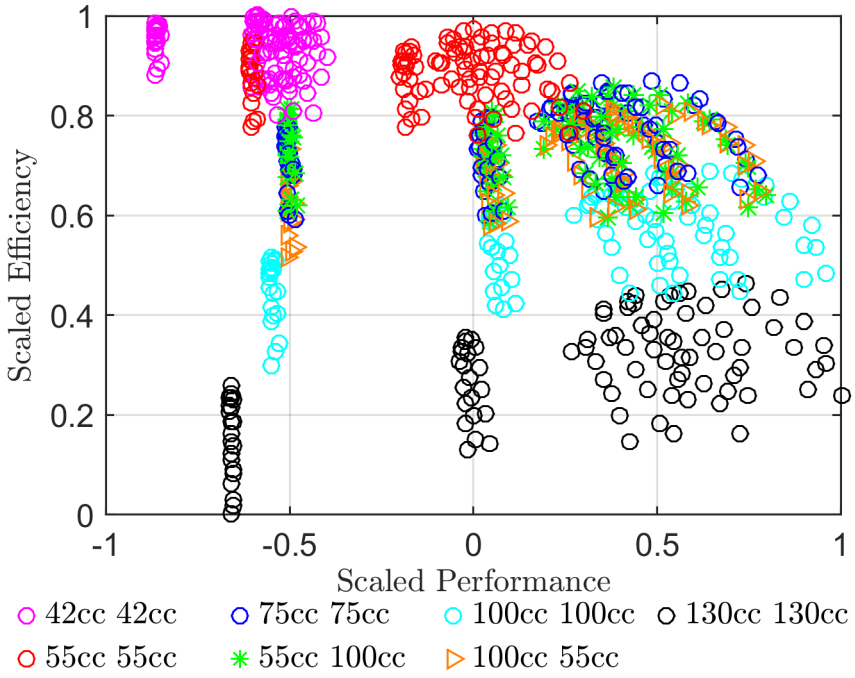

Figure 5.13. Combined efficiency and performance showing unit 2 and 3 trends.

Figure 5.13 shows the same pareto front with the size of unit 2 and 3 colored. This shows the great influence that units 2 and 3 have on efficiency. Smaller units create a more efficient transmission, this was shown before, but what this figure also shows is that smaller units will not provide the needed performance, only larger units coupled with larger pumps provide the necessary performance. What is misleading about this figure is that it suggests that a 55cc/rev unit 2 and unit 3 can provide nearly identical performance as the measured. This is because at the beginning of the performance run the transmission is slower than the measured but by the end of the run it is faster than the measured, therefore the distance traveled is approximately the same. When designing a transmission if it was important to maintain high acceleration at low speed this would not be desirable.

5.6.3 Accumulator Volume Combined Trends

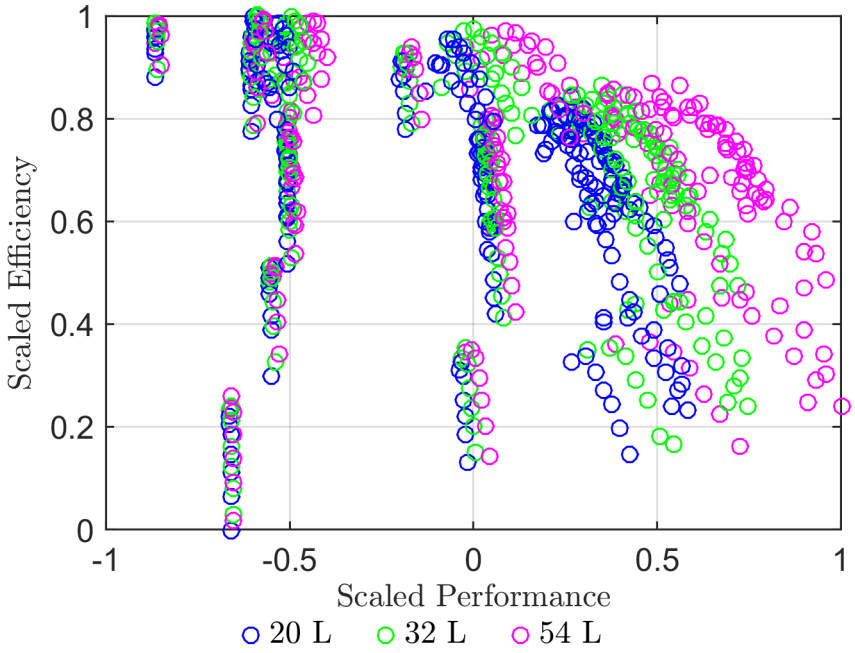

Figure 5.14. Combined efficiency and performance showing trends in accumulator size.

The effect of the HP accumulator volume on efficiency and performance is seen in Figure 5.14. This shows that for performance a larger accumulator increases acceleration due to the larger amount of energy stored in the accumulator. Similar to what was seen before, the accumulator size has very little effect on the overall transmission efficiency. What is not included in this model though is the effects of increased vehicle weight due to a larger accumulator.

For lower performing transmissions 5.14 indicates that the accumulator size doesnt affect performance or efficiency. For these combinations, the pump size is small and therefore is not able to extract all of the available engine power. As a result unit 2 and 3 are controlled in a manner that the pressure stays at 450 bar in order to extract as much engine power as possible, and therefore the power from the accumulator is not used. A different control strategy could be implemented that makes use of the

accumulator power for transmissions with smaller unit 1 sizes. This would result in similar trends in accumulator size as observed for larger unit 1 sizes, but at the compromise of using less energy from the engine.

5.6.4 Minimum Accumulator Pressure Combined Trends

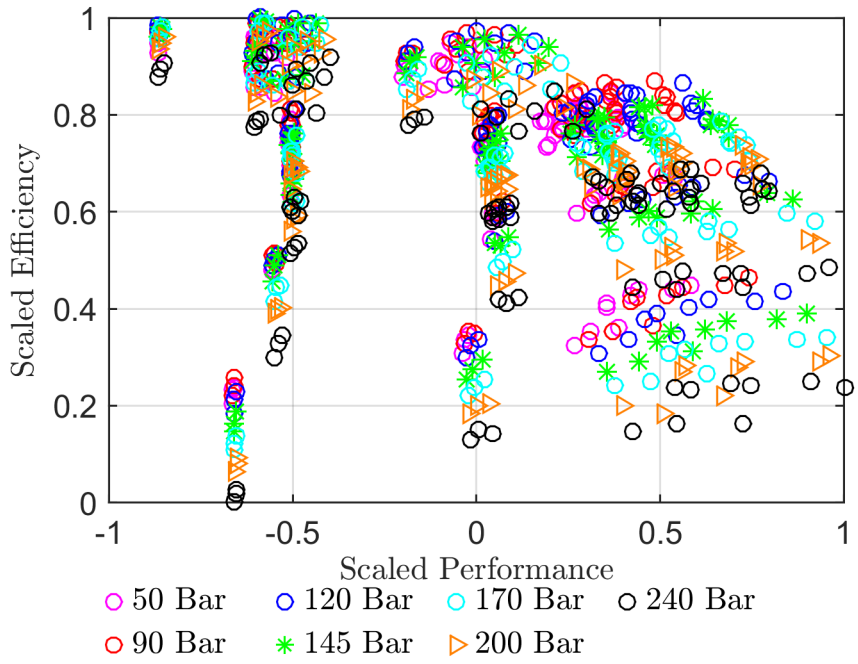

Figure 5.15. Combined efficiency and performance showing accumulator minimum pressure trends.

Lastly the effects of minimum accumulator pressure are presented in Figure 5.15. When comparing this figure to Figure 5.12 and Figure 5.13 it can be seen that for each combination of unit 1 and unit 2 and 3 there is a consistent trend of minimum pressure for efficiency, where higher efficiency is found at 120 and 90 bar, the reasons for this have been explained before. For low performing transmissions there is no influence of accumulator minimum pressure on performance because the accumulator energy is not being released, but for higher performing transmissions there is a trend that shows higher accumulator minimum pressure results in higher performance.

This is counter intuitive since it has been shown that maximum energy density of the accumulator for this work is achieved when the minimum pressure is 144 bar. What is happening in these simulations though is that the pressure is not decreasing to the minimum accumulator pressure, therefor the accumulator is unable to release all of its stored energy. To maximize performance the minimum pressure should be set to the minimum pressure needed for unit 1 to fully load the engine. By doing this the transmission is able to extract all of the engine power and all of the energy stored in the accumulator. Consequently though a minimum accumulator pressure greater than the minimum pressure needed during acceleration to load the engine would also perform worse because less energy would be stored in the accumulator.

Figure 5.16 shows the effects of performance due to minimum accumulator pressure and the size of Unit 1. For this figure the same maximum performance runs were done as were performed before on five different transmission combinations. Each transmission used a 75 cc/rev unit 2 and 3 and a 32 L HP accumulator. The only difference between each transmission was the size of Unit 1 and accumulator minimum pressure. 18 different accumulator minimum pressures from 50 to 400 bar were tested and the results were scaled the same as Figure 5.12 to 5.15. These results are consistent with what has been discussed before. For small unit 1, 42 cc/rev and 55 cc/rev, minimum pressure didn't have a noticeable impact on performance because the pressure stayed at 450 bar. For larger unit 1 sizes, 75, cc/rev, 100 cc/rev and 130 cc/rev the performance has a bell shaped curve. The peak of these curves correspond to the pressure needed to fully load the engine for the given pump, that is why the max for a 75 cc/rev unit has a peak performance at a higher minimum pressure than a 130 cc/rev unit.

The correlation between torque and volumetric losses and minimum pressure are seen in this figure. If torque and volumetric losses were neglected the peak performance would continue to increase as the size of unit 1 increased until the minimum pressure dropped below the minimum pressure that maximized energy density. This is because the amount of energy stored in the accumulator would begin to decrease

at lower minimum pressures. As seen in the figure though, a 100 cc/rev unit has increased performance over the larger 130 cc/rev unit because the torque and volumetric losses of this unit are be higher than the 100 cc/rev unit. These results show that minimum pressure plays a key role in maximizing the acceleration performance of the powertrain.

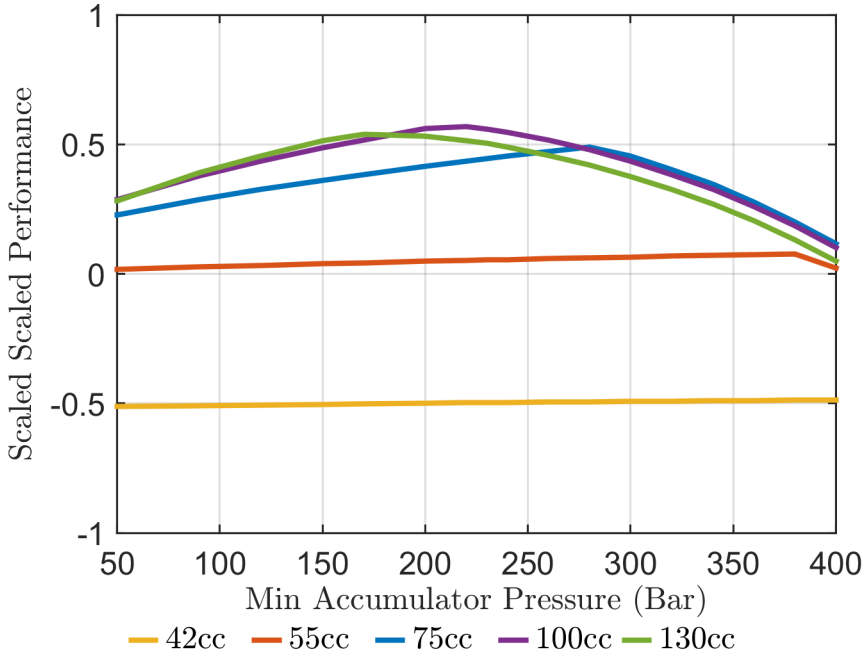

Figure 5.16. Scaled performance according to minimum pressure and unit 1 size.

5.7 Conclusions

In this chapter a new methodology was presented for sizing a hydraulic hybrid transmission for both performance and efficiency, and the methodology was applied to a blended hydraulic hybrid transmission. To fully understand how each component effects efficiency and performance a total of 735 different component combinations were investigated by varying unit 1, unit 2 and 3, Accumulator, and HP Accumulator minimum pressure. All transmission combinations were optimally controlled using

dynamic programming for the UDDS cycle. This allowed a fair comparison between transmission combinations because inefficiencies due to control were no longer a factor.

These results showed that efficiency is greatly influenced by unit 2 and 3 size, where a smaller unit 2 and 3 create a more efficient transmission. Unit 1 results showed an interaction with unit 2 and unit 3 when optimizing for efficiency. On average a 100 cc/rev unit 1 was more efficient but the most efficient transmission combinations consisted of a small unit 1 and a small unit 2 and 3. Accumulator size showed only slightly higher efficiency with a larger accumulator. On the other hand though the HP accumulator minimum pressure had a large impact on efficiency, lower minimum pressures resulted in higher efficiencies, except when the pressure dropped below the required pressure for braking, at these pressures the efficiency was less due to energy being lost through friction braking.

Performance was also simulated for each transmission combination by maximizing acceleration for 20 seconds. This was compared to the measured acceleration for the application vehicle. This procedure showed that unit 1 size has the greatest impact on performance. Unit 1 must be large enough to convert all the engine power to fluid power. Similarly unit 2 and 3 only impacts the performance at slow speeds when the engine is able to provide more power than unit 2 and 3 can convert to the wheels. It was also evident performance increased with increased accumulator size due to the increased amount of energy coming from the larger accumulator. Lastly performance was influenced by the minimum pressure in the HP accumulator. In order to extract all the energy from the accumulator the minimum system pressure seen during the acceleration run must be more than the minimum pressure required to load the engine. From these results it was found that a highly efficient blended hydraulic hybrid transmission can be developed for an on highway SUV that still meets the performance characteristics of the current vehicle.

6. THE BLENDED HYBRID TEST VEHICLE

One of the main goals of this thesis is to retrofit a production SUV with a blended hydraulic hybrid transmission. As discussed before the application vehicle for this work is a 1999 Range Rover 4.0 SE. In preparation for retrofitting the vehicle, the original automatic transmission was removed including the torque converter and transfer case. The only items left from the original power train was the 4.0 liter V8 engine, and the front and rear differential with a 3.54 gear ratio. This chapter will outline the application of the blended hydraulic hybrid transmission into this vehicle and initial testing results. following

6.1 Component Selection

The analysis and sizing done so far in this work are for the main components in the system. When actually designing a system to be implemented there are many other components that are needed. This section details the components that were selected for this project, and how each of them were selected.

Hydraulic Units and HP Accumulator

Chapter 5 details the process of sizing hydraulic units and accumulator for the blended hydraulic hybrid. Taking these results into consideration the units were selected to achieve high performance and high efficiency.

Table 6.1. Hydraulic units selected for Range Rover.

Unit	Model	Size	Max Pressure	Max Speed
Unit 1	Danfoss S90	100 cc/rev	450 bar	3650 RPM
Unit 2	Danfoss S90	75 cc/rev	450 bar	3950 RPM
Unit 3	Danfoss S90	75 cc/rev	450 bar	3950 RPM

As discussed before a gear box was placed between the engine output and unit 1. This resulted in a larger unit 1, but it also allows unit 1 to operate at slower speeds, which decreases noise. This gear box was donated by Durst and the specifications are seen in Table 6.2.

Table 6.2. Gear box selected for Range Rover.

Manufacturer	Model	Ratio	Max Power	Max Input Torque
Durst	1PD06	1.48	396 kW	1414 Nm

The high pressure accumulator chosen for this project was provided by Hydac. A low weight accumulator that is wrapped in kevlar was chosen to reduce overall weight. In addition to low weight, a special accumulator that has the gas volume filled with foam was also selected. In a typical accumulator without foam, an increase in pressure causes the gas temperature rise, heat then transfers through the shell and to the surrounding, when heat is transfered the gas cools and the pressure drops. With a foam filled accumulator the gas is insulated and limits the temperature drop and therefore pressure drop that would normally occur after a braking event. Table 6.3 shows the specifications of the accumulator chosen for this project.

Table 6.3. High pressure accumulator specifications.

Nominal Volume	Dry Weight	Maximum Pressure	Pre-charge Pressure	Length	Diameter
32 L	71 kg	500 bar	150 bar	1422 mm	227 mm

When braking, units 2 and 3 pump fluid into the high pressure accumulator, during this time unit 1 is at zero displacement. For unit 2 and 3 to pump fluid there needs to be low pressure flow going to these units. The low pressure accumulator solves this problem. When braking flow from the low pressure accumulator goes to unit 2 and 3 allowing them to pump high pressure fluid into the HP accumulator. As discussed in Section 4.1.2 a different minimum and maximum accumulator pressure will change the amount of fluid the accumulator can store. Because of this the low pressure accumulator can not simply be the same size as the high pressure accumulator. Using Equation (4.11) the high pressure accumulator with a pre-charge pressure of 145 bar and a max pressure of 450 bar results in approximately 16.1 liters of fluid in the accumulator. Using the same equations on the low pressure accumulator with a pre-charge pressure of 14.5 bar and a max pressure of 30 bar requires a 38 liter accumulator to store 16.3 liters of fluid.

Table 6.4. Low pressure accumulator specifications.

Nominal Volume	Dry Weight	Maximum Pressure	Pre-charge Pressure	Length	Diameter
42 L	– kg	350 bar	14.5 bar	880 mm	274 mm

With this sizing in mind, a 42 liter accumulator was chosen. This accumulator was manufactured by Hexagon Lincoln and is made of carbon fiber in order to reduce weight. Table 6.4 details the specification of the carbon fiber accumulator used for this project.

Charge Pump

The charge pump is necessary for a closed circuit system, it provides flow to the control system, and accounts for the losses in the hydraulic units. Dynamic simulation was used to size the charge pump for the blended hybrid test vehicle. The cycle used to size the charge pump was take from the beginning of route 5 run 1 of the baseline fuel measurements, which is a very aggressive stop and go cycle. The size of the charge pump was selected to ensure that the pressure in the low pressure system did not drop below 15 bar. Thus the system will have enough pressure to control the hydraulic units, and avoid cavitation. Figure 6.1 shows the results of using a 26.4 cc/rev charge pump.

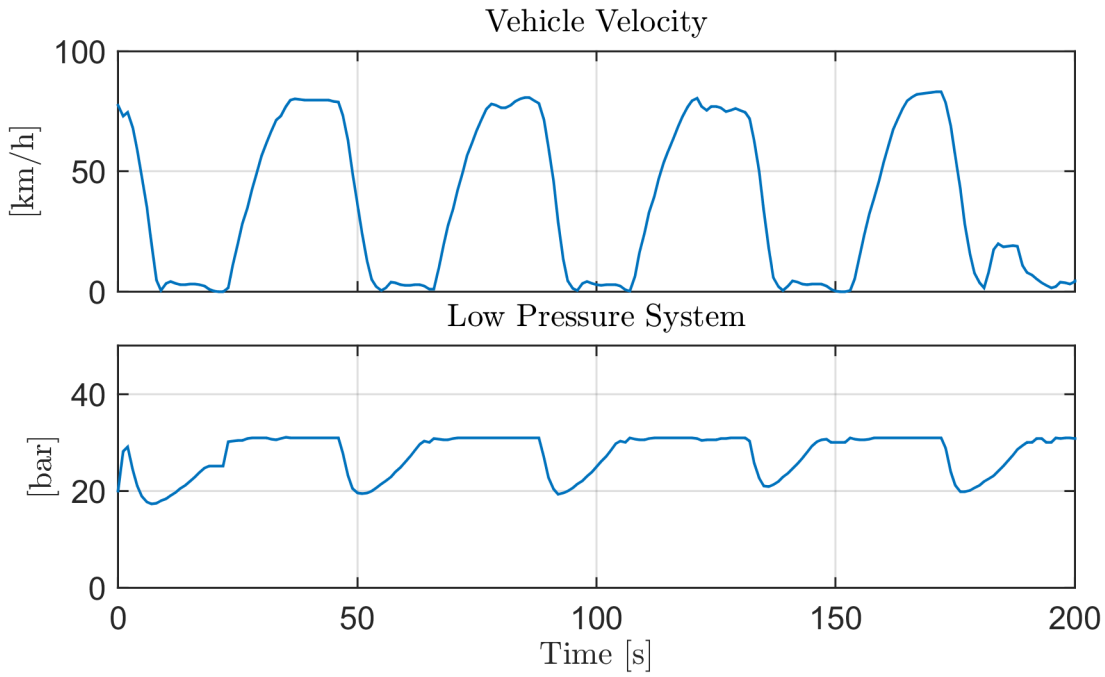

Figure 6.1. Simulated average energy loss and cooler flow rate for route 5 run 1.

Notice that the highest demand of the charge pump is during braking, because unit 1 goes to zero displacement, and all the flow through units 2 and 3 must come from the low pressure accumulator and the charge pump.

For this work a 26.4 cc/rev charge pump was used for the blended hybrid Range Rover. Table 6.5 shows the specifications of the charge pump that was donated by Cassapa for this project. The rated maximum speed is at maximum pressure, because the pressure in the low pressure system is much less, this pump is capable of running at the much higher speeds.

Table 6.5. Oil cooler specifications.

Manufacturer	**Model**	**Displacement**	**Max Pressure**	**Max Speed**
Casappa	Polaris 20-25	26.4 cc/rev	210 bar	2500 rpm

Hydraulic Oil Reservoir

The hydraulic reservoir serves a few different purposes. First is allows time for the entrained air to be released, second is that the reservoir often acts as a cooling mechanism, where hot oil is allowed to cool. Lastly is that when not in use the reservoir holds fluid that drains from the accumulators. The following equation is used in sizing the reservoir:

$$Res_{vol} = \sum V_i \tag{6.1}$$

Where V_i is the volume in each component. For this system the resulting minimum volume of the reservoir is 70 liters. For this work an 80 liter accumulator was selected.

Cooler

An important component in the system that has not been discussed before is the oil cooler. In every component including the hydraulic units, hoses, and vales there is energy loss during operation. This energy lost from the system is converted

to heat and therefore a mechanism to dissipate the heat is required. To size the cooler for the blended hydraulic hybrid Range Rover, dynamic simulation was used to estimate the amount of power loss and therefore heat that must be rejected through the cooler. For much of this work the UDDS cycle was used for sizing components of the transmission, for sizing the cooler though a much more aggressive cycle is needed to ensure the proper amount of cooling is available. To accomplish this the vehicle was simulated using a portion of the baseline measured data from route 5, run 1 seen in Figure 6.2.

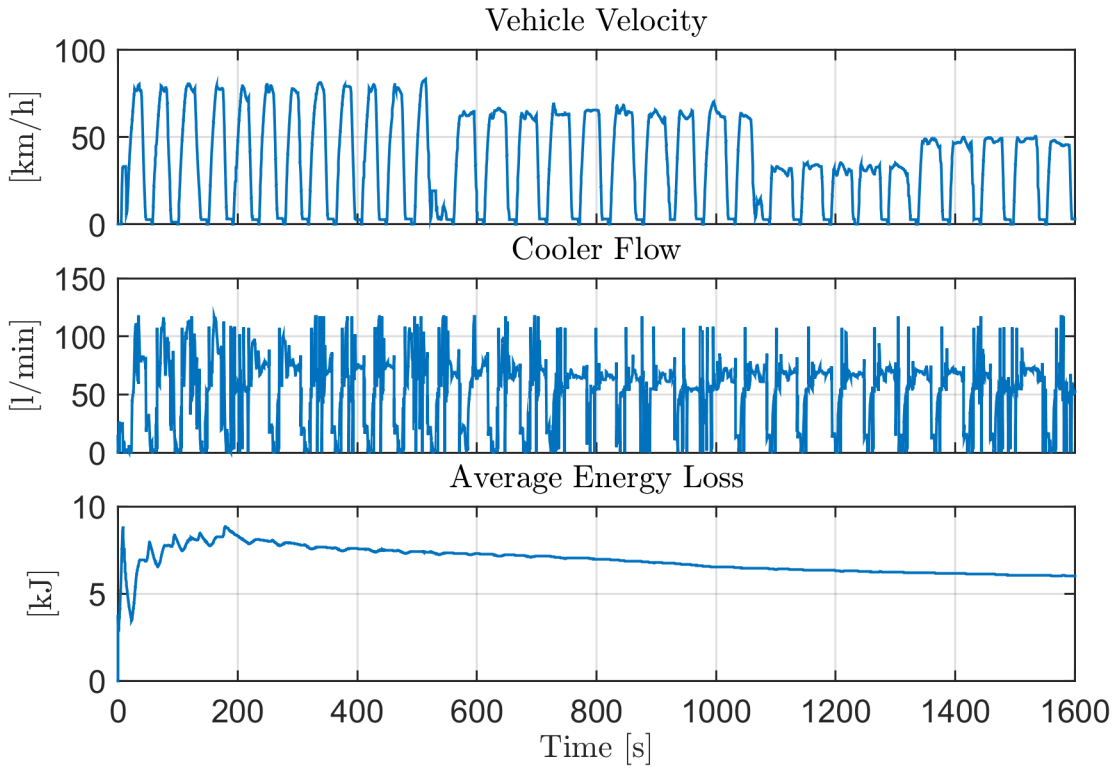

Figure 6.2. Simulated average energy loss and cooler flow rate for route 5 run 1.

Table 6.6. Oil cooler specifications.

Manufacturer	**Model**	**Heat Rejection @ 37.8 °C ETD**	**Max Pressure**	**Max Temperature**
AKG	D20-12	15 kW @ 100 l/min	26 bar	121 °C

Figure 6.2 shows the amount of flow through the cooler and the average amount of heat needing to be rejected is also calculated. From the results above a cooler was selected. Table 6.6 shows the specifications of the cooler selected for the blended hybrid test vehicle.

Figure 6.3 shows the placement of the cooler the Range Rover. The heat exchange for the air conditioning and the transmission oil cool were removed and the remaining space in front of the engine was fitted with the oil cooler and fan. The original engine oil cooler and radiator were left intact.

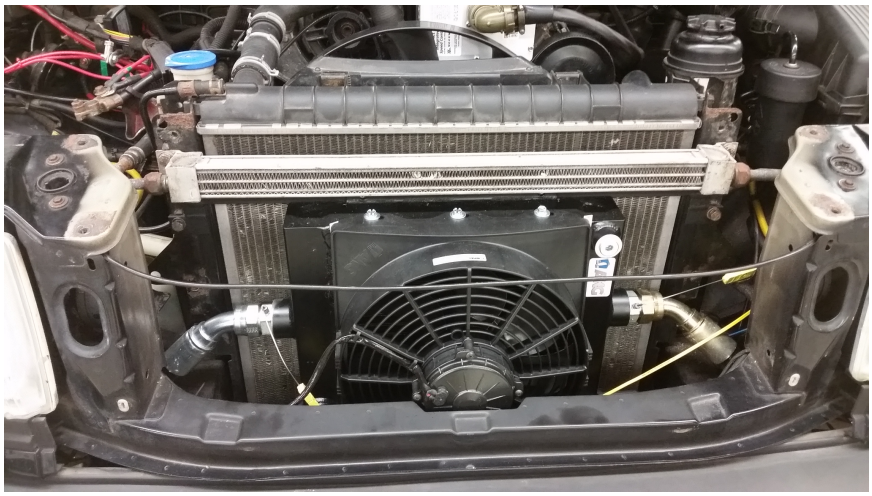

Figure 6.3. Packaging of oil cooler in Range Rover.

Filter

In all hydraulic systems it is necessary to filter the oil, this ensures that contaminants do not damage the hydraulic units and valves. For this systems all fluid enters the system through the charge pump and into the low pressure system. Figure B.1 shows the final circuit design that was implemented in the Range Rover. This figure shows that the filter was placed after the charge pump so all fluid entering the system is clean of containments. Table 6.7 shows the specifications of the cooler selected for this work.

Table 6.7. Filter specifications.

Manufacturer	**Flow Rate**	**Filter Size**	**Max Pressure**
Parker	75 l/min	10 micron	34 bar

6.2 System Packaging and Design

This section overviews the efforts taken to package the blended hydraulic hybrid in the application vehicle. One of the difficult aspects of this project is the packaging was limited to the space originally used by the automatic transmission.

Gear Box, Unit 1, and Charge Pump

A major challenge of this work was packaging and designing a solution to couple the engine to unit 1 and the charge pump. In the conventional automatic transmission the engine flywheel coupled to a flex plate and torque converter which also mechanically connected to the transmission. The bell housing provided a structural member to couple the engine block to the automatic transmission housing. For the blended hydraulic hybrid the engine output is designed to be coupled to a gear box which is coupled to unit 1 and the charge pump.

To accomplish this a custom bell housing was designed which used dowel pins to align the center of the bell housing to the engine fly wheel, and a centering ring was machined into the opposite side of the bell housing to align the gear box shaft to the engine flywheel. A pocket was also machined on the side of the bell housing to accommodate for the starter gear which interfaces with the flywheel. Figure 6.4 shows the design and the manufactured bell housing.

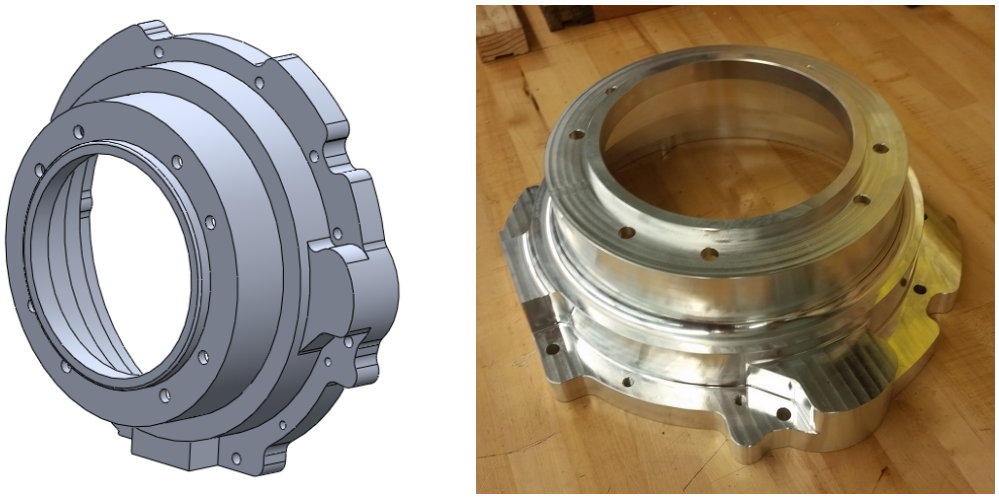

(a) Bell housing design. (b) Manufactured custom bell housing.

Figure 6.4. Bell housing design.

Figure 6.5 shows the entire assembly from the engine to unit 1 and the charge pump. In addition to the bell housing a significant challenge with this project was coupling the engine output to the gear box and unit 1. In the conventional automatic transmission the flywheel is coupled to a flex plate which is then mounted on the torque converter which has a female splined shaft that couples to the transmission. To couple the flywheel to the splined inputs shaft of the gear box a custom adapter plate and pre-manufactured flex plate where used. The custom adapter ensured that the flex plate was aligned to the flywheel. 60 teeth where machined on the perimeter which allowed for a hall affect sensor to provide the speed feedback to the engine controller. For safety and comfortable driving, the adapter was dynamically balanced

as well. The flex plate coupled the splined engine shaft and the custom adapter plate together, this device also allowed for some miss alignment of the shafts.

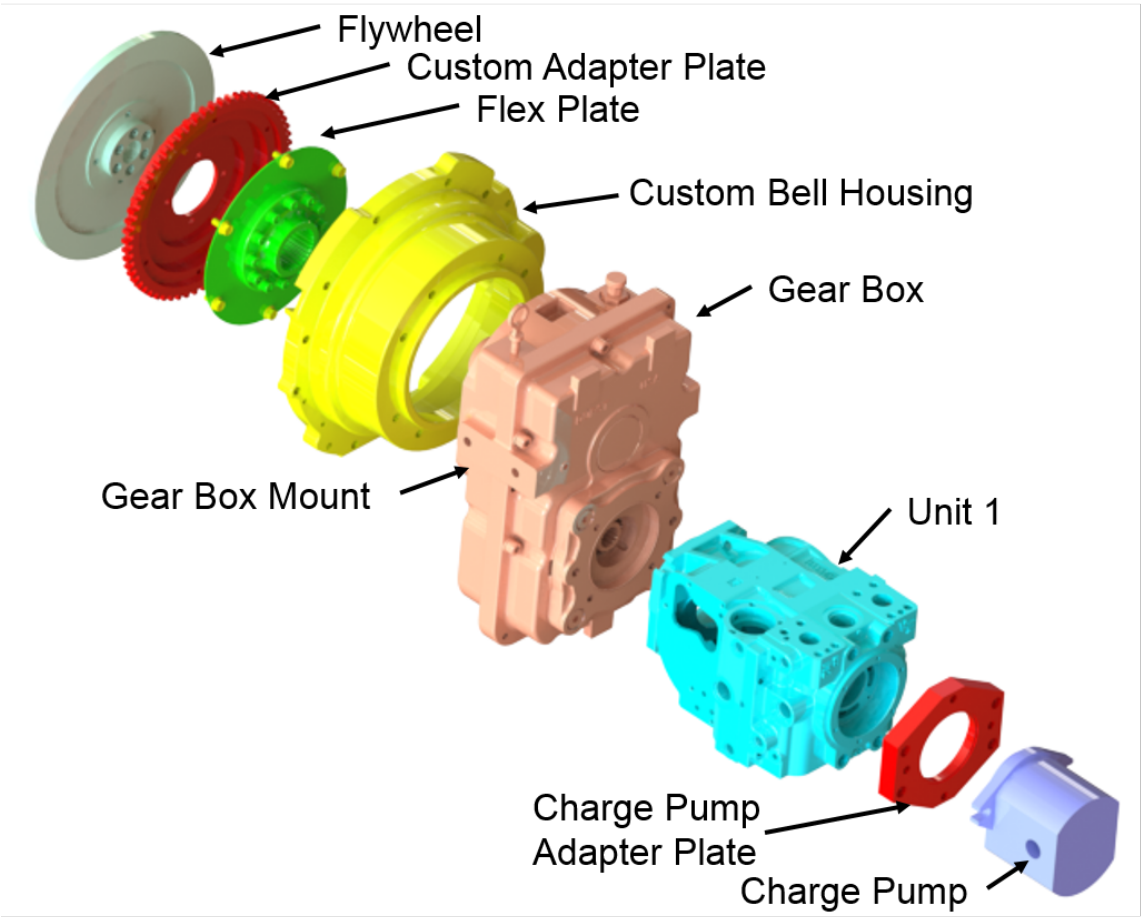

Figure 6.5. Exploded view of engine flywheel to unit 1 assembly.

As can be seen in Figure 6.5 unit 1 coupled to the gear box using the existing pump mounting pad. The charge pump mounted to the back of unit 1 though a custom pump adapter plate. This plate had slots for o-rings machined on both sides to ensure that leakage in this interface could be contained, likewise this adapter plate aligned the charge pump to unit 1.

The engine has only two in-line mounting points which hold the engine up, but do not limit the engine from rotating. Because of this the unit 1 assembly needed to be

mounted to the vehicle frame and the engine face. The bell housing mounted to the engine face and the gear box was mounted to the frame using the gear box mounts and vibration isolators. Figure 6.6 shows the installation of the bell housing, gear box, and unit 1. Because packaging constraints were very tight, the charge pump is not visible in the picture, it is above the frame member. Vibrations from the engine, unit 1 and the charge pump have potential to seriously affect driver feel and noise. For this reason vibration isolators were selected and placed between the vehicle frame, and the mounting point of the gear box. The specifications for the vibration isolators is shown in Table 6.8.

Table 6.8. Unit 2 and unit 3 vibration isolator specifications.

Manufacturer	**Model**	**Type**	**Max Load**	**Spring Rate**
LORD	LM-CB-1180-1	Center Bonded	400 lbs	2963 lbs/in

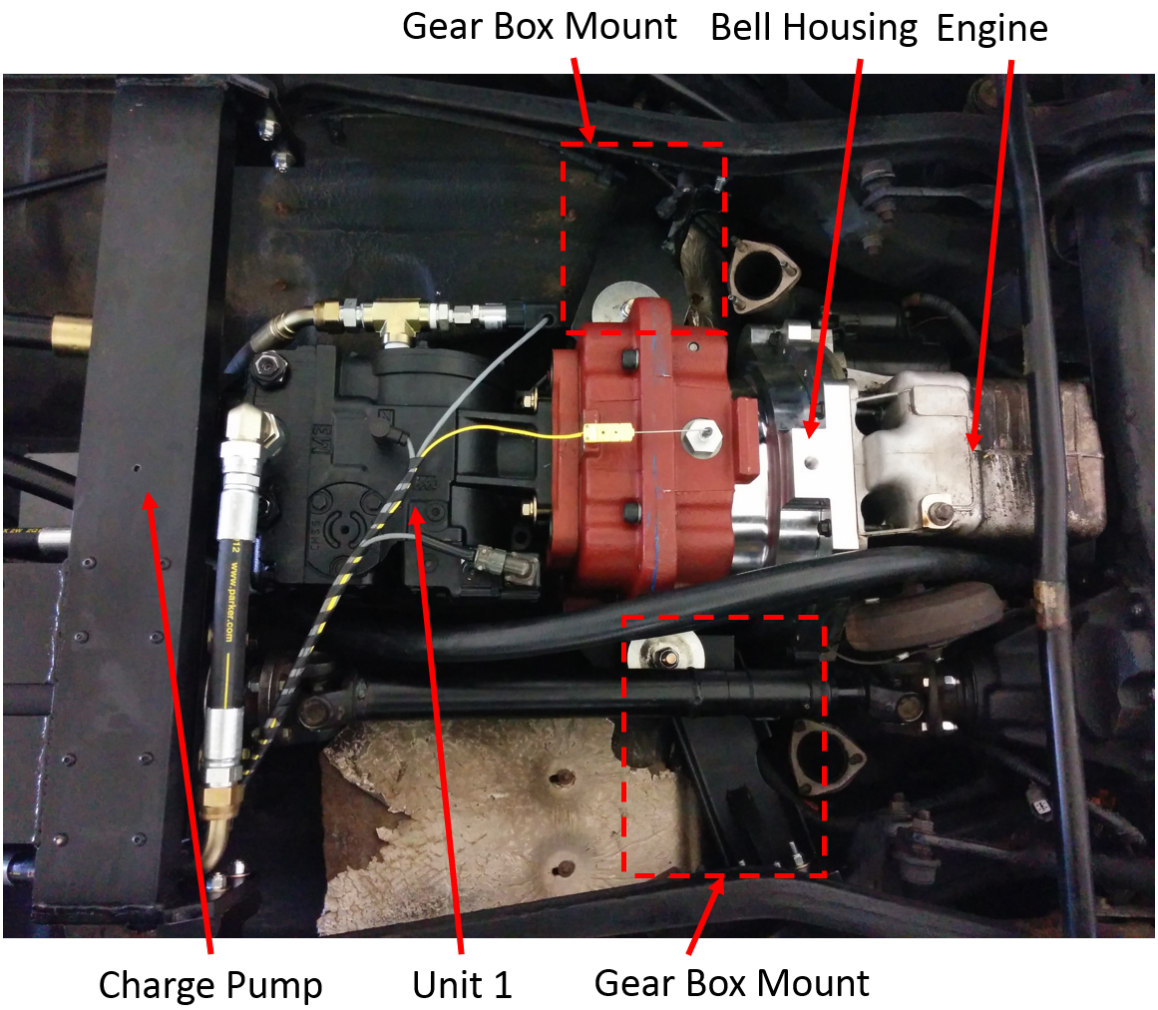

Figure 6.6. Install of unit 1 assembly.

Unit 2 and Unit 3 and High Pressure Accumulator

The packaging of unit 2 and unit 3 required special effort to meet space requirements and loading requirements. Figure 6.7 shows an exploded view of the packaging of unit 2, unit 3, and the HP accumulator. A new frame was designed out of 4 inch wide C-channel. This allowed for a very stiff structure, this also aided in a more compact design because the vibration isolators fit conveniently in the channels. At

high pressures and high speeds the hydraulic units can emit harsh vibrations, Table 6.9 shows the specifications of the vibration isolators selected for unit 2 and 3, these isolators are designed for loads in any direction, which is necessary in when resisting the torque from the hydraulic units. Additionally two mounts were designed and manufactured for mounting unit 2 and 3 using the mounting face on the units.

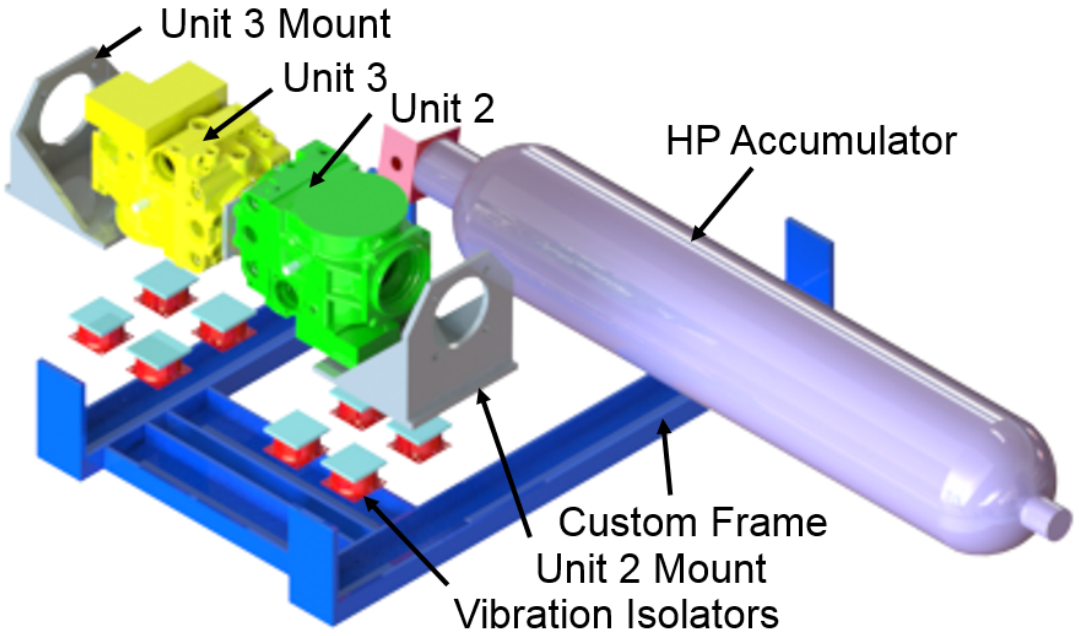

Figure 6.7. Unit 2, unit 3 and HP accumulator exploded view.

Table 6.9. Unit 2 and unit 3 vibration isolator specifications.

Manufacturer	**Model**	**Type**	**Max Load**	**Material**
ACE Controls	CM-US2-25-S	Cup Mount	250 *lbs*	Silicon

The high pressure accumulator was placed under the vehicle longitudinally, it was mounted using two accumulator straps to a structural member on the bottom of the

vehicle and the frame created for the valve block. Because of limited space with the hydrualic units there was only one feasible spot for the accumulator to go. The frame for units 2 and 3 was required to allow room for the 9 inch diameter accumulator. Figure 6.8 shows the installation of unit 2 and 3 and the space provided for the HP accumulator under the vehicle.

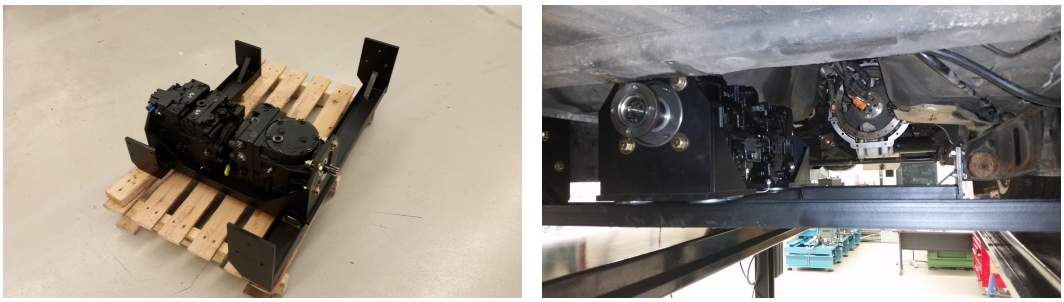

(a) Unit 2 and unit 3 assembly.

(b) Unit 2 and unit 3 installation.

Figure 6.8. Unit 2 and unit 3 assembly and installation.

Valve Block

Appendix B shows the hydraulic circuit implemented on the blended hybrid Range Rover. Figure B.1 details how the circuit was configured to assist in packaging. To conserve space, minimize complexity, and minimize points of failure a valve block was made that contained all of the check valves, flushing valve, and the enabling valve. This component was donated by Sun Hydraulics and can be seen in Figure 6.9.

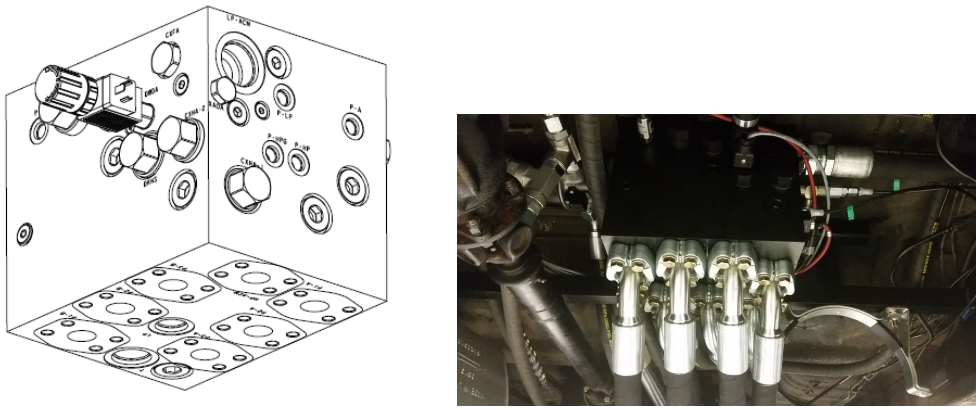

(a) Valve block design.

(b) Valve block installed in vehicle.

Figure 6.9. Valve block design and installation in vehicle.

The valve block was placed beneath the rear seats of the vehicle. Vibration dampening pads were used to isolate the valve block which vibrates due to pressure pulsations. A frame was build beneath the car to hang the valve block from, this can be seen in Figure 6.9(b). Special effort was taken to ensure hose routing functioned appropriately with the packaging of the hydraulic units and accumulators.

Low Pressure Accumulator

The low pressure accumulator was placed in the trunk of the vehicle because of space constraints. This is the only hydraulic component that was placed inside the vehicle. Figure 6.10 shows the installation of the low pressure accumulator. The hose was routed through the space occupied by the original filler tube of the gas tank, and then to the valve block under the car.

Drive Shafts

In the original transmission the drive shafts coupled the output of the transfer case to the front and rear differential. In all vehciels the drive shafts extend and contract

Figure 6.10. Low pressure accumulator packaging.

with the motion of the suspension. In the blended hydraulic hybrid Range Rover the drive shafts couple unit 2 and unit 3 to the front and rear differentials, and still allow extension and contraction. Because of the new design the length of these drive shafts had to be altered. Figure 6.11(a) shows the packaging and suspension travel for the blended hybrid Range Rover. The drive shaft and suspension have different centers of rotation and therefore each drive shaft must be able to extend and retract. The front drive shaft has a required minimum and maximum length of 25.5 inches and 27.5 inches respectively, while the rear drive shaft has a minimum and maximum length of 31 inches and 33 inches respectively. The original drive shafts were shortened to these lengths and rebalanced. Figures 6.11(b) and 6.11(c) show the installed drive shafts in the vehicle.

Hydraulic Reservoir and Fuel Tank

As discussed previously an 80 liter hydraulic reservoir was used for this project. Also a 5 gallon fuel tank was manufactured in order to take fuel measurements. The fuel tank was retrofitted with the original fuel pump and a no-drip quick disconnect fitting was used to minimize the amount of fuel lost when removing the tank for fuel

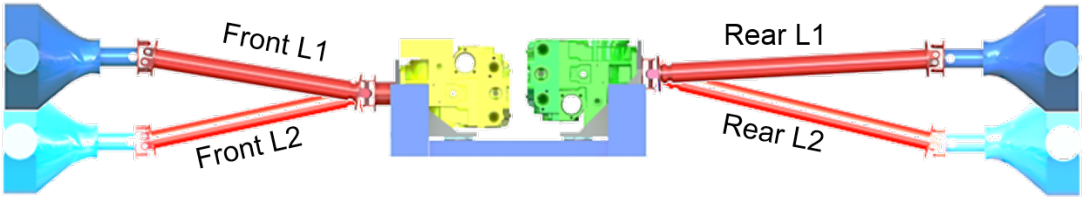

(a) Drive shaft packaging and design.

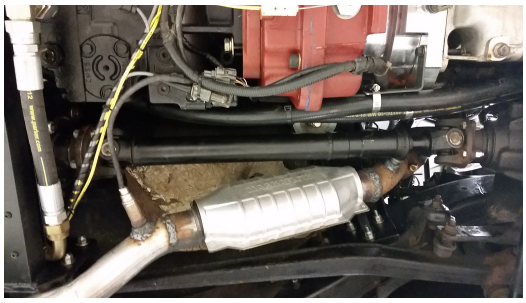

(b) Front drive shaft installed in vehicle.

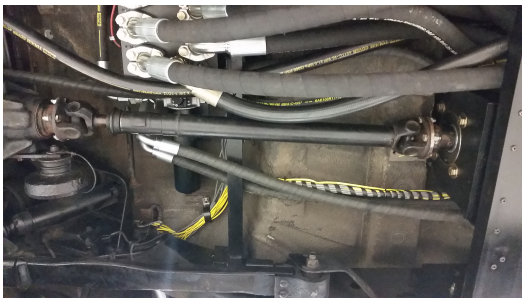

(c) Rear drive shaft installed in vehicle.

Figure 6.11. Design and installation of drive shafts.

consumption measurements. Figure 6.12 shows the assembly of the reservoir and fuel tank outside and inside the vehicle.

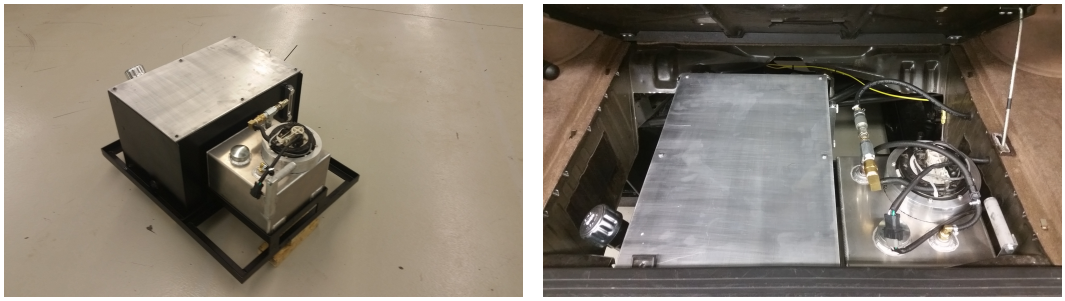

(a) Resevoir and Fuel Tank on Cradle. (b) Installed Resevoir and Fuel Tank.

Figure 6.12. Oil reservoir and fuel tank assembly.

As seen in Figure 6.12(b) the reservoir and fuel tank were placed behind the rear axle in the compartment that initially contained the spare tire.

Final Design

As discussed before the limited space under the Range Rover necessitated a detailed 3-dimensional model of the new blended hydraulic hybrid transmission. Using this tool allowed for more precise designs and aided in overcoming difficult packaging constraints. Figure 6.13 shows the overall packaging design for the blended hydraulic hybrid Range Rover. The only items missing from this design are the low pressure hoses, filter and wiring. Figure 6.14 show the finished design and installation for this project. The only possible view is from the bottom of the vehicle, as can be seen the finished design is almost identical to the 3-dimensional packaging design.

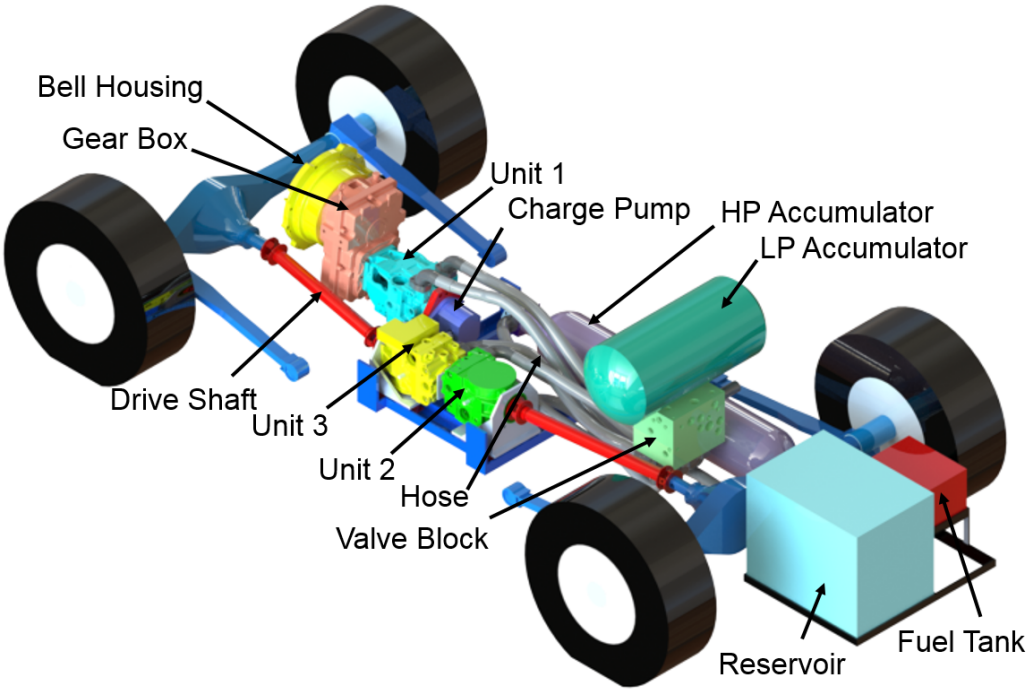

Figure 6.13. Final packaging design of the blended hydrualic hybrid.

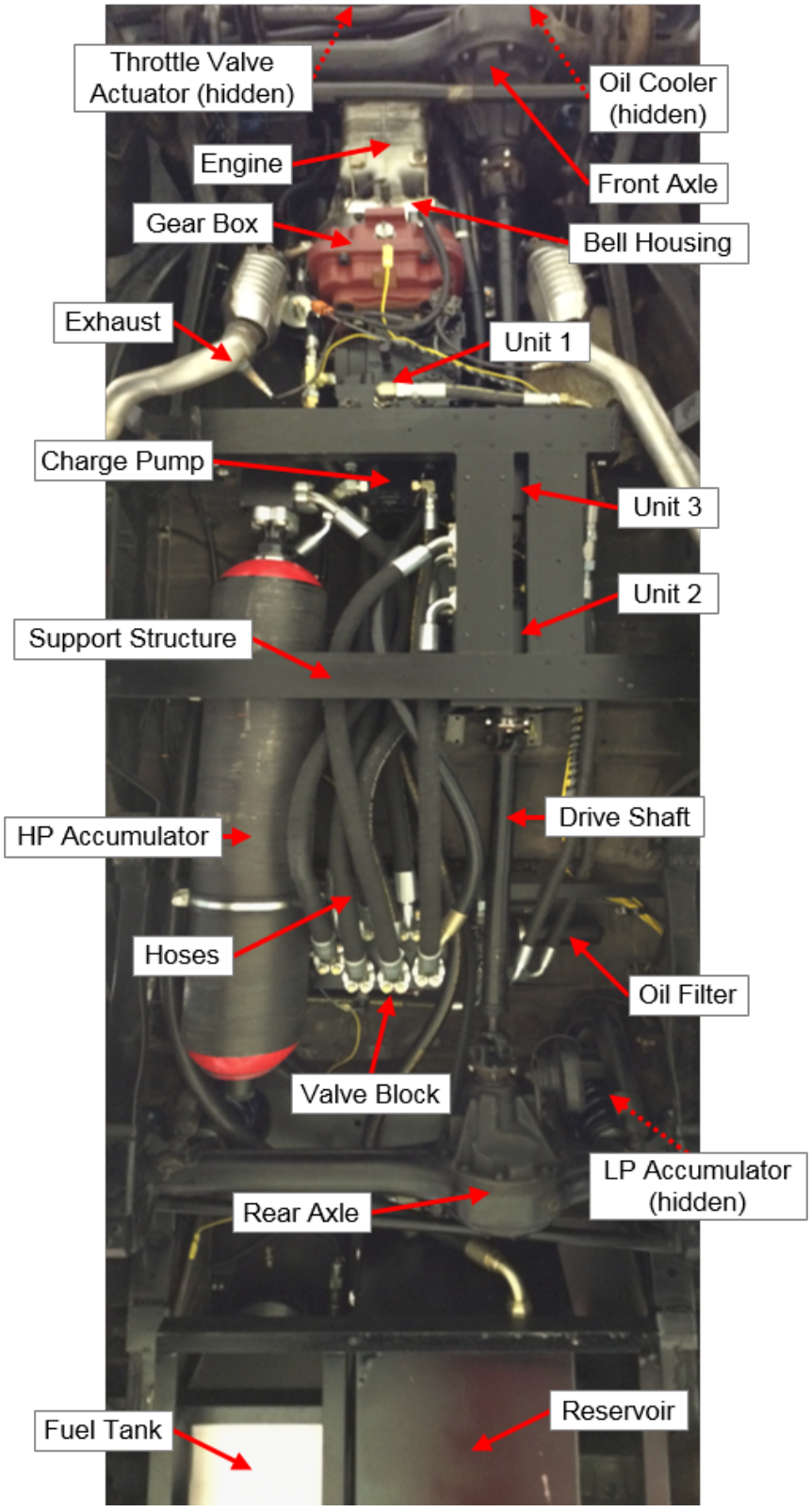

Figure 6.14. Final installation of the blended hydrualic hybrid.

6.3 Instrumentation

To fully understand and document the operation of the blended hydraulic hybrid implemented in a sport utility vehicle many sensors were used. In a production vehicle only a few additional pressure, and temperature sensors would be necessary. This section outlines much of the instrumentation needed for this project, a detailed description of the wiring and placement of sensors can be found in Appendix B and C.

6.3.1 Accelerator and Braking Inputs

In simulation the input to the system is a desired velocity profile that the vehicle attempts to follow. In operation though the user has only two inputs, the brake pedal and the accelerator pedal. In the original vehicle these inputs were connected to mechanical linkages. The accelerator opened the engine throttle with a cable resulting in an engine torque. The brake pedal was mechanically connected to the master cylinder, when a force was applied the pressure increased in the brake cylinder which actuated the brake calipers. These two inputs provided the acceleration and deceleration commands to the vehicle.

For the blended hybrid these same inputs must be used to determine the demands from the driver, but in this system multiple actuators are used increase or decrease the speed. This includes the engine throttle for increased combustion torque and the original friction brakes to slow the vehicle, but also the swashplate of the hydraulic units and the enabling valve must all be used in accelerating or decelerating the vehicle. To obtain the driver commands linear potentiometers where installed to determine the position of the brake and accelerator pedal as seen in Figure 6.15. Table 6.10 shows the specification for the linear potentiometers.

Figure 6.15. Accelerator and brake pedal assembly.

Table 6.10. Linear potentiometer specifications.

Manufacturer	**Model**	**Measurement Range**	**Resolution**	**Non-Linearity**
Sensor Connection	LPPS-100	100 mm	infinite	±0.08%

For the accelerator pedal, the cable connecting the pedal to the engine throttle was removed. For the blended hybrid test vehicle the only input to the system comes from the potentiometer, this signal can then be used to determine engine throttle, unit displacements, and enabling valve operation when accelerating.

An important issue for the braking system is the use of hydrualic regenerative braking and friction braking. During most operating points regenerative braking is required, but in some events the friction brakes are necessary. This includes extreme braking events when regenerative braking does not provide adequate braking torque, or for safety in an event when control pressure is lost and the units are no longer able to provide braking torque. For these reasons a solution was needed to allow a

braking input from the user that could be used for actuating both regenerative braking through the hydrualic units and friction braking with the existing brake system.

This was accomplished by modifying the mechanical linkage of the brake pedal. Originally a revolute joint coupled the pedal to the master cylinder as seen in Figure 6.16(a). A new mechanism was designed, as seen in Figure 6.16(b), to incorporate a sliding joint instead of a revolute joint.

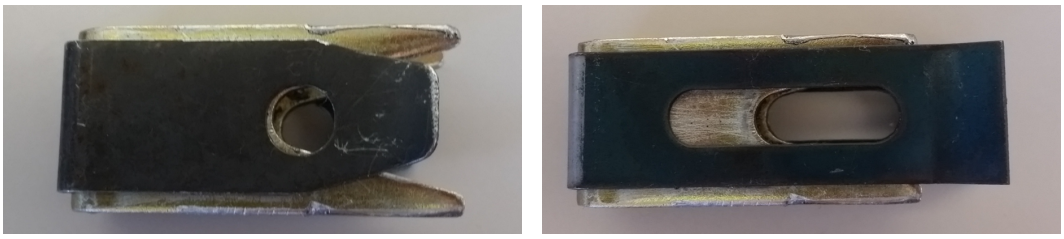

(a) Old linkage with revolute joint.

(b) New linkage with sliding joint.

Figure 6.16. Brake pedal linkage modification.

With this design the friction brakes are not actuated while the pedal travels through the slot, when the pedal reaches the end of the slot it begins applying a force on the master cylinder. Figure 6.17 shows a diagram of how this old design works compared to the new design. Notice that in the new design a portion of the travel does not actuate the master cylinder because of the added slot.

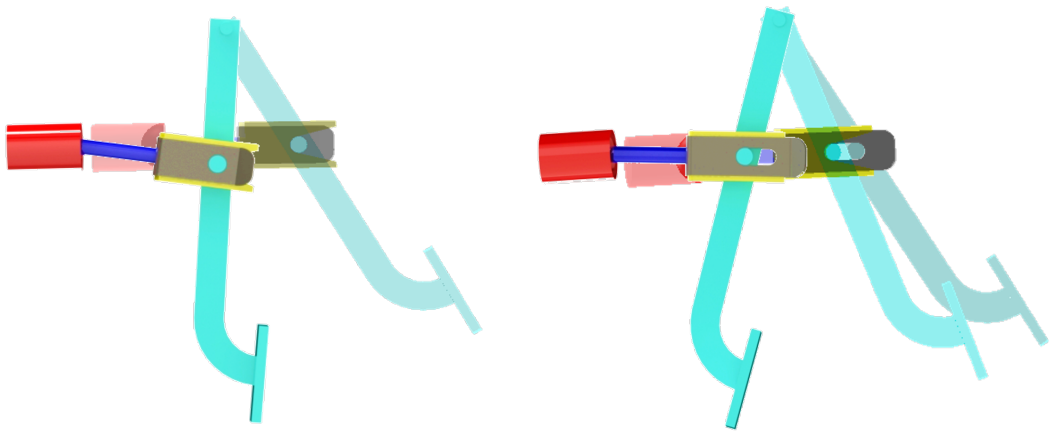

(a) Old brake pedal operation. (b) New brake pedal operation.

Figure 6.17. Old and new brake pedal assemblies and operation.

Figure 6.18 shows the resulting relationship between the pressure in the original braking system and brake pedal position when implemented on the vehicle. This shows that the modified braking mechanism results in the first 35% of the brake pedal travel has no affect on the friction brakes. With this alteration the first 35% of the brake pedal travel will be used as the input for regenerative braking. Likewise if more braking torque is required by the operator than is available in the hydraulic system the operator will depress the brake pedal more to actuate the original friction brakes.

6.3.2 Engine Speed Controller

In the traditional automatic transmission the engine speed is determined by a torque balance between the combustion torque of the engine and the resistive torque coming from the wheels and through the transmission and torque converter. If the torque from the engine is larger than the torque coming from the wheels than the engine speed increases, likewise if the torque coming from the wheels is greater than the engine torque than the engine speed decreases, this loop is closed by the driver

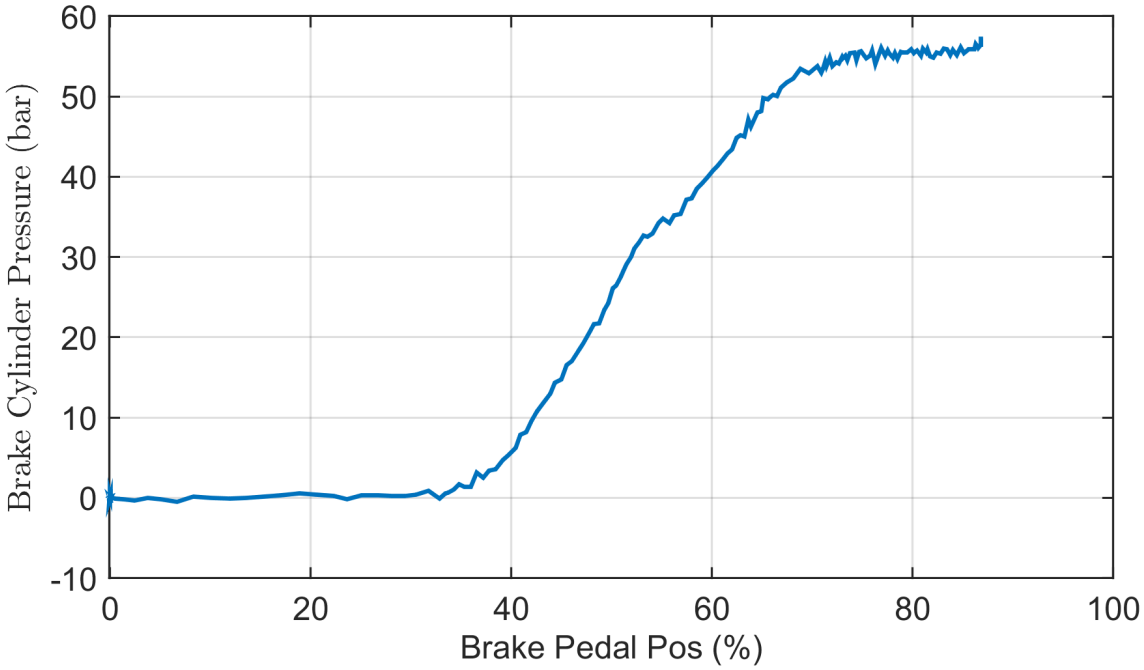

Figure 6.18. Brake pedal position vs. brake cylinder pressure.

through the accelerator pedal which controls engine torque. For a hybrid continuously variable transmission the speed of the engine is now independent of the speed of the wheels and therefore the engine speed can now be selected by a supervisory controller. Also with the use of power coming form the accumulator, the accelerator pedal input does not always result in a power demand from the engine. For these reasons a separate actuator for the engine throttle is necessary, and a controller must be designed to control the engine speed.

To accomplish this a throttle actuator and integrated speed controller designed by Woodward was selected for this work. Typically this controller is used on large diesel and natural gas engines. Figure 6.19 shows the actuator used for this project and Table 6.11 details the specifications of the engine speed controller.

Figure 6.19. Engine speed controller and actuator.

Table 6.11. Engine controller specifications.

Manufacturer	Woodward
Model	ProAct ISC Model II
Voltage	18-32 V
Max Transient Power	251 W
Slew Rate	1000 deg/sec
Steady State Speed Band	0.5 % of rated

One struggle in applying the engine speed controller is that the shaft rotates 75 deg while the throttle needs to rotate 90 deg. To accomplish this a four bar mechanism was designed using graphical analysis to ensure that the 75deg rotation of the actuator resulted in a rotation of 90deg of the throttle. The design and assembly of the four bar mechanism can be seen in Appendix D.

To package the engine speed controller it had to be placed near the engine throttle which could not be moved. To do this the pump for the air conditioning was removed

and a custom bracket was manufactured and used to mount the engine speed controller to the top of the engine. It was necessary to have the controller mounted to the engine because the controller must always move relative to the engine, or else the system could become unstable. The final packaging and implementation engine controller can be seen in Figure 6.20(a).

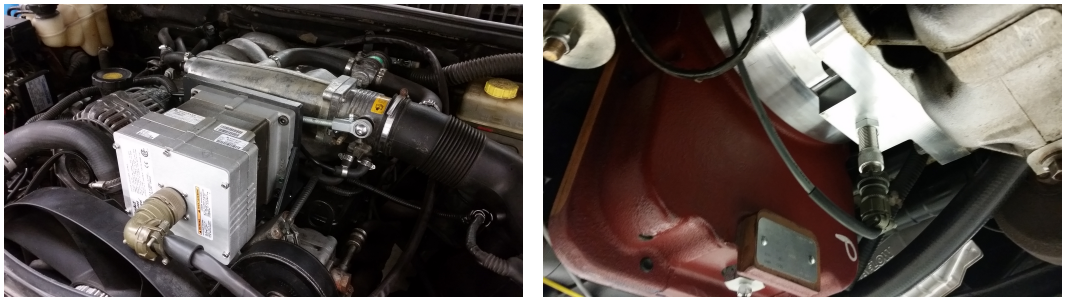

(a) Installed engine speed controller and actuator.

(b) Engine speed sensor used for feedback.

Figure 6.20. Installed engine speed controller and speed feedback sensor.

In order to follow a desired engine speed the actual engine speed must be fed back to the controller. This is done through a magnetic pick up sensor that was installed in the bottom of the bell housing and outputs a pulse each time the teeth of the custom adapter plate passes the sensor. The assembly of this sensor in the bell housing is seen in Figure 6.20(b).

The focus of this thesis is in implementation of the blended hybrid and not controls, as such only a simple PI control strategy was used for controlling the engine speed. Though the blended hybrid is a multi input multi output (MIMO) system, for this work the engine speed was treated as a single input single output (SISO) system. Figure 6.21 shows the block diagram for the negative feedback control system that was used for this work.

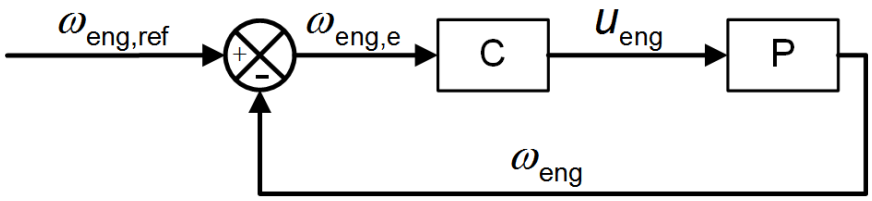

Figure 6.21. Engine speed control block diagram.

6.3.3 Control Unit and Data Acquisition System

For data acquisition and control a National Instruments CompactRio real-time controller was used. This controller has a modular design that allows up to 8 different input/output cards to be used for both control and data acquisition. Table 6.12 details the real-time controller and DAQ cards used for the blended hydraulic hybrid Range Rover

Table 6.12. Electronic control unit and data acquisition system.

NI cRio-9074	Real-Time Controller, 400 MHz, 128 MB RAM, 256 MB Storage
NI Module 9205	± 10 V Analog Input, 32 Channel
NI Module 9264	± 10 V Analog Output, 16 channels
NI Module 9213	16 Channel Thermocouple Module
NI Module 9401	5 V Bidirectional Digital Input Output, 8 Channel deg/sec
NI Module 9474	24 V, Soursing Digital Output, 8 Channel

NI Veristand was the software chosen to develop the data acquisition and control. This software package allows controller development in Matlab Simulink which can then be uploaded onto the cRio. In addition to Veristand, Field Programmable Gate Array (FPGA) was used for obtaining the speed of the three hydraulic units. The speed of the hydraulic units is measured by a frequency coming from a hall affect

sensor installed in each unit. FPGA was used to calculate the time between each pulse, which was then used to determine the unit's rotational speed.

6.3.4 Electrical Wiring

Figure 6.22 shows the enclosure that houses the controller, cRio modules, relays, terminal blocks, and voltage to current converters. Figure 6.23 shows the wifi router and 12 to 24 volt power converter that is installed on the opposite side of the vehicle. Both of these units are located in the trunk of the vehicle.

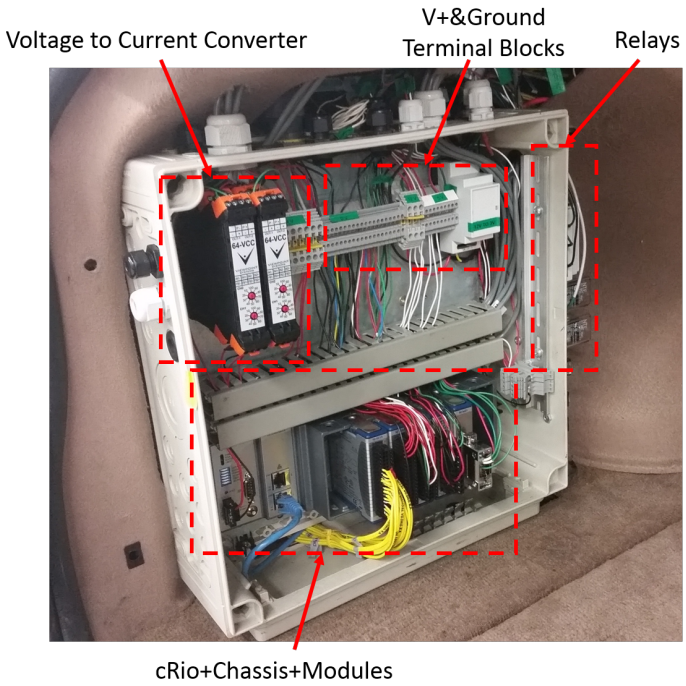

Figure 6.22. Industrial wring enclosure.

In addition to the instrument pack discussed, it was important that the operator had some physical control of the instrumentation. Figure 6.24 shows the instrument panel set up in this vehicle. The original gear shifter and parking brake were removed, in their place on-off switches for the sensors and controller, a lamp to indicate that the controller is operational, an E-stop switch, HP and LP accumulator gauges, and

Figure 6.23. Wifi router and power converter.

a three way toggle switch which controls forward reverse and neutral operation was added.

Appendix E details the logic that was used to create the forward neutral and reverse commands. For safety this logic makes it impossible to switch the driving command when moving. This switch ensures that during forward operation unit 2 and 3 have a positive swash plate displacement, when in reverse unit 2 and 3 have a negative swash plate displacement, and in neutral all units are set to zero percent displacement.

When the E-Stop is triggered all hydraulic units are sent to zero displacement, and the engine speed controller is disabled. This forces the engine to go to idle and no power can be transmitted to the wheels. Keeping the engine at idle allows for power steering and the brake pump to still be operational.

Appendix C shows a detailed wiring diagram of the data acquisition system and controls. An important detail shown in the wiring diagram is the use of two 12V batters and a batter separator. Having this set up allows the controller to be powered by a separate battery and therefore will not loose power during engine start.

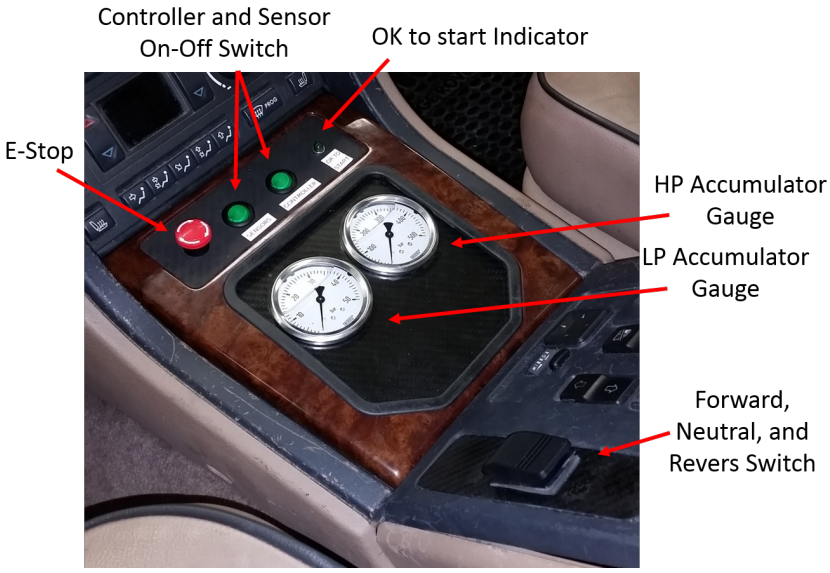

Figure 6.24. Instrument panel.

6.4 Control, Operation and Testing

As discussed before the blended hydraulic hybrid transmission has multiple modes of operation. These include, hydrostatic driving, blended driving, which is a combined hybrid and hydrostatic driving, full hybrid driving, and regenerative braking. Figure 6.25 shows a top level operation diagram for the blended hydraulic hybrid. The controller receives inputs from the operator via the accelerator and brake pedals, additionally the wheel speed, engine speed, and HP accumulator pressure are measured and used by the controller. The controller commands the necessary engine throttle position, on or off of the enabling valve, and the displacements of unit 1, unit 2 and unit 3.

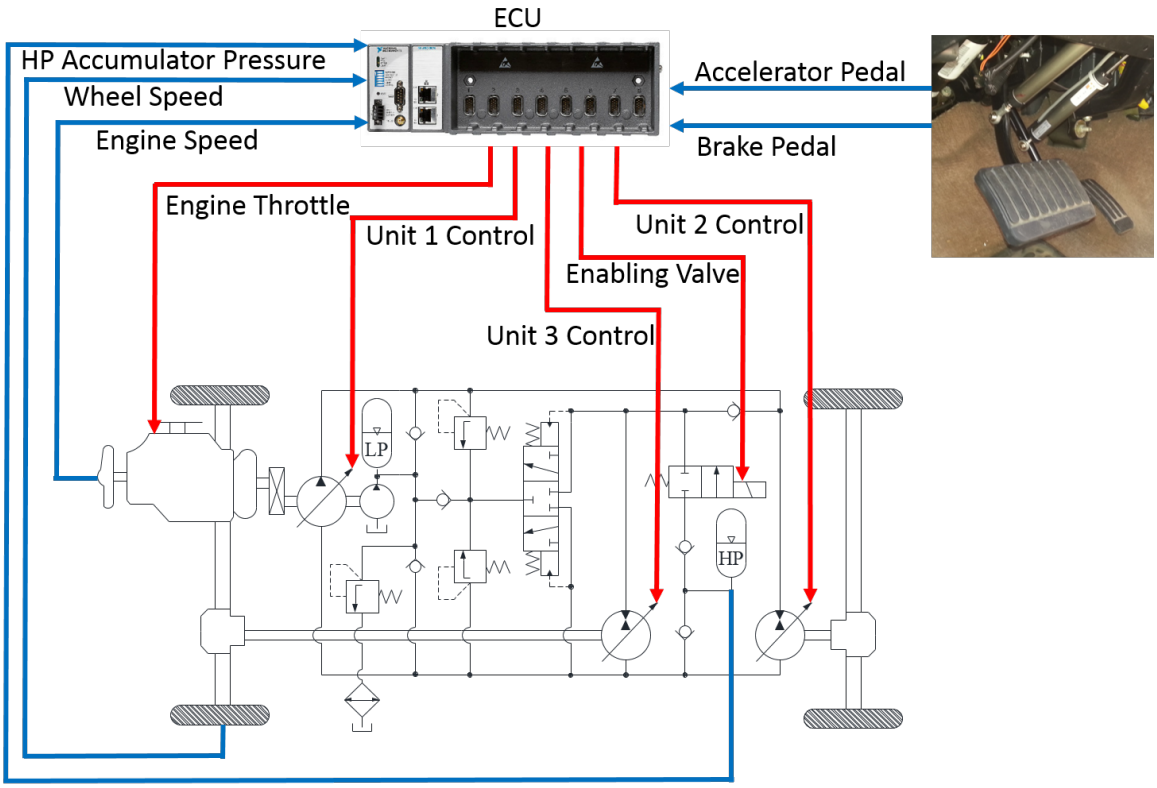

Figure 6.25. The blended hybrid top level control diagram.

6.5 Control

The following sections discuss the control strategy that was implemented and subsequent testing results to validate that all operating conditions are able to be met with this prototype transmission. For this work only the simplest of controllers were implemented, this consist primarily of feed forward control, and very simple feed back control.

6.5.1 Desired Vehicle Speed Algorithm

The control strategies used for this work are taken from Sprengel et al. (2015). The first goal in controlling the blended hybrid was to create a similar pedal feel

as a conventional automatic or manual transmission. The hydrostatic transmission is flow controlled, meaning the flow from unit 1 must be absorbed by unit 2 and 3, and therefore a vehicle speed can be calculated using the current engine speed and the displacement of the hydraulic units. In off-highway vehicles, which typically have a set engine speed, the accelerator pedal corresponds to a set vehicle speed. On-highway vehicles on the other hand operate very differently, the accelerator pedal input is a desired torque, thus the pedal is adjusted continuously by the operator to either demand more or less torque.

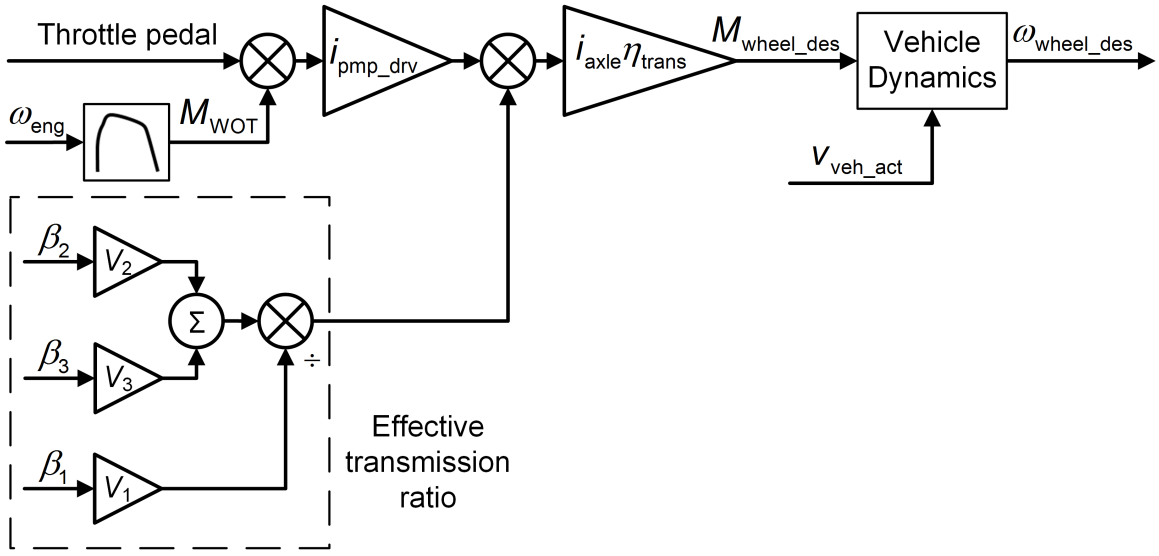

Figure 6.26. Desired vehicle speed algorithm (Sprengel et al. 2015).

It would be impractical to use the accelerator pedal position as a commanded vehicle speed, but the simplest way to control the HST is with a speed command. Figure 6.26 shows the algorithm that was used to transform the accelerator pedal input from a desired torque to a desired wheel speed command. This algorithm uses the throttle pedal position to determine the percentage of available engine torque to propagate through the transmission. The current unit displacements create an effective gear ratio that multiplies the available engine torque to the wheels. This

desired wheel torque is then processed through a vehicle dynamics model, which accounts for rolling resistance and aerodynamic drag at to the current vehicle speed, and outputs a desired wheel speed. This desired wheel speed is used in the different controllers to determine unit displacements.

6.5.2 Hydrostatic Driving Controller

As discussed before, the flow of the system determines the vehicle speed when operated as an HST. This mode occurs when accelerating the vehicle with the enabling valve closed. Figure 6.27 shows the block diagram of this control strategy.

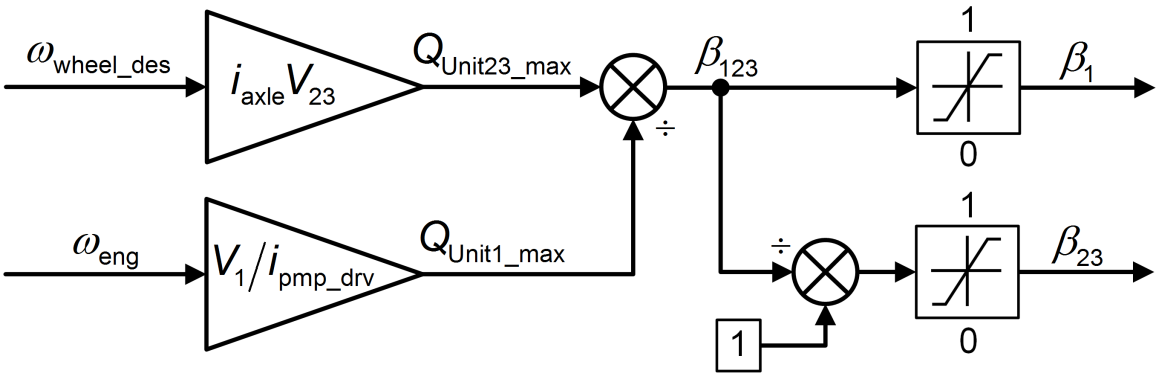

Figure 6.27. HST controller (Sprengel et al. 2015).

The inputs are the current engine speed and the desired wheel speed coming from the desired vehicle speed algorithm. From these values the maximum flow that unit 1 and units 2 and 3 could provide are calculated. Because sequential control is used in HST mode and unit 2 and unit 3 are operated at the same displacements these two flows determine the required displacement of each unit. As can be seen this is a purely feed forward control strategy.

6.5.3 Hybrid Driving Control

An important factor of the blended hydraulic hybrid transmission is the use of stored energy in the hydraulic accumulator. A second mode of operation for this vehicle is accelerating the vehicle by releasing the stored energy from the accumulator. This mode occurs when the enabling valve is open and unit 1 and unit 2 are at zero displacement. Thus high pressure fluid in the accumulator is used to motor unit 3 and propel the vehicle. Figure 6.28 shows the block diagram for this control strategy.

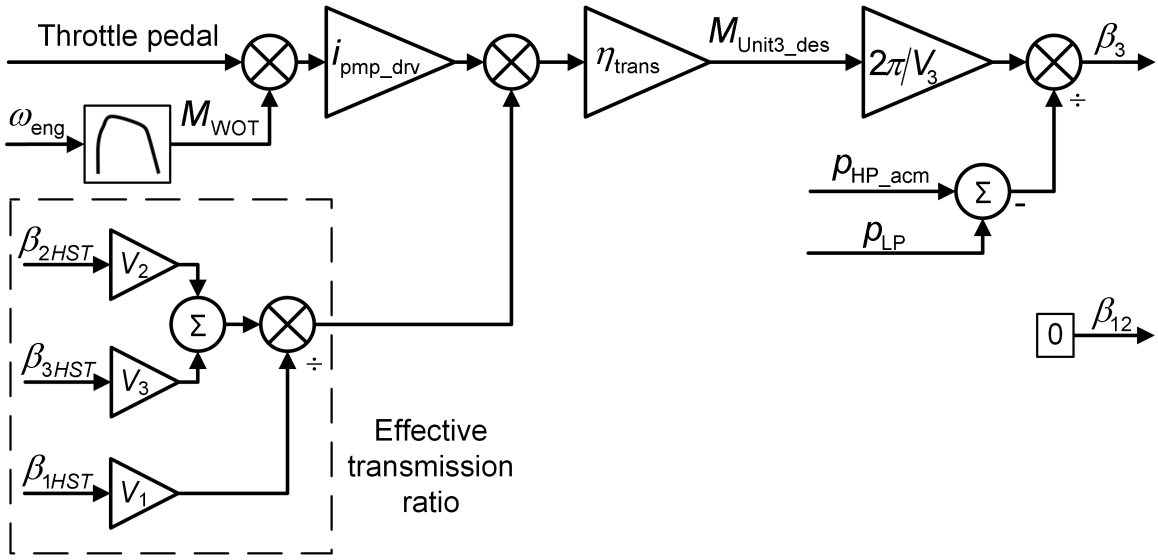

Figure 6.28. Hybrid propulsion controller (Sprengel et al. 2015).

Using the same concept from the desired vehicle speed algorithm in Section 6.5.1 the accelerator pedal position is used to determine a desired torque at the wheels. For this control strategy though the effective transmission ratio is determined using the unit displacements from the HST control. The desired torque is then met by calculating the required unit 3 displacement according to the current accumulator differential pressure.

6.5.4 Blended Driving Control

A third mode of vehicle propulsion is found when combining the hydrostatic mode and the hybrid mode of propulsion. In this mode the desired torque determined from the accelerator pedal is met partly from hybrid control on unit 3 seen in Figure 6.28 and hydrostatic control on unit 2 as seen in Figure 6.29. In this mode flow from unit 3 is not considered when determining the displacements of unit 1 and unit 2. Therefore in this mode unit 1 only provides flow to power unit 2, and the accumulator provides flow to power unit 3.

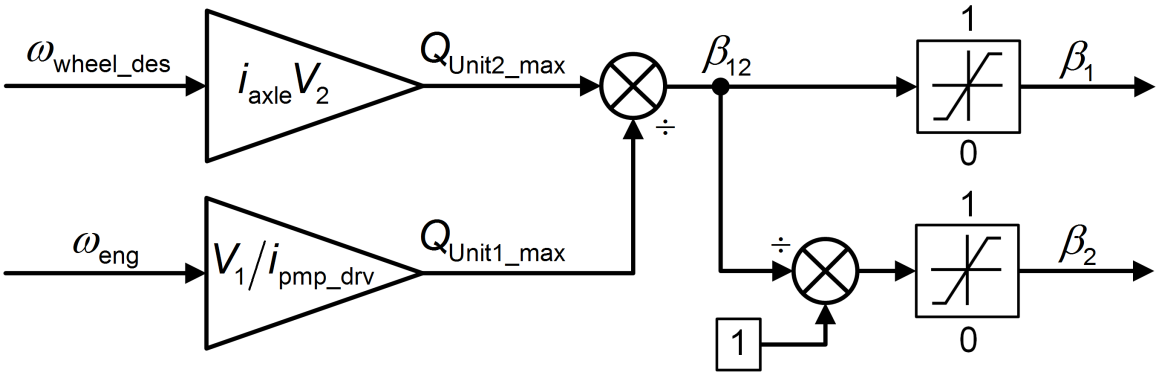

Figure 6.29. Hybrid mode controller (Sprengel et al. 2015).

6.5.5 Regenerative Braking Control

The last operating mode for this work is regenerative braking. It is desired that all kinetic energy from the vehicle be transformed and stored as high pressure fluid in the accumulator, but on top of this the operator must have the braking control they desire, meaning the braking torque must be controlled by the operator. Figure 6.30 shows the block diagram used for regenerative braking. The operator depresses the brake pedal, which results in a desired braking torque. With the desired braking

torque and the current system pressure, a required unit 2 and unit 3 displacement are determined.

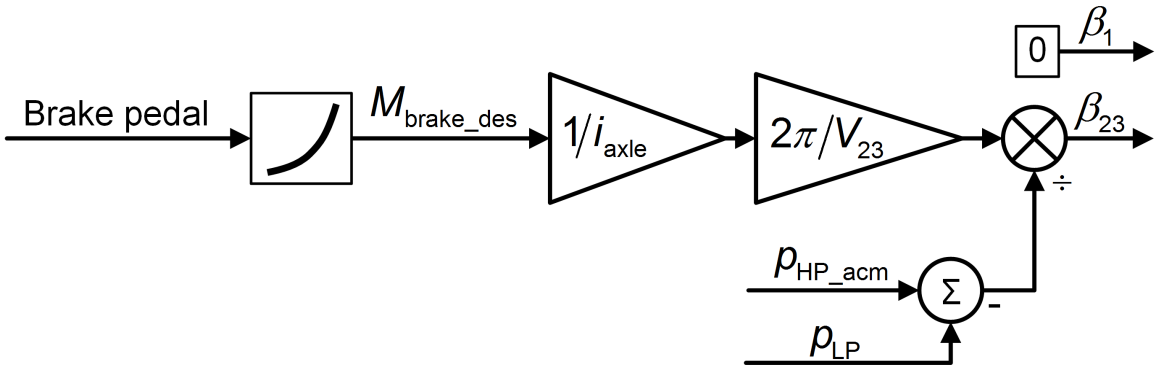

Figure 6.30. Regenerative braking controller (Sprengel et al. 2015).

6.6 Results

The following sections show the results of implementing the control strategies discussed previously.

6.6.1 Forward Operation

As discussed in previous sections the blended hydraulic hybrid has multiple modes of operation. Figure 6.31 shows the measurement results of a simple acceleration and deceleration cycle. During this cycle all modes of operation are realized. This shows that during the beginning of the cycle the transmission is in hydrostatic mode. Then the transmission switches to blended mode, as can be seen the enabling valve opens and exposes line C to the pressure in the HP accumulator, at this point unit 3 is operated using the hybrid controller and units 1 and 2 are operated in hydrostatic mode. Following this the transmission switches to full hybrid mode, in which unit 1 and 2 are sent to zero displacement and all propulsion is delivered by unit 3 with

pressure and flow coming form the accumulator. During the braking event, line B increase in pressure to that of the accumulator, units 2 and 3 change their displacement to provide the required braking torque and the accumulator pressure increases, storing the brake energy. Additionally it is important to notice that the accelerator pedal does not correspond to a set vehicle speed, this shows how the desired vehicle speed algorithm worked successfully in mimicking a torque controlled power train.

6.6.2 Four Wheel Drive Turning Event

As discussed in previous sections, one goal of this work is to operate safely in four wheel drive at all times. In simulation it was shown that this transmission was capable of operating in four wheel drive during turning events. Figure 6.32 shows measurement results while doing multiple turning events. This figure does not show turning command from the operator, but it does show the yaw rate and lateral acceleration of the vehicle which in vehicle dynamics are the necessary values in describing a turning event. Thus the yaw rate shows the rate of rotation of the vehicle and the lateral acceleration shows how quickly it moves laterally. For this driving event multiple S turns were performed. This figure also shows that during these turns the speed of unit 2 and unit 3 are different and therefore validates our model that this system has no trouble operating in four wheel drive at all time, and no control effort is needed to allow units 2 and 3 to operate at different speeds.

6.6.3 Reverse Operation

Reverse operation is very simple in the blended hydraulic hybrid. For this system, units 2 and 3 are simple operated over center to provide torque in the opposite direction, all other operation is the exact same. Figure 6.33 shows the measurement results of operating in reverse. Notice in this figure the vehicle is first operated in forward operation and then at approximately 32 seconds units 2 and 3 are switch to the opposite swash plate angle and the vehicle is operated in reverse. Additionally

when braking in reverse the accumulator charged by units 2 and 3. What is not shown here, is that the blended hydraulic hybrid is capable of operating in all operating modes in reverse, including blended and hybrid mode.

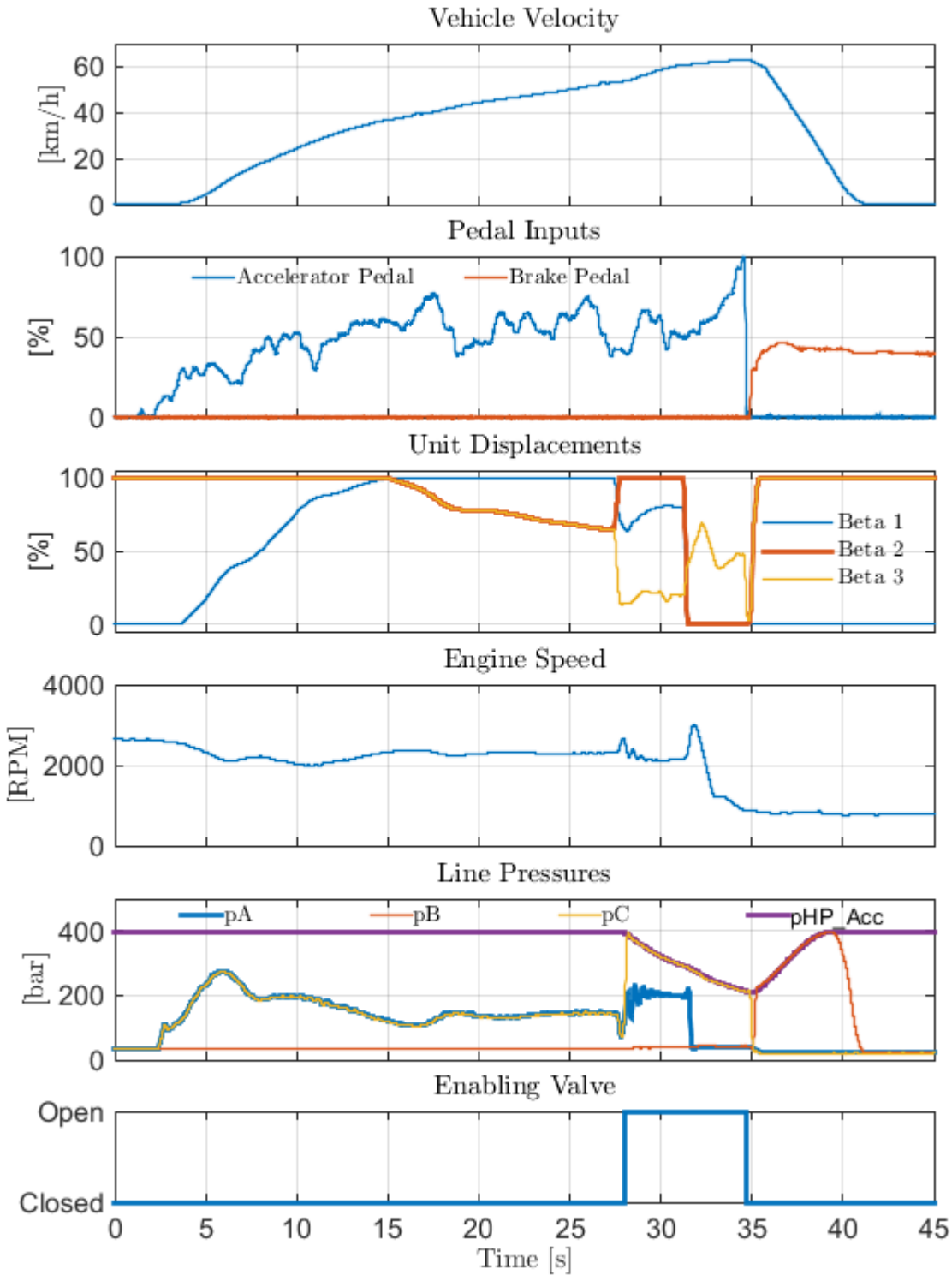

Figure 6.31. Measurement results showing all modes of operation.

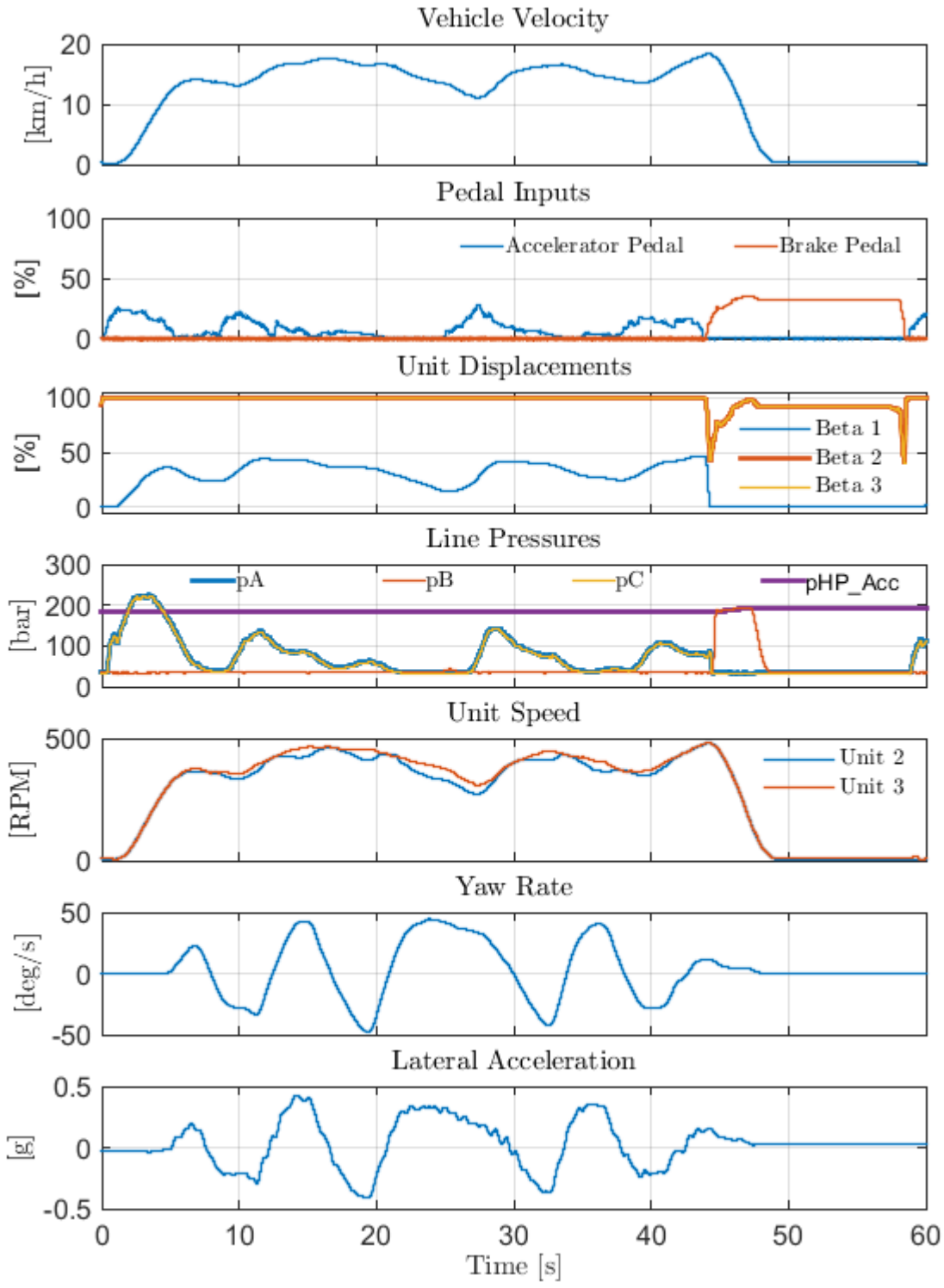

Figure 6.32. Measurement results for four wheel drive turning.

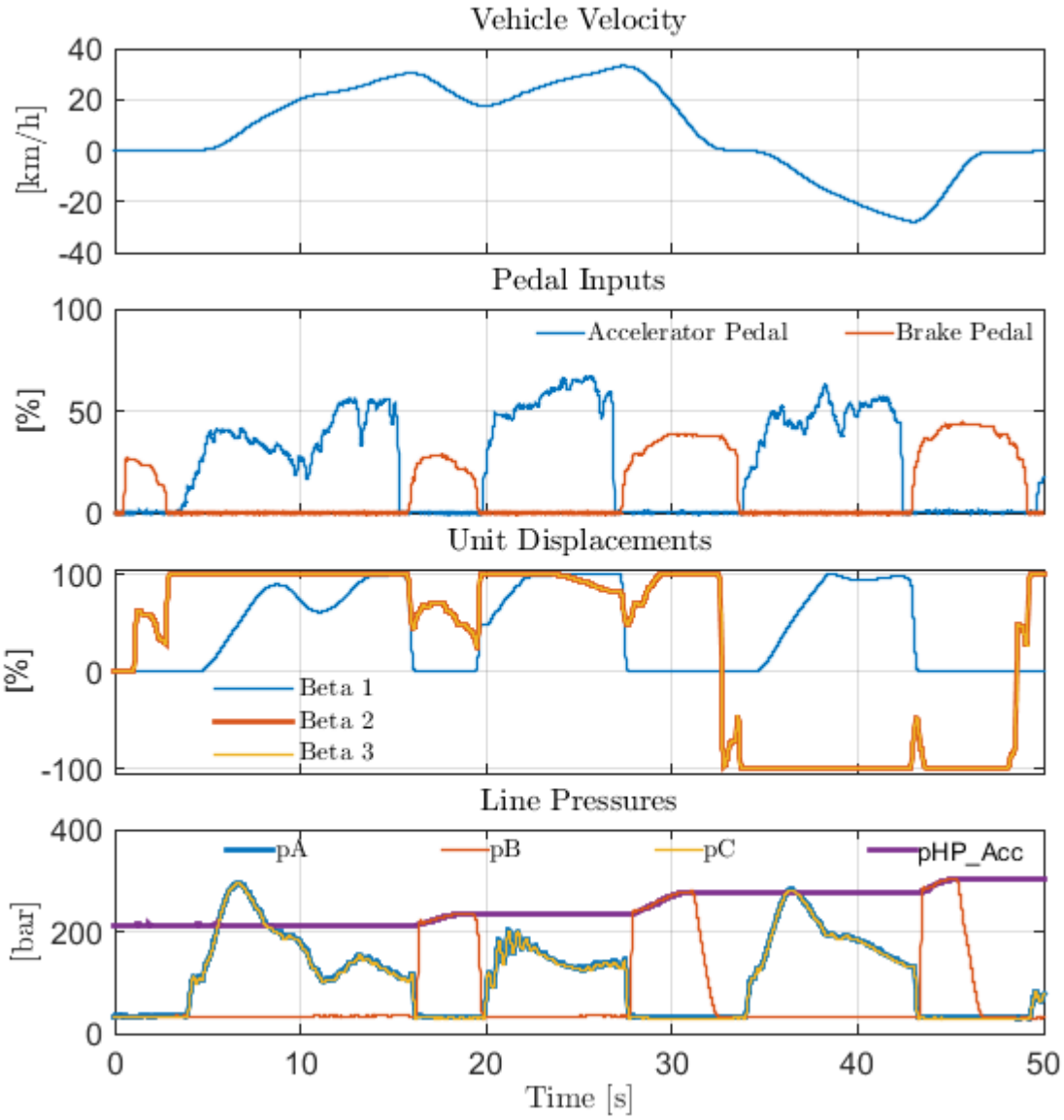

Figure 6.33. Measurement results for reverse operation.

6.7 Conclusions

This chapter outlined the extensive work that was done in order to transform an on-highway SUV into a fully operational blended hydraulic hybrid.

Modeling tools were used to design custom parts that made this transmission a reality, in addition modeling enabled a successful implementation because packaging constraints were extremely tight. Similarly this chapter overviews the instrumentation and installation that took place. In addition control algorithms were presented and implemented on the machine with measurement results that validated the work that was preformed.

7. SUMMARY

The goal of this work was to implement a blended hydraulic hybrid transmission on a four wheel drive SUV. This began with modifying the blended hydraulic hybrid circuit to allow for four wheel drive operation, simulation was used to verify operation during turning events.

To properly size the transmission a new methodology for sizing of hydraulic hybrid transmissions was presented. A parameter study was done in which 735 different designs were investigated using an optimal control tool called dynamic programming, to compare efficiency over the UDDS cycle. Additionally dynamic simulation was used to investigate the performance capabilities of each design. From this work it was evident that a smaller unit 2 and 3 create a more efficient transmission, while a larger unit 2 and 3 aid in low speed acceleration. Unit 1 showed an interaction with unit 2 and 3 with efficiency and performance, where a larger unit 1 had highest efficiency on average but when paired with a small unit 2 and 3 a small unit 1 showed the best efficiency. Overall though, a larger unit 1 increased the performance capability of the transmission because it was able properly extract engine power. Accumulator size showed only minimal changes in efficiency, where a larger accumulator resulted in higher efficiency, likewise a larger accumulator resulted in higher performance. The HP accumulator minimum pressure had a large impact on efficiency, high minimum pressure decreased efficiency, while a low minimum pressure increased efficiency but only to 90 bar. For maximizing performance a minimum pressure that was still able to load the engine resulted in the highest performance.

The main aim of this work was to implement the blended hydraulic hybrid transmission in an on-high way SUV. For this work a 1999 Range Rover 4.0 SE was selected as the application vehicle. a 100 cc/rev unit 1 and two 75 cc/rev unit 2 and 3 were selected, along with a 32 liter accumulator were selected. 3D modeling was used

for packaging the transmission and designing custom parts in order to integrate the system. The engine throttle was controlled in an effort to control engine speed, and accelerator and brake pedal were modified to create inputs for the hybrid system. A control strategy was presented and measurements were taken which showed the vehicle operation at in hydrostatic mode, blended mode, full hybrid mode, and reverse. Additionally it was shown that all time four wheel drive operation was possible with this circuit design.

LIST OF REFERENCES

LIST OF REFERENCES

Automobile Catalog (2015), '1999 range rover 4.0 detailed performance review and accelerations chart'. [Online; accessed 21-May-2015] *http://www.automobile- catalog.com/performance/1999/1398950/range_rover_4_0.html.*

Baseley, S., Ehret, C., Greif, E. & Kliken, M. (2007), 'Hydraulic hybrid systems for commercial vehicles', *SAE Commercial Vehicle Engineering Congress* (SAE Technical Paper 2007-01-4150).

Bellman, R. (1957), *Dynamic Programming*, Princeton University Press, New Jersey.

Cross, M. (2011), Optimal control: An effective method for designing hydraulic hybrid vehicles, Master's thesis, Purdue University.

Davis, S., Diegel, S. & Boundy, R. (2014), 'Transporation energy data book: Edition 33', (ORNL-6690).

Dewey, C., Elder, F. & Otis, D. (1974), 'Accumulator-charged hydrostatic drive for cars saves energy', *Hydraulics and Pneumatics* pp. 180-183.

Dunn, H. & Wojcienchowski, P. (1972), 'High-pressure hydraulic hybrid with regenerative braking', *7th Intersociety Energy Conversion Engineering Conference* pp. 207-209.

Dunn, H. & Wojcienchowski, P. (1974), 'Energy storage and conversion efficiency in a hydraulic/gas-turbine hybrid', ASME (74-GT-107).

Dunn, H. & Wojcienchowski, P. (1975), 'Energy regeneration and conversion efficiency in a hydraulic-hybrid propulsion system', *High Speed Ground Transportation Journal* pp. p:282-392.

Elder, F. & Otis, D. (1973), 'Simulation of a hydraulic hybrid vehicle powertrain', ASME (73-ICT-50).

Heggie, W. & Sandri, R. (1979), 'Simulation of a hydraulic hybrid vehicle powertrain', ASME (79-WAIDSC-15).

Heskitt, M., Smith, T. & Hopkins, J. (2012), 'Design & development of the lco-140h series hydraulic hybrid low floor transit bus', BUSolutions Final Technical Report.

Hugosson, C. (1993), 'Cumulo hydrostatic drive a vehicle drive with secondary control', 3rd Scandinavian International Conference on Fluid Power.

Kepner, R. (2002), 'Hydraulic power assist - a demonstration of hydraulic hybrid vehicle regenerative braking in a road vehicle application', (SAE Technical Paper (2002-01-3128).

Kirk, D. (2004), Optimal Control theory: An Introduction, Dover Publications, Mineola, New York.

Kumar, R. (2010), A Power Management Strategy for Hybrid Output Coupled Power-Split Transmission to Minimize Fuel Consumption, PhD thesis, Purdue University.

Lammert, M., Burton, J., Sindler, P. & Duran, A. (2014), 'Hydraulic hybrid and conventional parcel delivery vehicles' measured laboratory fuel economy on targeted drive cycles', SAE Technical Paper 2014-01-2375.

Martini, S. (1984), 'The m.a.n. hydrobus: A drive concept with hydrostatic brake energy recovery', *International Symposium on Advanced and Hybrid Vehicles.*

Nakzawa, N., Kono, Y., Takao, E. & Takeda, N. (1987), 'Development of a braking energy regeneration system for city buses', (SAE Technical Paper 872265).

PSA-Peugeot-Citroen (2014), 'Hybrid air, an innovative full hybrid gasoline system'. [Online; accessed 02-May-2015] *http://www.psa-peugeot-citroen.com/en/automotive-innovation/innovation-by-psa/hybrid-air-engine-full-hybrid-gasoline.*

Shiber, S. (1979), 'Automotive energy management system', *National Conference on Fluid Power* pp. 141-147.

Shiber, S. (1980), 'Mutli-mode transmission'. US Patent 4196587.

Sprengel, M., Bleazard, T., Haria, H. & Ivantysynova, M. (2015), 'Implementation of a novel hydraulic hybrid powertrain in a sports utility vehicle', *4th IFAC Workshop on Engine and Powertrain Control, Simulation and Modeling.*

Sprengel, M. & Ivantysynova, M. (2012), 'Novel transmission configuration for hydraulic hybrid vehicles', *Proceedings of the International Sci-Tech Conference "Machine Dynamics and Vibro Acoustics"* pp. 207-209.

Sprengel, M. & Ivantysynova, M. (2013a), 'Control strategies for a novel blended hydraulic hybrid transmission', *22nd International Conference on Hydraulics and Pneumatics* (SICFP2013).

Sprengel, M. & Ivantysynova, M. (2013b), 'Investigation and energetic analysis of a novel hydraulic hybrid architecture for on-road vehcles', *Proceedings of the 13th Scandinavian International Conference on Fluid Power* pp. 15-22.

Sprengel, M. & Ivantysynova, M. (2014a), 'Hardware-in-the-loop testing of a novel blended hydraulic hybrid transmission', *Proceedings of the 8th FPNI PhD Symposium on Fluid Power* (FPNI2014).

Sprengel, M. & Ivantysynova, M. (2014b), 'Investigation and energetic analysis of a novel blended hydraulic hybrid power split transmission', *Proceedings of the 9th IFK International Fluid Power Conference.*

Sprengel, M. & Ivantysynova, M. (2014c), 'Recent developments in a novel blended hydraulic hybrid transmission', *SAE 2014 Commercial Vehicle Engineering Congress* (SAE Technical Paper 2014-01-2399).

U.S. Department of Energy (2015), '1999 Land Rover Range Rover'. [Online; accessed 20-May-2015] *http://www.fueleconomy.gov/feg/noframes/15552.shtml.*

Wendel, G., Baseley, S., O'Briend, J., Kargul, J. & Ellis, M. (2007), 'Hydraulic hybrid vehicle system panel', Michigan Clean Fleet Conference.

Wouk, V. (1995), 'Hybrids: Then and now', Spectrum, IEEE pp. 16-21.

Wu, P., Luo, N., Fronczak, F. & Beachley, N. (1985), 'Fuel economy and operating characteristics of a hydropneumatic energy storage automobile', (SAE Technical Paper 851678).

Zhao, M. (2012), Optimal control based design of output coupled power split hydraulic hybrid, Master's thesis, Purdue University.

APPENDICES

Appendix A. Base Line Fuel Consumption Measurments

Figure A.1. Fuel consumption route 1.

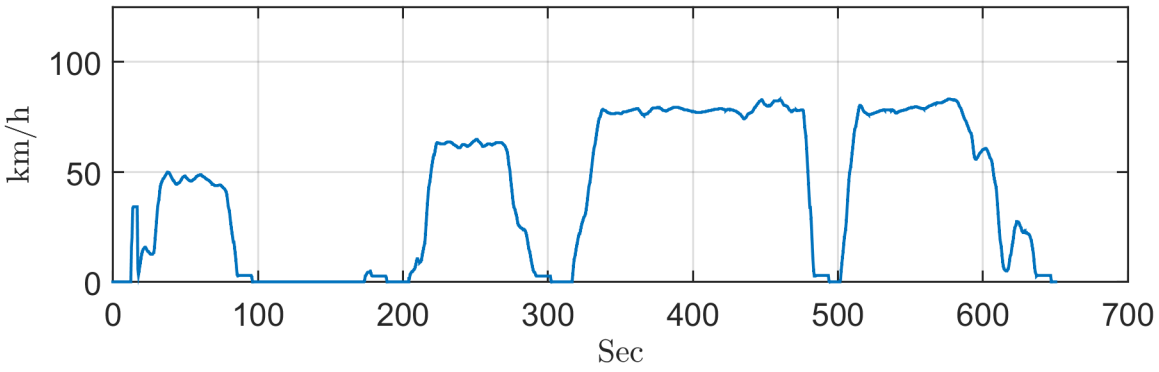

Figure A.2. Route 1, run 1, velocity profile.

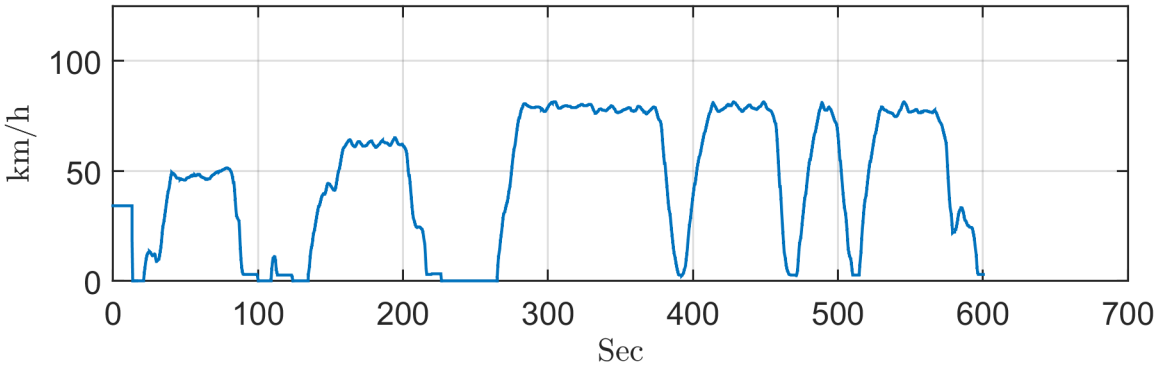

Figure A.3. Route 1, run 2, velocity profile.

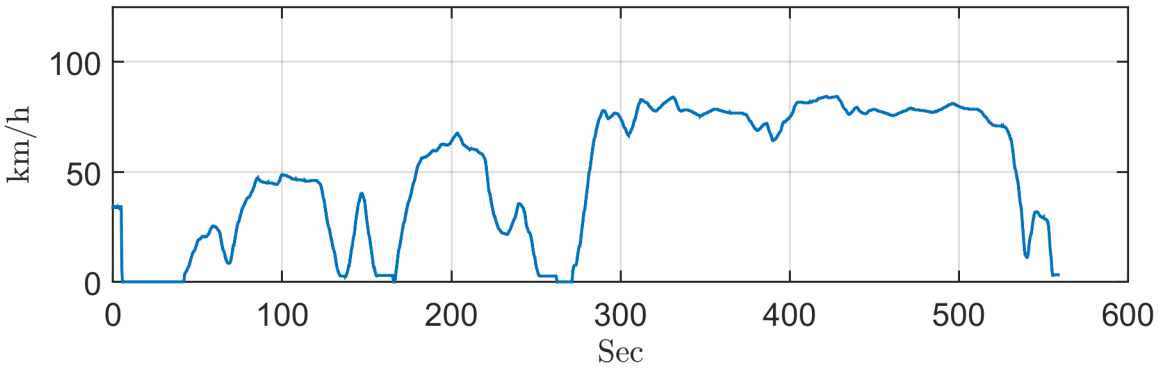

Figure A.4. Route 1, run 3, velocity profile.

Figure A.5. Fuel consumption route 2.

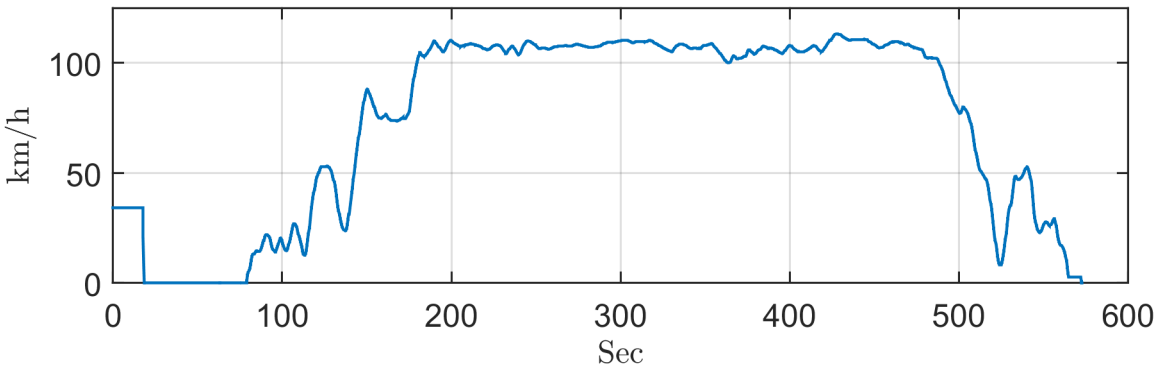

Figure A.6. Route 2, run 1, velocity profile.

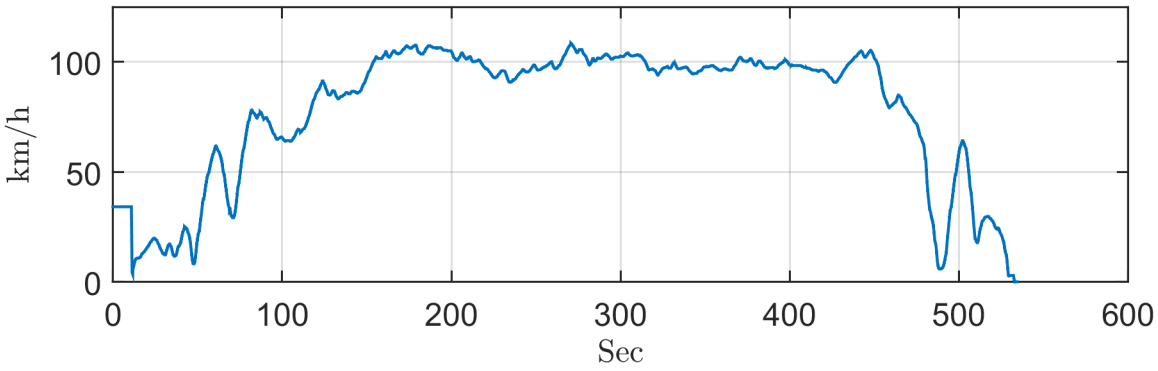

Figure A.7. Route 2, run 2, velocity profile.

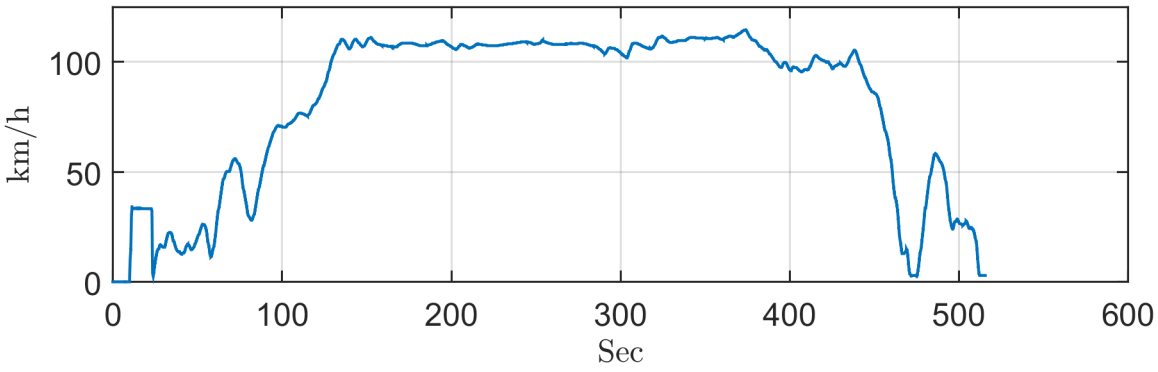

Figure A.8. Route 2, run 3, velocity profile.

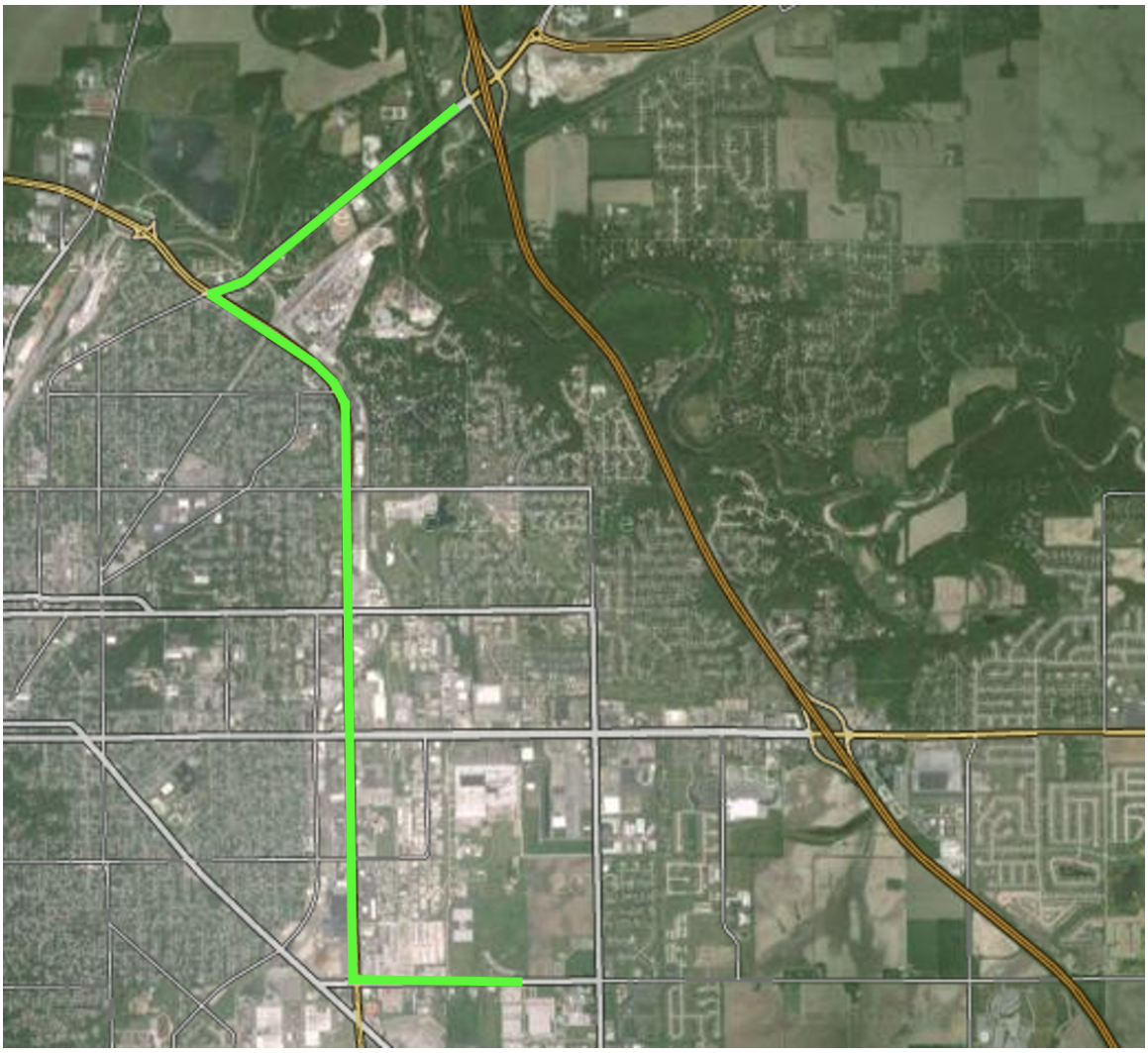

Figure A.9. Fuel consumption route 3.

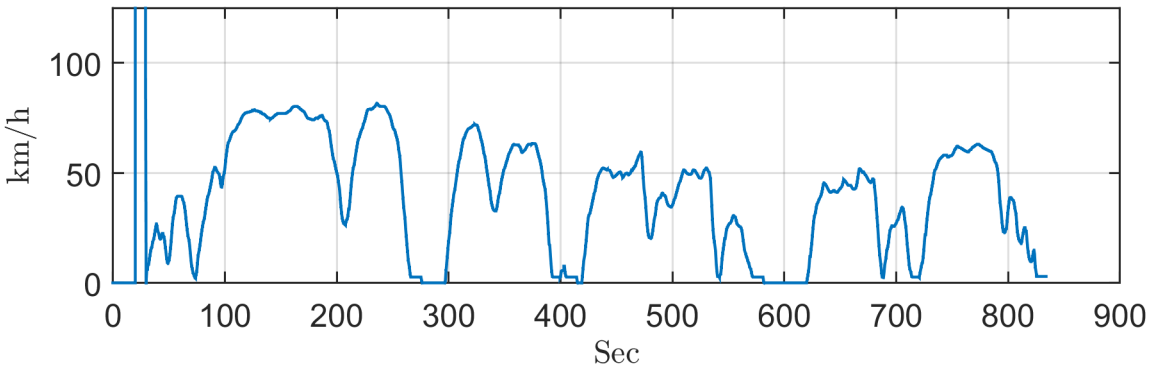

Figure A.10. Route 3, run 1, velocity profile.

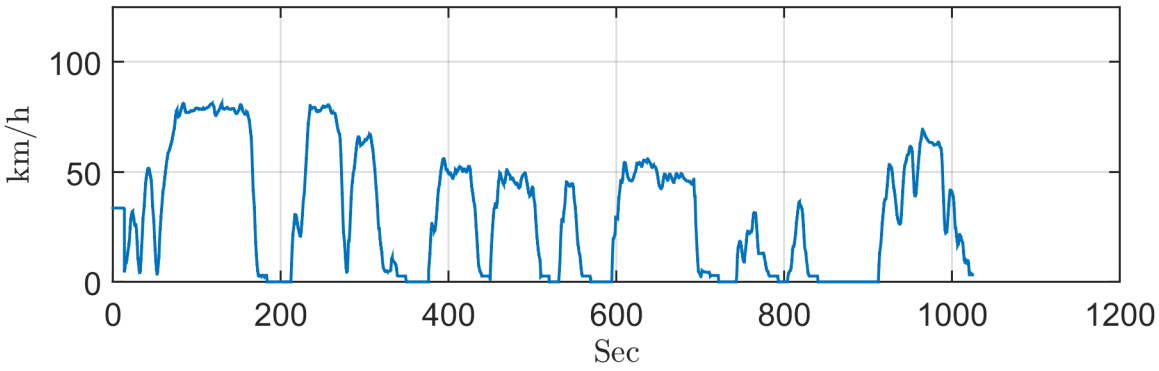

Figure A.11. Route 3, run 2, velocity profile.

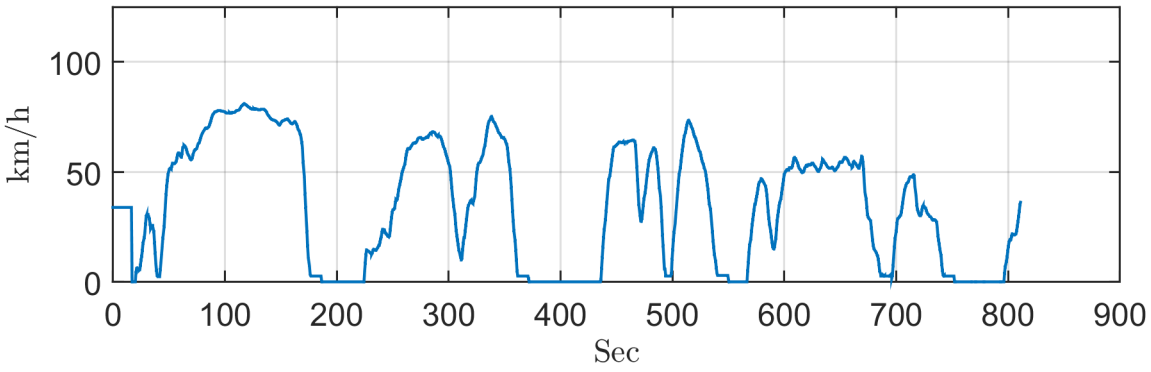

Figure A.12. Route 3, run 3, velocity profile.

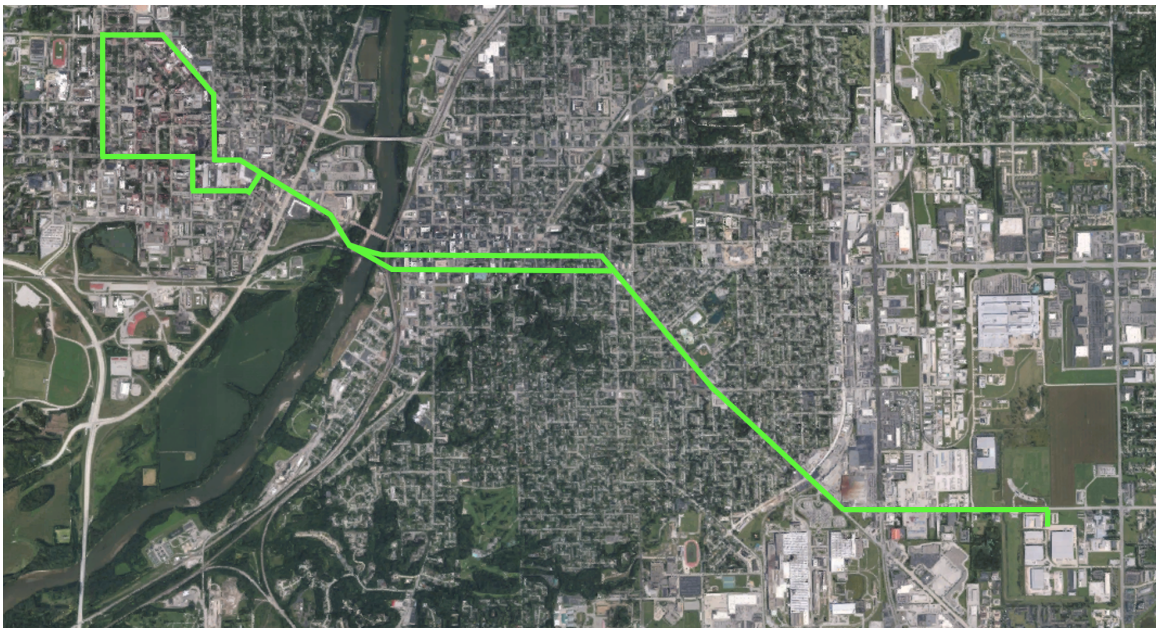

Figure A.13. Fuel consumption route 4.

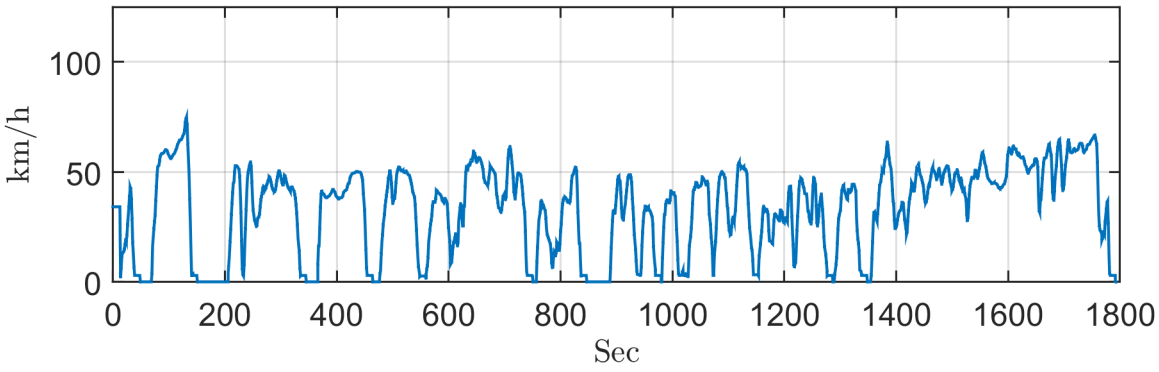

Figure A.14. Route 4, run 1, velocity profile.

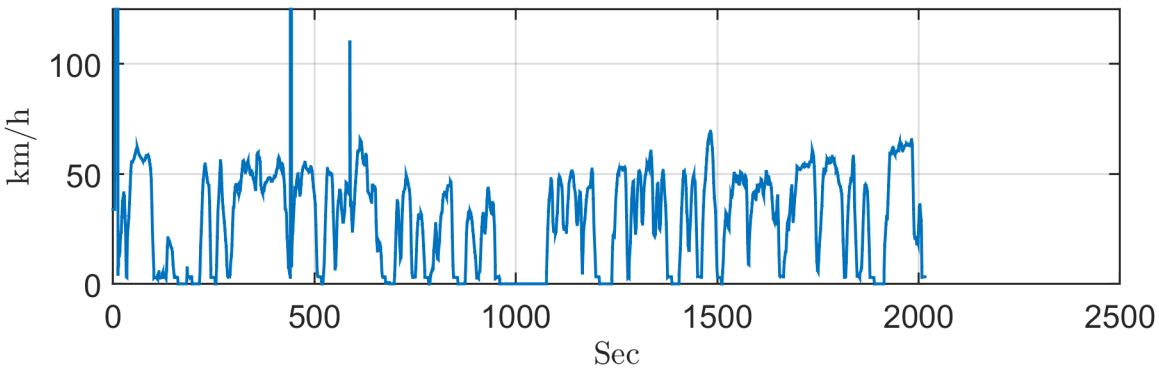

Figure A.15. Route 4, run 2, velocity profile.

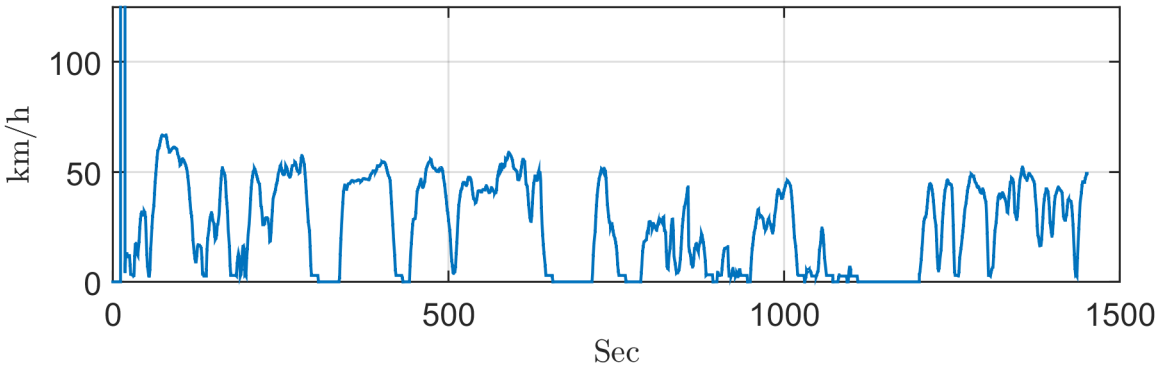

Figure A.16. Route 4, run 3, velocity profile.

Figure A.17. Fuel consumption route 5.

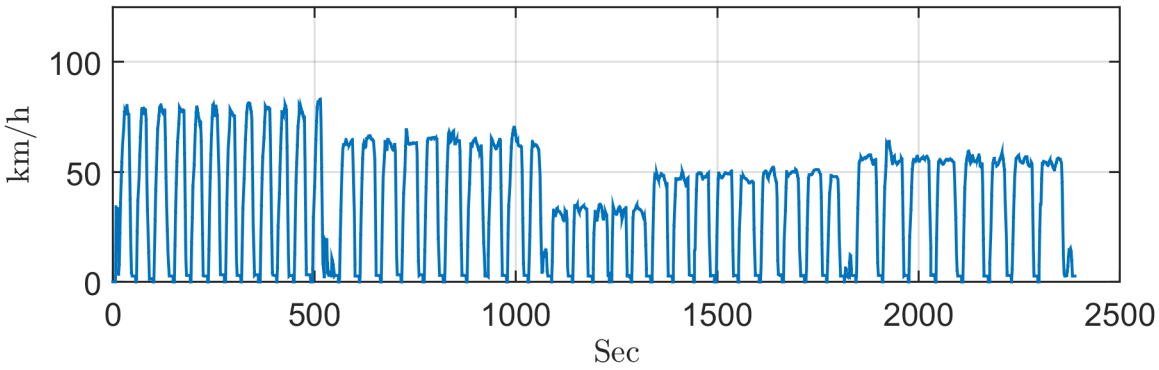

Figure A.18. Route 5, run 1, velocity profile.

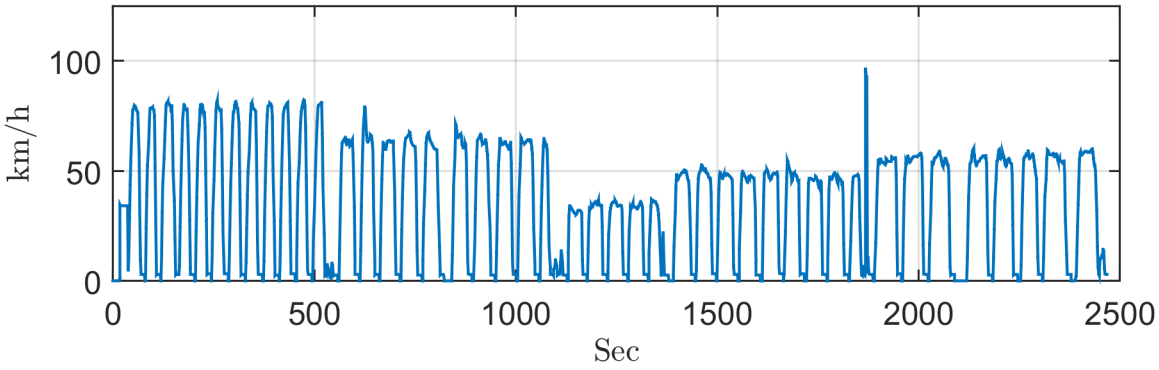

Figure A.19. Route 5, run 2, velocity profile.

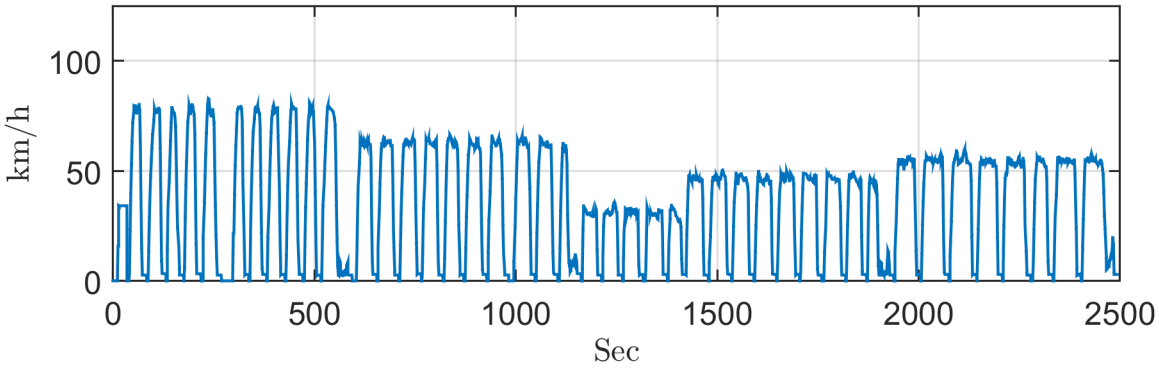

Figure A.20. Route 5, run 3, velocity profile.

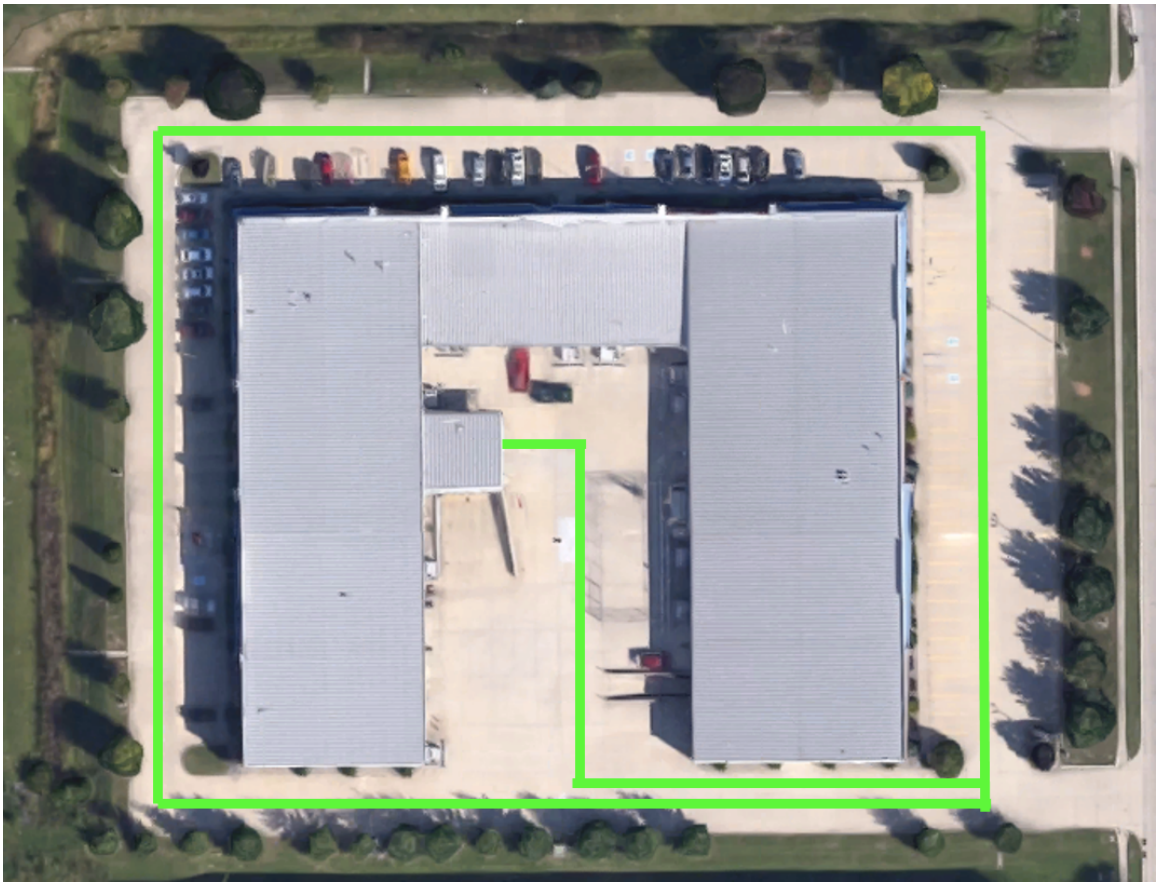

Figure A.21. Fuel consumption route 6.

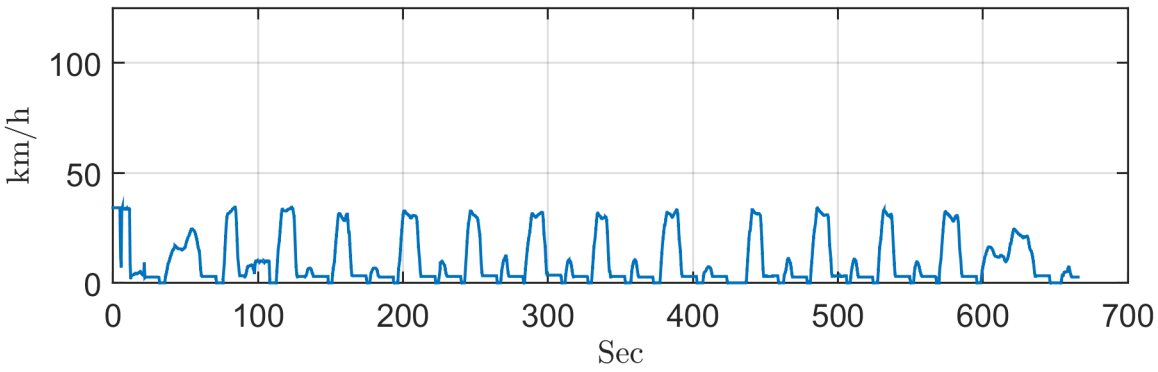

Figure A.22. Route 6, run 1, velocity profile.

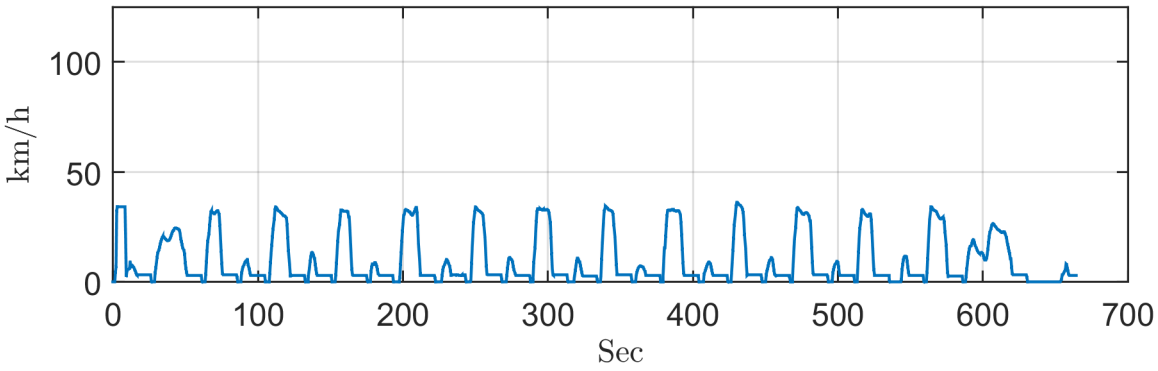

Figure A.23. Route 6, run 2, velocity profile.

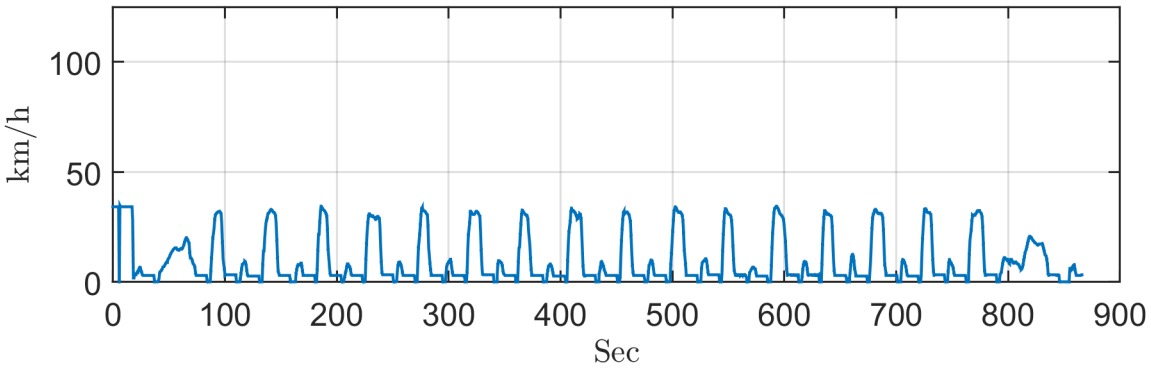

Figure A.24. Route 6, run 3, velocity profile.

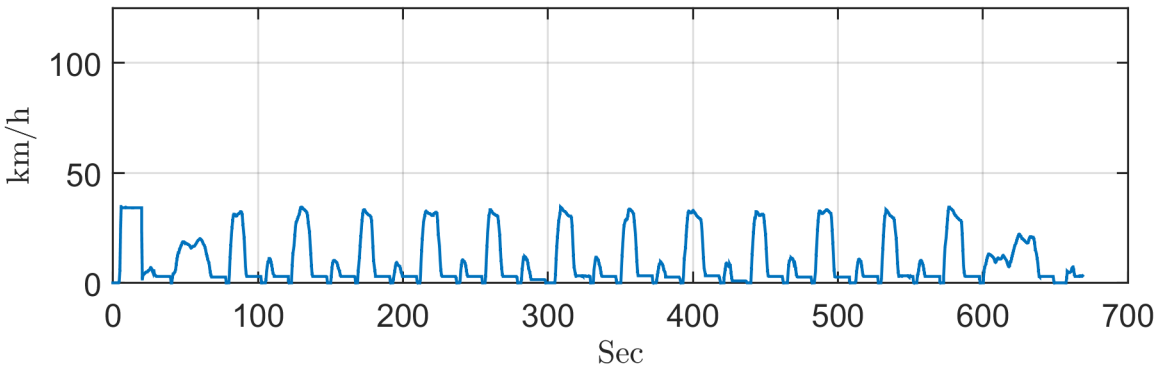

Figure A.25. Route 6, run 4, velocity profile.

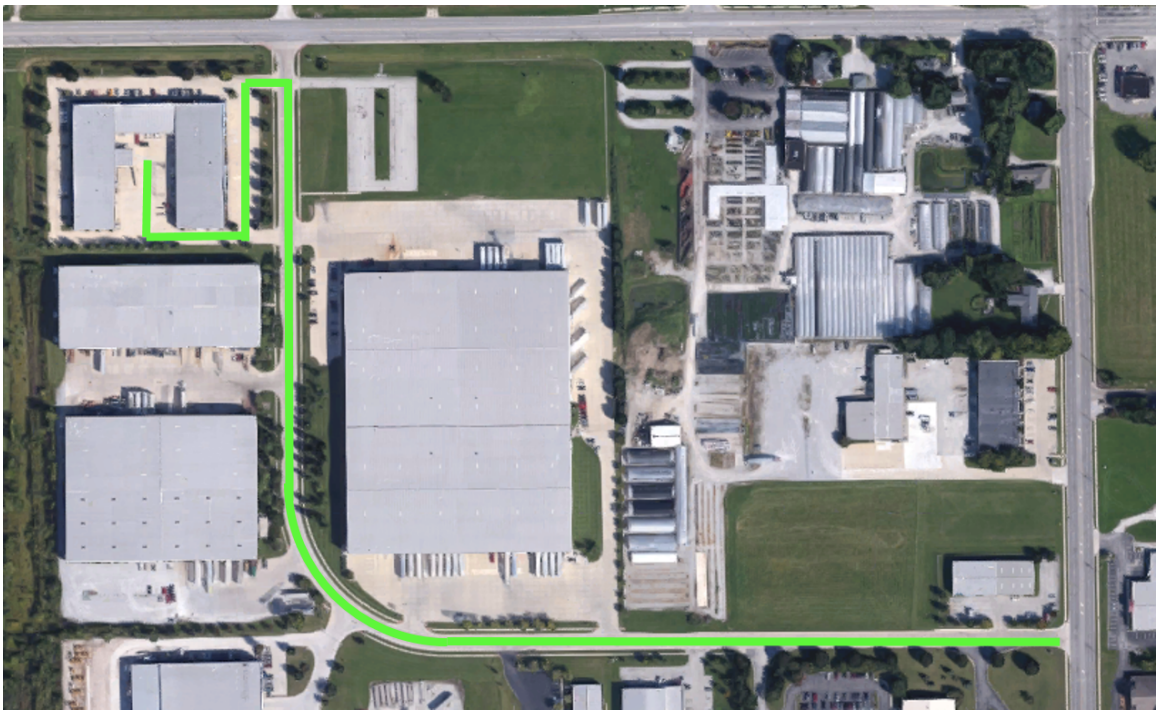

Figure A.26. Fuel consumption route 7.

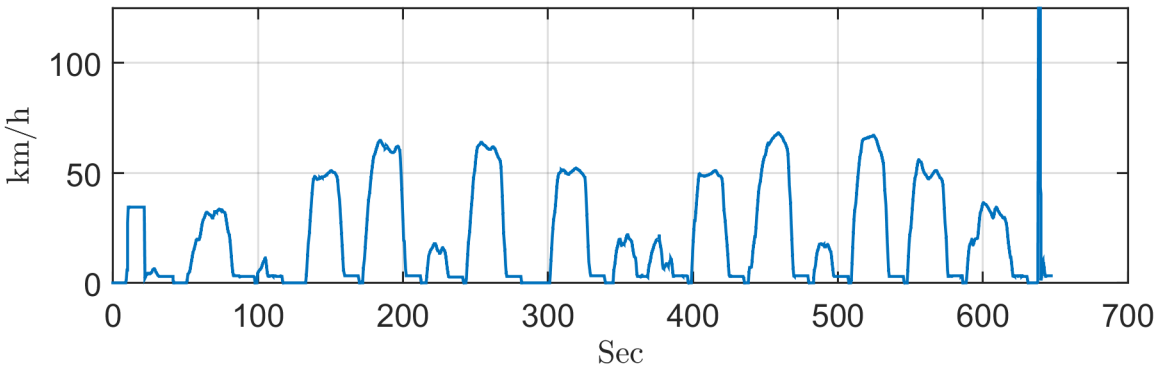

Figure A.27. Route 7, run 1, velocity profile.

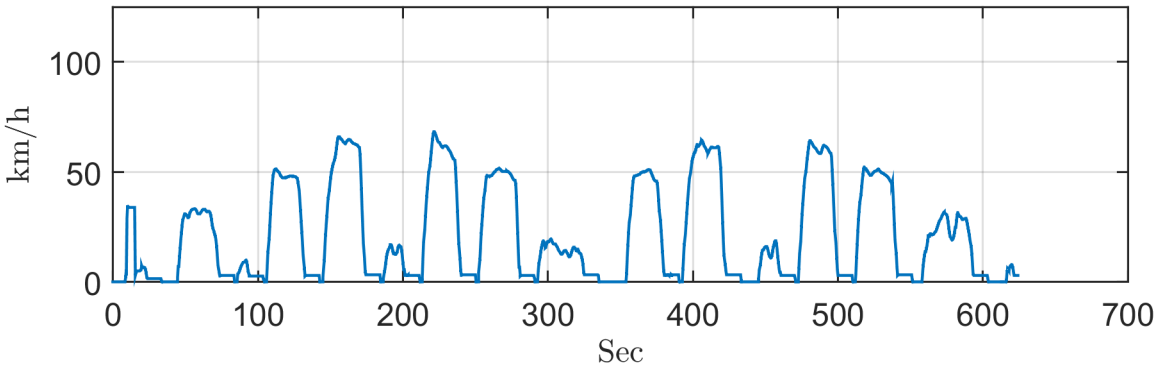

Figure A.28. Route 7, run 2, velocity profile.

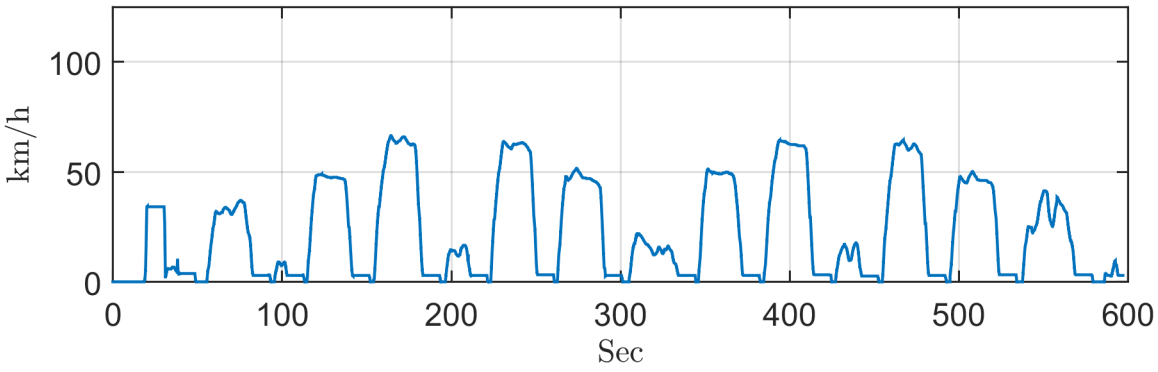

Figure A.29. Route 7, run 3, velocity profile.

Appendix B. Blended Hybrid Range Rover Hydraulic Circuit

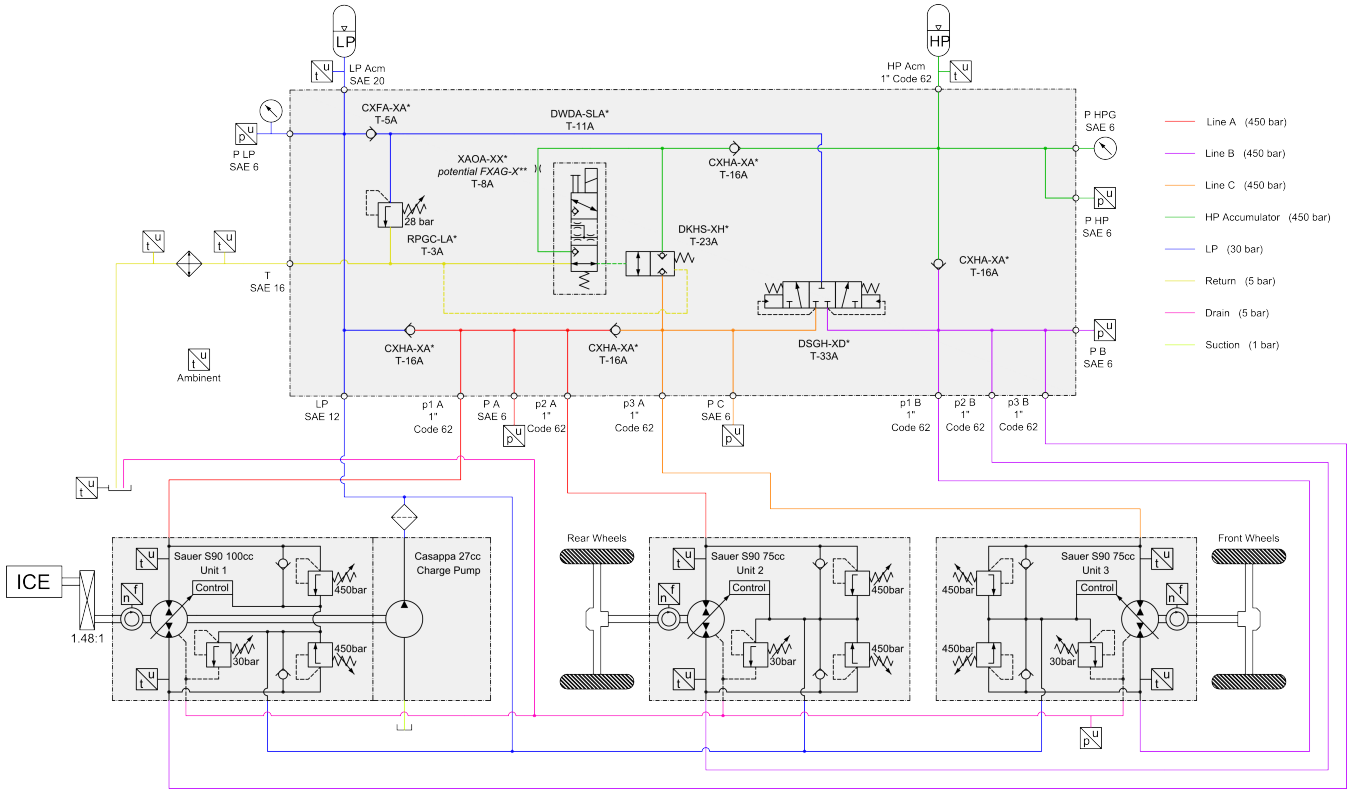

Figure B.1. Range rover hydraulic circuit.

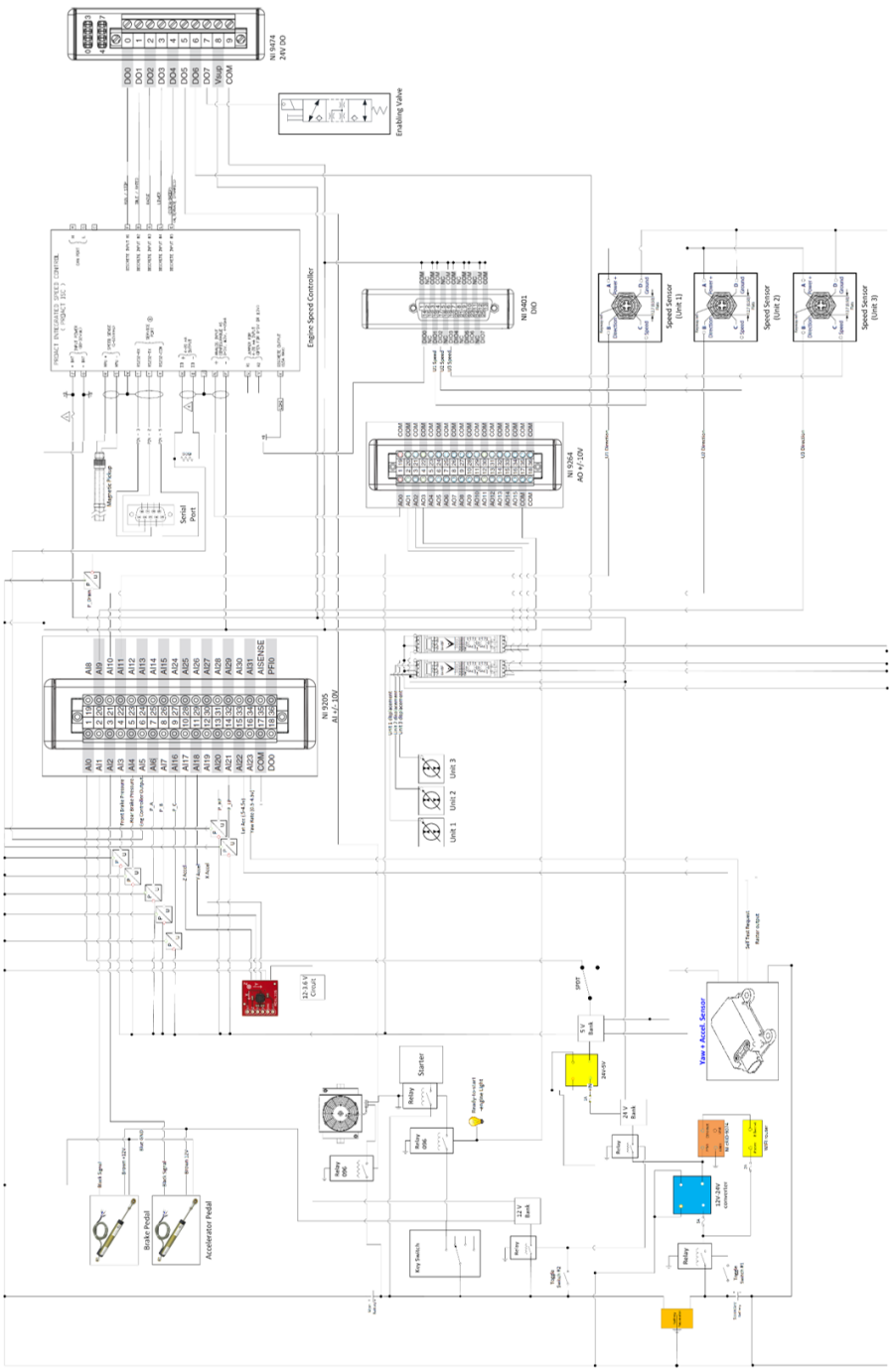

Figure C.1. Range rover wiring diagram.

Appendix D. Engine Speed Controller Four Bar Mechanism Design

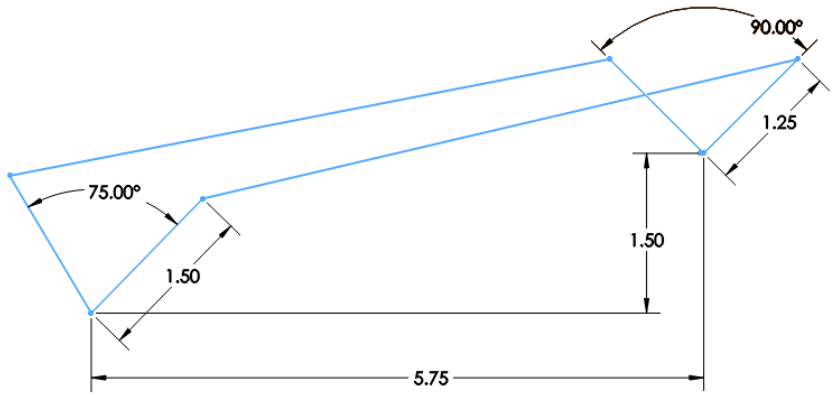

Figure D.1. Engine speed controller four bar mechanism graphical analysis design.

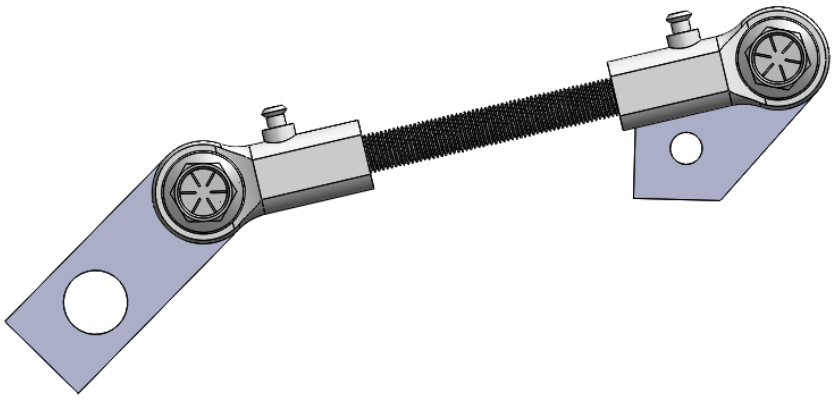

Figure D.2. Engine speed controller four bar mechanism assembly.

Appendix E. Forward, Neutral, and Reverse Logic

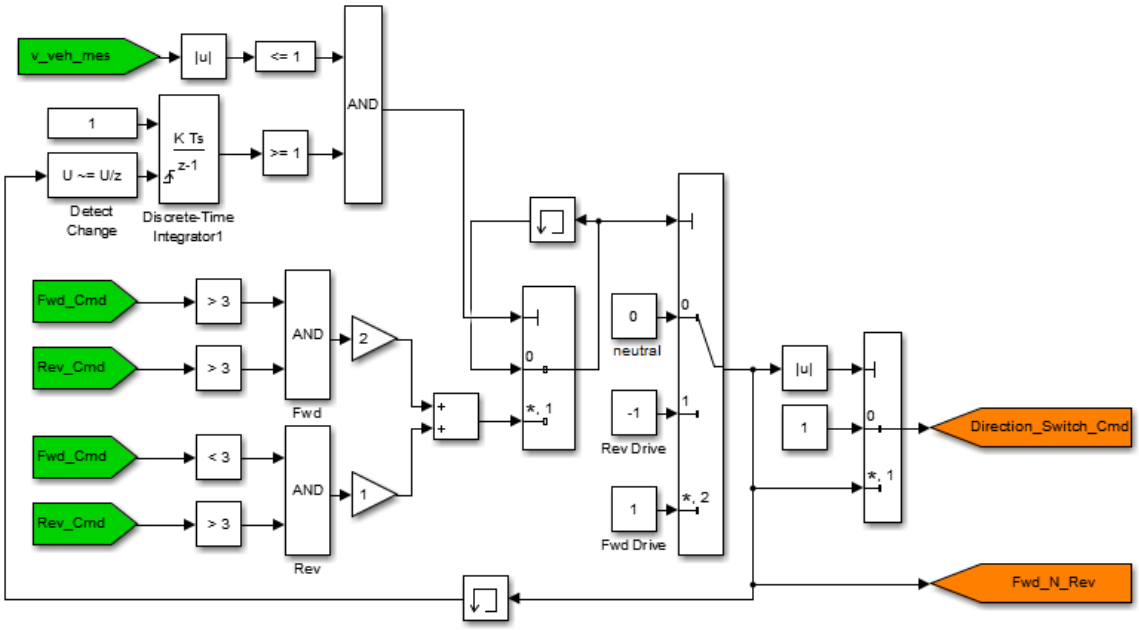

Figure E.1. Forward, neutral and reverse logic.